University of Strathclyde

Department of Pure and Applied Chemistry

Development of Novel Indicators

By Michael McFarlane

This thesis is the result of the author's original research. It has been composed by the author and has not been previously submitted for examination which has led to the award of a degree.

Signed:

Date:

Acknowledgements

First and foremost I would like to extend my deepest thanks to Professor Andrew Mills for giving me the chance to undertake my PhD and for his continued advice and guidance. The patience he has shown during many a confused and flustered presentation of data, and his calm correction of my many crazy/stupid ideas has not gone unnoticed or unappreciated.

I would also like to thank all the undergrads, PhDs and Postdocs that passed through the research group during my time there, with special mention going to Dr Ross "quick-pint-after-work" Archer. I wouldn't have enjoyed my time nearly as much without their support, friendship, and 'abuse'.

Last, but certainly not least, I would like to thank my closest friends and family. Without their belief I would never have had the motivation or the confidence to come as far as I have, and I know they will continue to push me further and higher. For that I am eternally grateful. To Sarah and Tony, the rest of the Cumbernauld crowd, Mum, Dad, Peter, Scott and Kate - thank you.

Abstract

Two indicating systems for measuring the dose of erythmal UV light have been developed. The first system is of a viologen salt, preferably benzyl viologen chloride, dissolved in poly(vinyl alcohol). This viologen dosimeter responds clearly to different wavelengths and intensities of UV light, although the colour change is hampered by the presence of oxygen, and completely reversed in the absence of UV light. Attempts are made to enhance the rate of the reaction of the viologens with UV light by changing the halide of the salt or adding electron donating species. There is no positive effect noted with the addition of these materials, but changing the halide does alter the UV spectrum of the viologen species, resulting in a slower reaction and thus providing a way of retarding the dosimeter if required. This dosimeter shows a demonstrable reaction to both artificial and natural sources of erythemal light.

The second UV dosimeter is based on the tetrazolium salts and is shown to behave in a similar way to the viologen dosimeter, with the neotetrazolium chloride salt as a preferred material for use in the dosimeter. This tetrazolium system is shown to respond clearly to different wavelengths and intensities of light, and shows a demonstrable response to erythemal levels of UV.

A solvatochromic indicator is developed, using Reichardt's dye adsorbed onto fumed silica to identify and measure the concentration of various solvent vapours. The fumed silica films are shown to be faster in response than polymer systems and have been shown to distinguish between different solvent vapours, but do not do so in a way that correlates with Reichardt's dye in the pure solvent. These films are shown to be more reliable in identifying alcohol vapours in a predictable manner.

A review is also carried out on existing methods of assessing the performance of photocatalytic films, comparing them with a new method developed within the Mills group.

Contents

1 Introduction *1*

1.1 Optical Sensors **1**

1.1.1 Advantages of Optical Sensors 2

1.2 Ultraviolet light **3**

1.2.1 Ultraviolet wavelengths 3

1.2.2 Ultraviolet sources 4

1.2.3 Health effects of UV exposure 4

1.3 UV Detection **8**

1.3.1 The UV Index 8

1.3.2 The Minimum Erythemal Dose 12

1.3.3 Electronic Detection 15

1.3.4 Other Commercial UV Sensors 16

1.3.5 Other UV Dosimeters 21

1.4 Detection Of Volatile Organic Compounds **26**

1.4.1 Sources of VOCs 26

1.4.2 Health Effects of VOCs 27

1.4.3 Sensors for VOCs 28

1.5 Aims **30**

1.6 References **31**

2 Experimental *39*

2.1 Materials Preparation **39**

2.1.1 Polymer Solutions 39

2.1.2 Dye solutions 42

2.1.3 Silica coated with Reichardt's dye 42

2.2 Spectroscopic Analysis **43**

2.2.1 Beer's Law 47

2.3 Gas Blending **49**

2.4 Sample Irradiation **49**

2.4.1 Instruments 50

2.4.2 UV Light Sources 51

2.4.3 Solar Simulation 52

3 A Viologen based UV dosimeter *54*

3.1 Methyl viologen in polymer (MV^{2+}-Polym.) **56**

3.1.1 MV^{2+}/PVA film's response to UV 57

3.1.2 Response to different UV wavelengths 62

3.1.3 Response to light intensity 64

3.1.4 Concentration Study 64

3.1.5 Film Thickness 67
3.1.6 Salt Concentration 68
3.1.7 Other Electron Donors 72

3.2 Benzyl Viologen 74
3.2.1 Spectral Properties 74
3.2.2 Response and Recovery 75
3.2.3 An Erythemal sensor 77

3.3 Conclusions 81

3.4 References 82

4 A tetrazolium based UV dosimeter 85

4.1 Neotetrazolium Chloride 86
4.1.1 Comparison with TTC 90
4.1.2 Oxygen Sensitivity 91

4.2 Response to UV light 93
4.2.1 Dye Concentration and Film Thickness 95

4.3 An erythemal sensor 97

4.4 Conclusions 98

4.5 References 99

5 A Solvatochromic Sensor for VOCs 100

5.1 Solvatochromism 100
5.1.1 The Franck-Condon Principle 100
5.1.2 Negative and positive solvatochromism 101
5.1.3 Applications of Solvatochromism 103

5.2 Reichardt's Dye 105
5.2.1 Reichardts dye-based Sensors 106

5.3 Riechardt's dye in Ethyl Cellulose (RD/EC) 107
5.3.1 RD/EC films for quantitative analysis. 110
5.3.2 Response and recovery characteristics of a RD/EC film 114

5.4 Reichardt's dye on fumed silica films (RD/SiO_2) 115
5.4.1 RD/SiO_2 films for qualitative analysis 116
5.4.2 Quantitative analysis 118
5.4.3 Response and recovery characteristics of a RD/SiO_2 film 120
5.4.4 RD/SiO_2 films and $E_T(30)$ values for alcohol vapours 123
5.4.5 RD/SiO_2 films and humidity detection 124

5.5 Conclusions 126

5.6 References 127

6 Optical Sensing Systems for Photocatalysis 129

6.1 Photocatalysis 129

6.2 Existing Methods of Analysis 130
6.2.1 The stearic acid (SA) test 130
6.2.2 The methylene blue (MB) test 134
6.3 Newly Developed Method of Analysis 140
6.3.1 The resazurin (Rz) ink test 140
6.4 Conclusions 145
6.5 References 146
7 Summary ***149***
7.1 Viologen Dosimeter 149
7.2 Tetrazolium Dosimeter 150
7.3 Solvatochromic VOC sensor 150
7.4 Sensor systems for Photocatalysis 151
7.5 Further Work 152

1 Introduction

1.1 Optical Sensors

Optical methods have been an active part of the analytical sciences for many years now. Colorimetry, photometry, spot tests, and various spectroscopic methods dealing with the visible region have all been used to qualitatively determine chemical and biochemical species. In recent times these techniques have expanded into the area of optical sensors.

According to Wolfbeis[1] the initial history of optical sensors can be traced through pH indicator strips, the O_2 sensor developed in the 1930s by Kautsky and Hirsch for monitoring photosynthesis[2], Bergman's O_2 sensor[3], and the CO_2 sensor developed by Lübbers and Opitz[4, 5]. The latter are even credited with creating two words to describe their device: optode (from the greek "οπτικοσ οδοσ" meaning optical way or path) or optrode (from optical electrode). Other than the pH strips all of these systems are based around the change in fluorescence of a species upon exposure to the relevant analyte. In truth all of these systems rely on the same methodology: the chosen analyte causes a change in the optical properties of the system which can be distinguished by sight, as in the pH strips, or via use of a spectroscopic device such as a fluorimeter. This method has now been used to create optical sensors for many analytes and physical conditions. In fact the method described is now commonly used as one of the 3 'generations' of fiber optic sensors:

1st Generation – Direct spectroscopic analysis of the optical properties of an analyte.

2nd Generation – An indicator system, when exposed to the analyte, undergoes a specific change in its optical properties. Monitoring of this property allows indirect analysis of the chosen analyte.

3rd Generation – In this instance an analyte must be chemically altered before any indicator species will fully react in its presence. Commonly a biocatalytic process may be used to transform the analyte, which is then exposed to a 2nd generation sensor.

The examples of early sensors listed above would be classed as 2nd generation sensors.

1.1.1 Advantages of Optical Sensors

As the field of optical sensing expands it continues to cover areas of detection which already have traditional sensing methods associated with them e.g. fluorescent indicators for O_2 in place of the Clark electrode. This may lead to questioning of the value of developing sensors where others already exist. However many traditional sensors are electrical systems and optical sensors have a few advantages over these. For example:

- Optical sensors do not require a reference signal for operation.
- They can be easily miniaturised to form very small, light and robust sensors. Many electrical systems are bulky and heavy by comparison.
- The use of fiber optics allows remote sensing over hundreds of meters, as well as having the ability to transmit greater levels of data over those distances than electric cable.
- Optical sensors are not prone to electric interference.
- Many can be used for non-destructive, real time analysis.
- Most optical sensors are very simple systems. This allows cheap manufacture and purchase of the devices in comparison to electrical goods.

This list demonstrates just some of the general advantages of most, if not all, optical systems. While it would be untoward to suggest that these systems do not have their disadvantages – light interference in fiber optics, stability of indicator phases, questions on equilibria formation and low dynamic ranges etc. – the listed advantages can often make a compelling argument for the use of optical systems over their electronic counterparts.

The intention of this thesis is to describe the development and characterisation of several new and different optical sensor systems.

1.2 Ultraviolet light

1.2.1 Ultraviolet wavelengths

The conclusion drawn after Ritter discovered UV light in 1801 was that light consisted of three parts; an oxidising component (infrared), an illuminating component (visible) and a reducing component (ultraviolet). Of course it is now understood that these 'separate' components are all part of the electromagnetic spectrum. We now also know that ultraviolet light (UV) can be further divided into separate wavelength regions, much like visible light can be split into a spectrum of colours. These different regions, although slightly arbitrary, are classified as follows[6]:

Table 1-1 – Wavelengths and names of the regions of ultraviolet (UV) light

Wavelength (nm)	Classification of light
1 – 30	Extreme UV
10 - 200	Far *or* Vacuum UV
200 - 290	UVC*
290 - 320	UVB*
320 - 400	UVA*†

*** These regions are generally classified as *near UV***

† Some groups have taken to further dividing this region into UVA1 and UVA2[6, 7]

1.2.2 Ultraviolet sources

A significant source of these wavelengths of UV is the sun. On an average sunny day in Melbourne an individual could be exposed to 5.9 mW cm^{-2} and 0.38 mW cm^{-2} of UVA and UVB respectively[6]. Terrestrial levels of the shorter wavelengths are negligible as these are blocked by our atmosphere. Even on a cloudy day we are constantly being exposed to UV. Not only that, but many tools of modern living are also sources of UV. Common fluorescent bulbs emit small levels of UVA ($\leq$ 4.8 $\mu W\ cm^{-2}$) and UVB ($\leq$ 9.3 nW cm^{-2})[8], black-light blue (BLB) bulbs are UVA lamps which are regularly used to check for fluorescent markings on banknotes, UVA and UVB fluorescent tubes are used in the tanning industry[9], and UVC lamps are even used for disinfection and sterilisation. Other devices such as welding arcs, plasma torches and some lasers are also sources of UV[10]. As such it is almost impossible for anyone to go through a typical day without being exposed to UV. Over the years a great amount of work has gone into understanding the effect of UV on human health.

1.2.3 Health effects of UV exposure

1.2.3.1 **Beneficial Effect**s

The best known beneficial effect of UV is the formation of vitamin D3, which is required for the intestinal absorption of calcium[11, 12]. UVB exposure causes provitamin D3 to be isomerized to pre-vitamin D3, which then spontaneously isomerizes to vitamin D3. After prolonged whole body exposure to UV light the circulating vitamin D levels in the blood increase by an order of magnitude (2 ng ml^{-1} to 24 ng ml^{-1} within 24 hours) and return to normal levels within a week[13].

UV radiation has also been used as a therapeutic agent for various skin diseases. It is reported that the topical application of natural psoralen followed by exposure to sunlight was used as a remedy for vitiligo by the ancient Egyptians. More modern studies reveal that oral administration of psoralens and irradiation with UVA is a highly effective treatment of psoriasis, as well as showing promise in the treatment of mycosis,

fungoides, and atopic dermatitis[14]. However, it has been pointed out that these therapies are "associated with acute and chronic side effects on human skin, which cannot be separated from the beneficial effects of UV irradiation"[14].

1.2.3.2 Irradiation of the Skin

UV is now well recognised as a potential health hazard, significantly with regards to its effect on human skin. The two most obvious and best known effects are *erythema* and tanning of the skin[14, 15]. The former is the familiar reddening of the skin that is more commonly known as sunburn, the latter is the equally familiar darkening of the skin caused by melanin production[15-17]. These effects usually occur over a number of days. There are other effects on the skin, however, that are not as obvious as these. The outermost layers of the skin will thicken over time to attenuate UV penetration to the deeper layers[16, 18]. Chronic over exposure to UV can also cause degenerative changes in the cells, fibrous tissue and blood vessels of the skin. These include freckles, nevi (moles), lentigines (liver spots) and diffuse brown pigmentation. UV radiation also accelerates skin ageing and can lead to a loss of skin elasticity[14-19].

Exposure to high levels of UV radiation has also been linked to the formation of non-melanoma skin cancers (NMSC) and malignant melanomas (MM). NMSC comprise basal cell carcinoma (BSC) and squamous cell carcinoma (SCC)[7, 17, 18, 20-22]. These conditions are rarely lethal but the surgical techniques used to treat them can be painful and disfiguring. The lack of reliable registration of NMSC makes it difficult to determine any trends in incidence with time. However, specific studies relating to personal exposure to UV have been carried out and the NMSC are most frequent on parts of the body that are commonly exposed to the sun[13]. The implication of this is that long term exposure to the sun contributes to the formation of NMSC.

Malignant Melanoma (MM) is the major cause of death from skin cancer. World Health Organization (WHO) statistics show that 132,000 melanoma skin cancers occur each year. Studies have shown that the risk of malignant melanoma is tied to a person's genetic characteristics as well as UV exposure behaviour. MM is shown to be more

common among people with a fair complexion as they have less protection against UV. This is demonstrated as increasing occurrence of MM in fair populations with decreasing latitude (higher UV levels), and there is a great amount of support showing an association between MM and a history of sunburn, especially sunburn at an early age.

1.2.3.3 Irradiation of the Eyes

Acute effects of UV exposure on the eyes include photokeratitis and photoconjunctivitis[13, 23]. Both of these effects, which are comparable to sunburn of the tissues of the eyeballs and eyelids, can be very painful but are reversible and neither has been shown to cause any long term damage to the eye. There are chronic effects of exposure to UV however, such as a contribution to the formation of cataracts within the eye. Cataracts are caused by the unravelling and tangling of proteins within the lens of the eye, causing a gradual clouding of the lens and, in some cases, eventual blindness. Current WHO estimates suggest that up to 20% of the 12 to 15 million cases of blindness caused by cataracts are due to overexposure to UV[13].

1.2.3.4 Effect on the Immune System

UV doesn't just affect the surface of our bodies. It has also been shown to alter the behaviour of our immune system. Experiments on animals, for example, have shown that UV radiation can modify the course and severity of skin tumours[17], people treated with immunosuppressive drugs have shown a greater incidence of SCC than the normal population, and exposure to environmental UV has been shown to alter the activity and distribution of cells responsible for triggering immune responses in humans[14, 24]. It can be assumed that, as well as causing skin cancers, exposure to solar UV may reduce the body's defences that limit the formation of skin tumours, as well as enhancing the risk of infection with viral, bacterial and parasitic infections. It may be that alteration to the immune response by high UV levels may decrease the efficacy of vaccines which could

have major consequences for public health, especially in the developing world, but much more work will be required to substantiate this.

The adverse health effects caused by exposure to UV light have seen an alarming increase in the last half century, especially instances of skin cancer. In 2003 over 1 million Americans were diagnosed as having skin cancer[20] and in 2004 it was predicted that 1 in 5 Americans would suffer some form of skin cancer, regardless of location[21]. In the mid-1990s it was calculated that the world had seen an 82 % increase in BCC and a 76 % increase in SCC *per decade* since the early 1960s. The calculated increase due to ozone depletion for this time had been 11.6 % for BCC and 21.6 % for SCC, thus something else has caused the rapid increase in NMSC[18]. This is most likely attributable to the cultural changes in the last century which Rona MacKie states have *"…resulted in complex psychological reactions to natural skin colour, such that pale-skinned Caucasians regard some degree of tan as cosmetically desirable, while dark-skinned Africans use destructive and expensive bleaching techniques to lighten their skin"*[25]. Professor MacKie's article also notes that the increase in cheap air travel in recent decades has allowed members of fair-skinned populations to accumulate many more hours of UV exposure than was the case at any point in recent history.

It is apparent then that exposure to UV is an increasingly significant health issue. As such there are an increasing number of studies aimed at finding the best methods of decreasing sun exposure, whether those methods are directly preventative, such as the use of sunscreens etc., or educational, such as programs to alter the behavioural patterns of Caucasian populations. It is imperative then that we have reliable techniques and devices for the immediate and quantitative detection of UV light. Accurate detection of UV light will not only benefit the collection of data for any study of UV effects on human health, but it may also help to provide more immediate protection against overexposure in the form of (personal dosimetry).

1.3 UV Detection

1.3.1 The UV Index[13, 23]

One system currently adopted for characterising ultraviolet radiation levels on the earth is the Global Solar UV Index (UVI). The UVI is a unitless scale ranging from 0 to 10+, with higher values indicating greater potential for harm to the skin over a shorter period of time. A summary of the exposure categories is shown in the table 1-2.

Table 1-2 – The UVI exposure categories as defined by the WHO

Exposure category	UVI Range
Low	**<2**
Moderate	**3 to 5**
High	**6 to 7**
Very high	**8 to 10**
Extreme	**11+**

The UVI values, when reported, should be used as a guide for the level of protection required for an individual. Recommended levels of protection are shown in table 1-3.

Table 1-3 – Recommended levels of protection of differing levels of UVI

UVI	Protection
1 – 2	No extra protection required.
3 – 7	Seek shade at midday. Use sunscreen. Wearing a shirt and hat recommended.
9 – 11	Avoid midday sun. Shirt, hat and sunscreen a must. Seek shade

The Global Solar UVI values are calculated using the International Commission on Illumination (CIE) reference action spectrum for UV-induced erythema on human skin. This is defined by the following equation[13]:

$$I_{UV} = k_{er} \cdot \int_{290nm}^{400nm} E_{\lambda} \cdot S_{er}(\lambda) d\lambda \tag{1.1}$$

Where E_λ = solar spectral irradiance in W m^{-2} nm^{-1}, $d\lambda$ = wavelength interval in the summation, $S_{er}(\lambda)$ = erythemal reference action spectrum, k_{er} = constant of 40 m^2 W^{-1}. From this equation UVI 1 = 25 mW m^{-2}.

This requires the measurement of the spectral irradiance of the sun at all wavelengths of light from 290 to 400 nm (figure 1-1). The values obtained are then multiplied by a weighting factor defined by the following equations:

$$\lambda_{290-298} = 1 \tag{1.2}$$

$$\lambda_{299-328} = 10^{0.094 \cdot (298-\lambda)} \tag{1.3}$$

$$\lambda_{329-400} = 10^{0.015 \cdot (139-\lambda)} \tag{1.4}$$

These equations define McKinlay and Diffey's erythemal action spectrum[26] (figure 1-2), which shows how effective each wavelength of light is at causing erythema of the skin. Once the action spectrum has been applied to the measured irradiances a plot is obtained which shows the erythemal irradiance of the sun (figure 1-3). The UVI is the sum of the irradiances of all wavelengths in this erythemal plot, multiplied by the constant k_{er}.

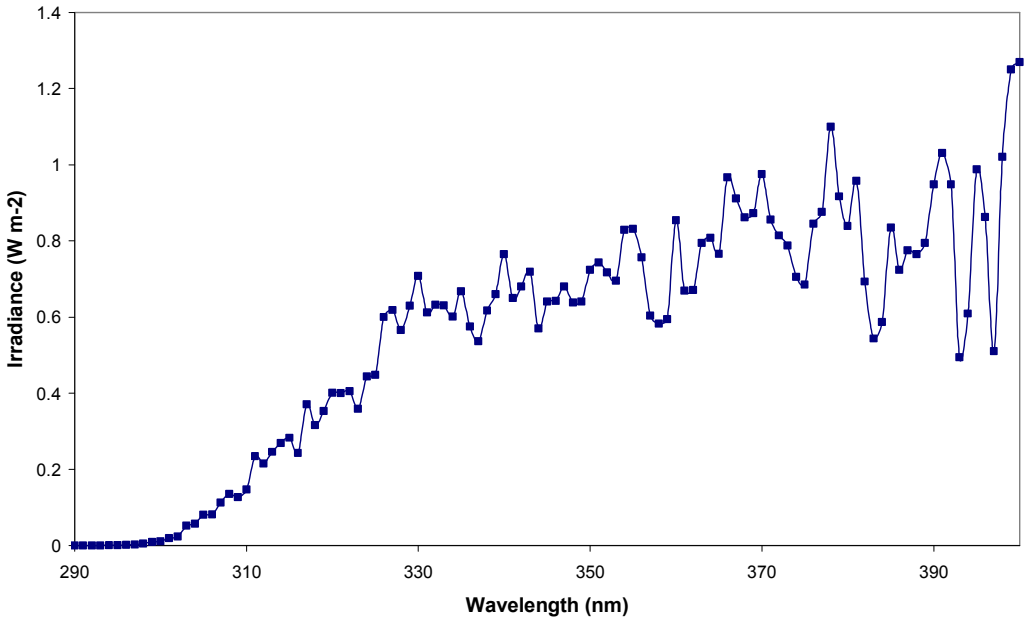

Figure 1-1 – A typical solar spectrum. This spectrum was recorded at noon on the 17th of January 1990 in Melbourne, Australia. Adapted from work published by Diffey[6].

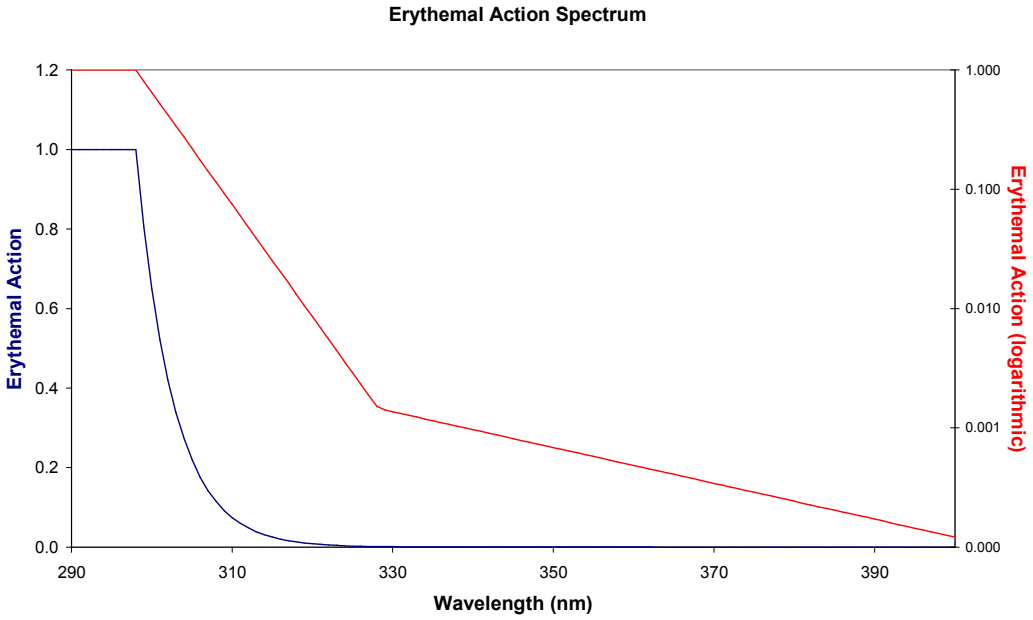

Figure 1-2 – McKinlay and Diffey's erythemal action spectrum on standard and logarithmic scales.

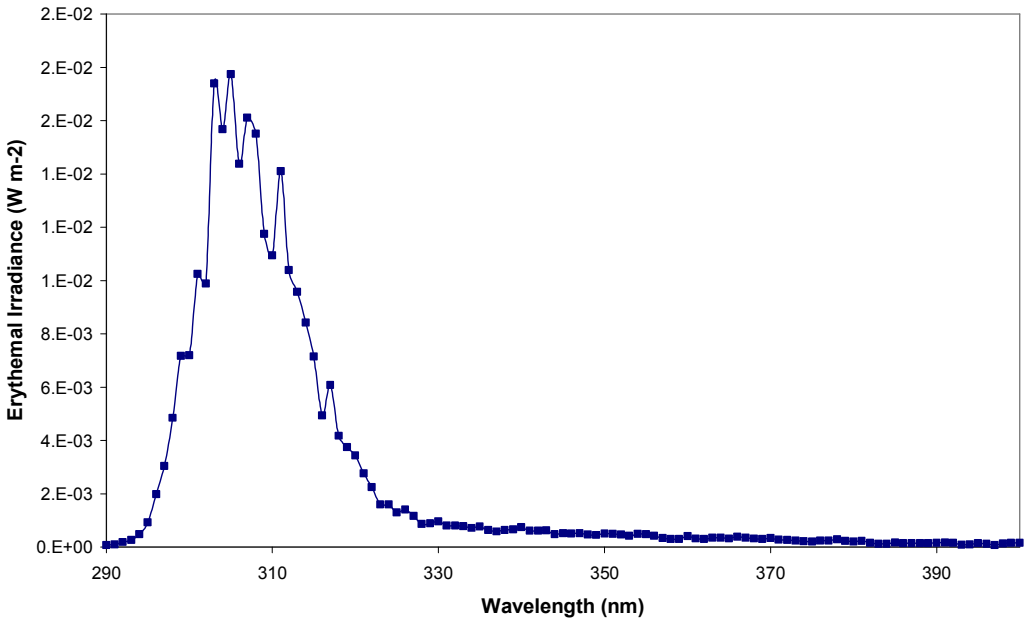

Figure 1-3 – A plot showing the erythemal effectiveness of the solar UV shown in figure 1. This equates to a UVI = 11.1

Figure 1-3 shows that it is the shorter wavelength, higher energy UVB radiation present in solar light which is the greatest contributor to erythema in human skin.

1.3.2 The Minimum Erythemal Dose

The erythemal dose describes the amount of erythemal radiation that has been cumulatively absorbed by the skin. The minimum erythemal dose (MED) is the minimum amount of radiation which is required to cause erythema, or reddening, of the skin[15, 27-29]. The MED for a particular individual depends largely on their skin type, as defined by Fitzpatrick[30]. These skin types can be described as shown in table 1-4. The MED for each is shown in table 1-5.

Table 1-4 – Classification of the Fitzpatrick skin types.

Skin type classification		Burns in the sun	Tans in the sun
I	Melano Compromised	Always	Seldom
II		Usually	Sometimes
III	Melano Competent	Sometimes	Usually
IV		Seldom	Always
V	Melano Protected	Naturally Brown Skin	
VI		Naturally Black Skin	

Table 1-5 – MED values for the Fitzpatrick skin types. The values shown are the minimum for each skin type, given in both Joules and milli-Watts.

Skin type classification		MED (J m^{-2} h^{-1})	MED (mW m^{-2})
I	Melano Compromised	200	55.6
II		250	69.4
III	Melano Competent	300	83.3
IV		450	125.0
V	Melano Protected	600	166.7
VI		1000	277.8

The MED values presented here can be used to calculate the amount of time which can be spent in the sun before erythema occurs i.e. the time to burn – TTB (units: h). Thus the calculation for exposure time in hours is simply:

$$TTB/h = \frac{MED\,(\text{in J m}^{-2}\ \text{h}^{-1})}{3.6 \times 25 \times UVI} \tag{1.5}$$

Or

$$TTB/h = \frac{MED\,(\text{in mW m}^{-2})}{25 \times UVI} \tag{1.6}$$

For example with skin type II we know MED = 69.4 W m^{-2}. Thus:

$$TTB = \frac{69.4}{25 \cdot UVI} = \frac{2.78}{UVI} \tag{1.7}$$

So at UVI 5 an individual with skin type II could expose themselves to 0.556 hours or 33.4 minutes of sunlight before their skin reached an erythemal condition. The same method can be applied to all skin types, allowing the development of the following table showing TTB for each UVI.

Table 1-6 – A table showing the TTB in minutes

UVI	Skin Types					
	I	**II**	**III**	**IV**	**V**	**VI**
1	133	167	200	300	400	667
2	67	83	100	150	200	333
3	44	56	67	100	133	222
4	33	42	50	75	100	167
5	27	33	40	60	80	133
6	22	28	33	50	67	111
7	19	24	29	43	57	95
8	17	21	25	38	50	83
9	15	19	22	33	44	74
10	13	17	20	30	40	67

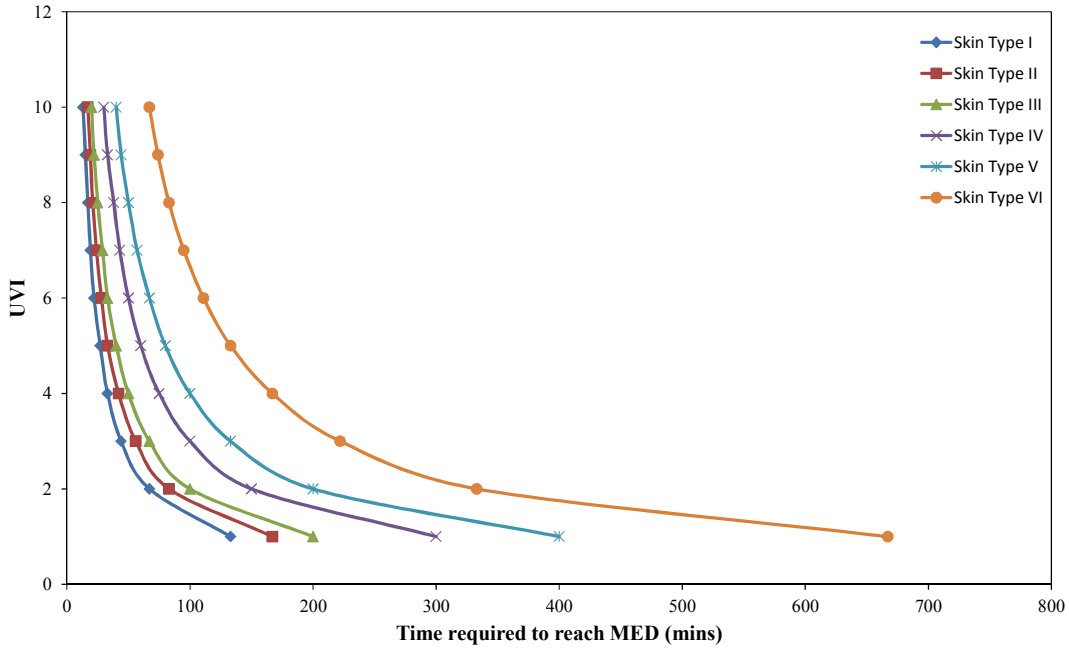

Figure 1-4 – A plot showing the exposure time required to reach MED as a function of UVI. Curves are shown for skin types I, II, III, IV, V, and VI.

NB: It is important to note that these times do not indicate the maximum amount of time that can safely be spent in the sun. The WHO is insistent that there is no such thing as a safe length of exposure to UV light, and as such asks those bodies which report the UVI not to report time to burn.

1.3.3 Electronic Detection

At the present time there are several devices available on the market which can be used to monitor personal levels of UV exposure, most of which are electronic in nature. Examples of these include the SafeSun Precision UV Meter produced by Optix Tech Inc, and IdeenWelt's UV Messgerät (UV instrument) – see figure 1-5.

Figure 1-5 – Two example electronic devices for monitoring the levels of solar UV. On the left is the Optix Safe Sun Precision UV Meter, and the right hand instrument is the UV Messgerät of Ideen Welt.

The Optix meter gives a real time measurement of the solar UV Index by applying the erythemal action spectrum to measured intensities of UV light. It also continually calculates the total absorbed dose of erythemal radiation (shown in units of MED) while the sensor is exposed to UV light. This calculation of the absorbed dose can be altered by programming in the user's skin type and the sun protection factor (SPF) of any

protective cream they may be wearing. Not only do these factors affect the calculation of absorbed dose but they also allow the device to calculate a recommended time for 'safe' exposure to sunlight. The UV Messgerät is a much simpler device, which works on a similar principle (photocell) as that of the Optix system. IdeenWelt's device does not calculate the UVI in real time, nor does it show the absorbed dose of radiation. Instead of real time analysis this device calculates the UVI as long as the user holds in a set button on the device. Once that button is released the last recorded UVI will be displayed on the front of the device and it is this value which is used to calculate recommended exposure times depending on skin type and SPF. This seems to be the method favoured by some other devices but, while it may work well under consistently clear conditions, the UVI can change quickly depending on weather conditions and time of day, making such, one-shot, predictive calculations unreliable.

Although these devices work well as UV meters they suffer from the same problems as many pieces of electrical equipment: they are expensive to buy individually (the SafeSun retailed for approx. £100 when purchased, while IdeenWelt's device retails for approx. £10), require lithium batteries to operate, require programming & calibration for each individual use, and are open to damage from careless handling and exposure to extreme environmental factors, such as immersion in water (a potential problem when considering use at the beach). The devices are also inconvenient to carry around unless placed in a bag or pocket, not ideal for continual assessment, or worn with a strap on the wrist or around the neck.

1.3.4 Other Commercial UV Sensors

There are of course methods of monitoring UV other than electronic devices. Many of these depend on a chemical reaction with exposure to UV which results in a change in an identifiable trait within the system that can be monitored and quantitatively related to the level of UV exposure. Thus, if the level of response is known it should be a simple matter to determine the level of exposure i.e. the received dose. For many of these systems, the light-induced chemical change is irreversible and so can be used to create a

UV dosimeter, rather than a UV index indicator. In this overview, most focus will be placed on chemical reaction based UV dosimeters.

An early example of this type of indicator is the polysulphone badge developed by Davis and Diffey[31-34]. Polysulphone has an absorption spectrum which approximates to the erythemal action spectrum and thus the erythemal response of human skin. When irradiated the polysulphone will begin to degrade, causing a noticeable change in the absorbance characteristics of the film. This is shown in figure 1-6. The standard set by Diffey et al. is to measure the absorbance of a 40 μm thick polysulphone film at 330 nm as a function of radiant exposure to UV in J m^{-2}, an example of which is shown in figure 1-7.

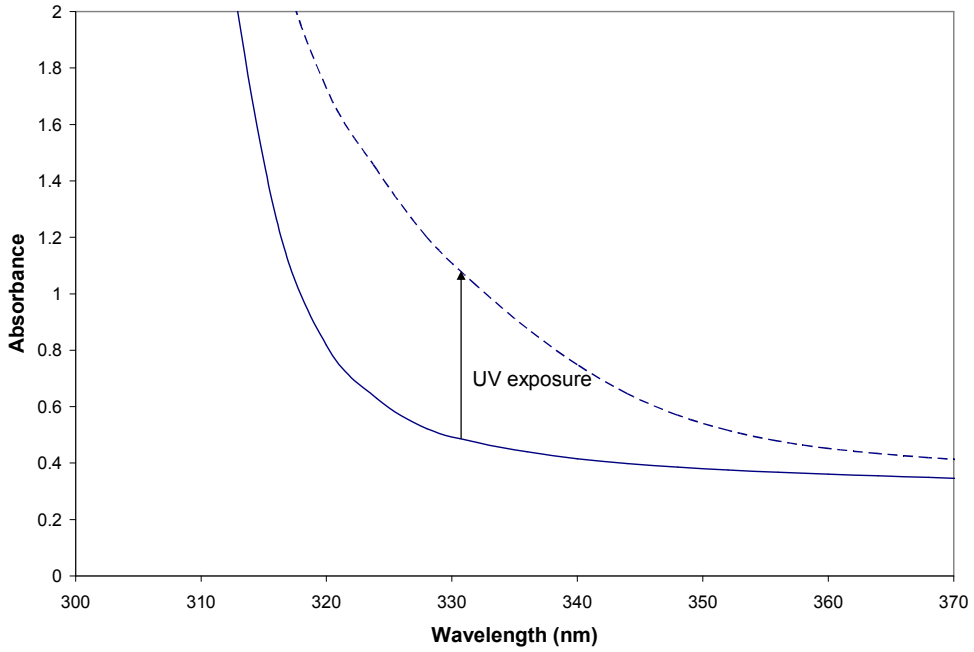

Figure 1-6 – The UV absorption spectrum of a polysulphone film before (---------) and after (- - - -) irradiation with UV light.

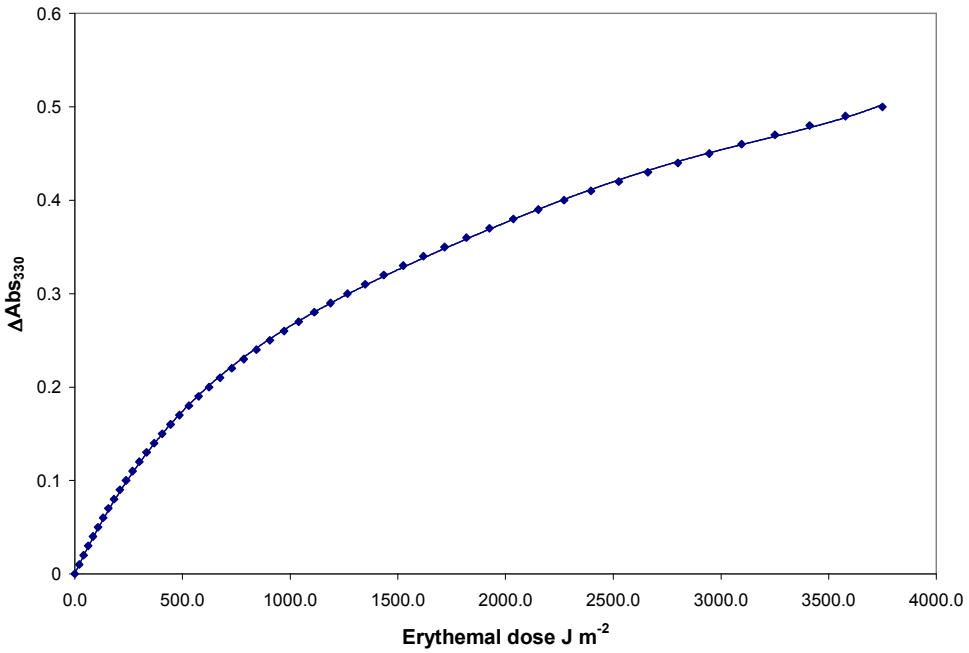

Figure 1-7 – The change in absorbance at 330 nm of a 40 mm polysulphone badge plotted as a function of erythemally effective dose as a result of sunlight exposure.

Exposure to sunlight leads to a consistent change in absorbance at 330 nm of approximately 0.13 at 1 MED (skin type II). This standard response makes the polysulphone an effective dosimeter and indeed it has been used in some industrial settings to test the UV exposure of workers under high intensity lamps etc. However the problem with this film is that it requires a spectrometer for analysis of the results and, as such, is not very effective as a personal dosimeter for real time analysis.

More useful than this to the average person are the wristbands developed by Solar Safe and Kids Label, which change colour upon exposure to UV and are supposed to act as indicators of when to apply sunscreen or get out of the sun. The Kids Label band is an indicator in the true sense of the word and only changes colour if the current intensity of sunlight is high, but shows no gradual change with time and as such does not let the user know how much UV they have been exposed to (figure 8) i.e. it is a rough UV index indicator but not a UV dosimeter. This sort of indicator is most suitable for, and is indeed aimed at, very small children who require a great deal of protection from the sun.

Figure 1-8 – The Kids Label wristband provided to holiday makers by Thomson. These images show the band before and after exposure to UV light. The phrase "cover me up" turns blue upon exposure to high intensity UV.

The Solar Safe band on the other hand is a UV dosimeter, gradually changing colour with increasing exposure to solar UV. The band changes colour from orange to purple upon initial exposure to UV and is then supposed to change to a brown colour, marking the need to put on more sunscreen, and finally to a flesh colour, indicating that you should now get out of the sun. This scheme is shown in figure 1-9.

Figure 1-9 – The proposed colour changing scheme of the Solar Safe wristband. The stages are, from top to bottom, pre-exposure to UV, initial exposure to UV, time to re-apply sun screen, and time to get out of the sun.

This wristband is approved of by the skin and cancer foundation of Australia and has received praise from several medical professionals as a good method for limiting the risk of skin cancer, due in part to the claim that the band will change colour and tell the user to get out of the sun before they have reached their MED. Not only that, but the manufacturer has been careful to instruct users to always wear sunscreen when using the band. However the manufacturers also admit in their own literature[35] that the band is calibrated for use with SPF 15 sunscreen. This raises questions around whether the band is useful in other situations. If an individual decides to use a different sunscreen such as SPF 8 (for those that want to tan) or SPF 30 (for extra protection) then it is unclear whether the band will be any use in giving an appropriate warning of impending erythemal harm. Bands exposed to UVI 5 solar light over 3 hours yield the images shown in figure 1-11.

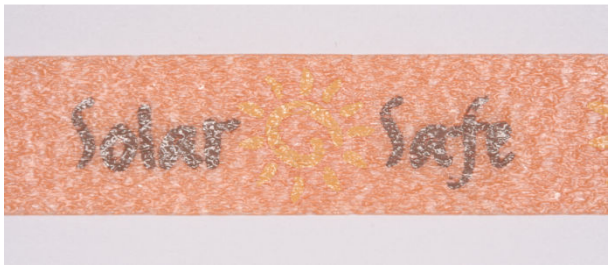

Figure 1-10 – A picture of the solar safe wristband before irradiation with UV light.

Figure 1-11 – Pictures of the centre of the SolarSafe wristband after irradiation with UVI 5 solar light. The pictures show, in order, the wristband after it has received 0, 1, 2, 3, 4, 5, 6 and 7 MED equivalents for skin type II.

It is understood that using these bands without any form of sun protection is against the manufacturer's guidelines and any medical advice but it must be assumed that a small percentage of customers may risk wearing the band without protection. From figure 1-11 it can be seen that the SolarSafe band has not undergone the colour change by the time it has been exposed to 1 MED, suggesting that the bands may not give correct warning unless using specific levels of protection. This is also complicated by the fact that many people do not apply sunscreen as directed on bottles, nor do they apply the exact amounts specified by many manufacturers. For a dosimeter to be truly effective at warning the user it must function under all conditions, ensuring that users in all extremes can be afforded its protection.

1.3.5 Other UV Dosimeters

As well as the commercially available materials, there are also many dosimeters which can be found in the literature. Some of these are shown in table 1-7. We can see from this table that UV dosimeters cover a range of materials and methods of analysis, from the growth and synthesis of biological species and chemicals to the optical and electronic properties of materials. A good comparison of the different types of UV dosimeter can be found in a review by Webb. [49] Each of the dosimeters listed are capable of giving accurate estimations of the level of UV-B exposure. However, as pointed out by Webb[49], there are some flaws associated with each method.

Table 1-7 – A list of some of the UV and solar UV dosimeters discussed in the literature.

Ref.	Author	Type of Dosimeter
[36]	Tzu-chien	Biological, using *B. subtilis* spores
[37]	Douglas Kerns	Electronic, using monolithic Si
[38]	Irene Horkay	Chemical, colorimetric, silver-mercury oxalate
[39]	Saad El Nagaar	Electronic
[40]	F. Abu-Jarad	Nuclear Track Detector
[41]	Ronal Rahn	Chemical, colorimetric, using iodouracil
[42]	J. Ramirez-Nino	Electronic, Optical
[43]	J. Garcia-Guinea	Chemical, thermoluminescence, using high-albite
[44]	Yasuhito Ishigaki	Biological, using stained DNA
[45]	Irina Terenetskaya	Chemical, colorimetric using vitamin D
[46]	J. Sandby-Møller	Biological, skin autofluorescence
[47]	Andrew Mills	Chemical, colorimetric, using methylene blue
[48]	A.A. Abdel-Fattah	Chemical, colorimetric, using Thymol-blue

For example the biological systems proposed by Ishigaki[44], Tzu-chien[36] and Sandby-Møller[46] require further treatment and/or analysis in the laboratory before any conclusions can be drawn. This means that there is no real-time analysis of exposure and, especially in Sandby-Møller's skin autofluorescence experiments, determination of health effects can only occur after the damage is done. With the electronic systems some specialist knowledge of their operation or interpretation may be required before any useful analysis can occur. The electrical dosimeters may also suffer from other problems: electrical interference, need for calibration or the problem of faults with power etc. associated with any electrical device are a few examples of such. Electrical devices can also be quite expensive. These issues are avoided by the dosimeters proposed by Horkay[38], Rahn[41], Abdel-Fattah[48], and Mills[47]. Each of their dosimeters are based on a colour change reaction in direct response to UV light. Some argument might be made that, for quantitative analysis, use

of a spectrometer or other device is required to measure the optical properties of these dosimeters. However, unlike the biological dosimeters, the colour change allows a visual estimation of the level of exposure. This can afford real time analysis without the problems associated with electronic devices.

Each of these colorimetric sensors can give accurate and reproducible measures of the UV exposure, showing varying levels of response depending on the intensity of the incident light. Both Mills and Abdel-Fattah also report that their systems may be adjusted to act as dosimeters for the UVA, UVB and/or UVC regions of the spectrum, thus making it possible that they may be useful as solar UVB sensors. Only Horkay and Rahn specifically target their dosimeters around solar UVB, although at the current time neither of these sensors has been shown to be ideal. A brief summary of each of these systems follows.

Abdel-Fattah's film[48] comprises an acid sensitive dye (thymol blue) and an acid releasing agent (chloral hydrate) embedded in a polymer film (polyvinyl butyral). Upon exposure to UV the chloral hydrate releases hydrochloric acid which protonates the (yellow) thymol blue, forming the (red) conjugated sulfonic acid. This reaction is shown in figure 1-12.

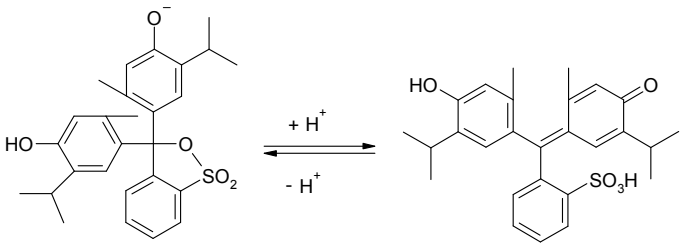

Figure 1-12 – The acid induced transformation of Thymol blue from its yellow basic form to a red acidic form.

In their work Abdel-Fattah and his team demonstrated that the rate of reaction varied with irradiation wavelength (increasing with decreasing wavelength) and with the concentration of the chloral hydrate. This makes it possible, with proper preparation, to develop a sensor for UVA, UVB and/or UVC light.

The film developed by Mills et al.[47] consists of nanocrystalline titania dispersed in a film of hydroxyl ethyl cellulose containing a mild reducing agent, triethanolamine, and a redox indicator, methylene blue. Upon irradiation with UV light the methylene blue is photocatalytically reduced to colourless leuco-methylene blue. This system makes a very good UV sensor although the leuco-methylene blue reoxidises in air. The application of a layer of Sellotape™, which acts as an oxygen barrier, prevents this from happening and allows the system to act as a dosimeter. It was demonstrated that the level of colour change is dependent on the concentration of titania and the intensity of the incident light, making the system an effective UV indicator. Mills also suggests that, as the technology is quite generic, it should be possible to develop sensors and dosimeters for specific wavelengths of light (UVA, UVB and UVC) by altering the semiconductor used.

The SUNTEST dosimeter proposed by Horkay[38] and her group is based on the colour change of a silver-mercury(I)-oxalate suspension. This suspension is embedded in gelatine and then mounted on a paper strip. Increasing UV exposure changes the colour of the sample as so: white → yellow → brownish → dark brown. This is due to the reaction sequence shown below (where ox = oxalate)

$$2Hg_2(ox) \longrightarrow 3Hg + ox^- + 2CO_2 + Hg^{2+} \quad (1.8)$$

$$Hg + Ag^+ \longrightarrow Hg^+ + Ag \quad (1.9)$$

As with the other sensors the degree of colour change is dependent on the level of incident radiation. Having correlated the colour change with the MED of various skin types, it is the group's recommendation that this sensor is exposed to the sun for 5 minutes and checked against a colour reference card to give some idea of the maximum allowed sunbathing time. It is also stated that SUNTEST takes into account the "variables influencing the length of sunbathing" such as type of skin, latitude, season, time of day etc. However, there is no guarantee that the level of exposure during a 5 minute test will remain constant during any sunbathing period. The UVI can rise

steadily during a recommended half hour, for example, increasing the level of UV exposure and therefore decreasing the time that the individual should be spending in the sun.

Ronald Rahn's sensor on the other hand is based around a solution of iodouracil (IU) and potassium iodide in a borate buffer which turns blue upon exposure to UVB[41] (response is reduced by 98.5% when a UVB filter is in front of the light source).

$$IU + h\nu \longrightarrow U^{\bullet} + I^{\bullet} \tag{1.10}$$

$$2I^{\bullet} + I^{-} \longrightarrow I_3^{-} \tag{1.11}$$

While Rahn and his team have shown a varying response in relation to the UVB intensity there has been no further work in moving away from the solution phase, or indeed relating the response to doses which will cause erythema in the skin. The measurements made are over a period of several hours and relate more directly to measuring large doses of radiation, such as those received at the earth's surface over the period of a day. However it is suggested that this solution could be developed into a personal dosimeter.

While none of these systems can be said to develop colour changes directly related to erythemal exposure – Horkay's dosimeter is predictive while the others need more formulation work – they have shown that relatively simple chemical systems can be successfully used for the monitoring of UV light.

As a consequence part of this work is to develop a colorimetric dosimeter which undergoes a quantifiable and reproducible colour change upon exposure to erythemal levels of UV. This colour change should be easy to distinguish with the naked eye.

1.4 Detection Of Volatile Organic Compounds

The abbreviation VOC is commonly used in the literature to describe volatile organic carbons or volatile organic compounds. The exact definition of the term depends on which piece of literature or legislation is referred to. For the purpose of this work the definition put forward by the World Health Organisation will be followed: a VOC is any carbon compound which exhibits a vapour under standard temperature and pressure and has a boiling point with a lower limit of 50^{o}C and an upper limit of 260^{o}C.

1.4.1 Sources of VOCs

Human beings are routinely exposed to VOCs. Sources for these compounds range from the apparently innocuous, such as household materials[50-52], to the more obviously hazardous like industrial waste[53]. A list of some of the suspected sources of hazardous VOCs is shown in table 1-8.

Table 1-8 – A selection of the sources of environmental VOCs

Sources of VOCs	
Building Materials[50, 52, 54]	Home Printers[55, 56]
Furnishings[50, 51]	Some open fires[57]
Traffic[58]	Aircraft cabins[59]
Paint and other household solvents[60-62]	Landfills[63, 64]
Insecticides and household sprays[61, 65, 66]	Sewage[67]
Ventilation systems[52, 68, 69]	Industrial Waste[53]

1.4.2 Health Effects of VOCs

According to a World Health Organisation report on indoor air quality[70], VOCs can be divided into 3 categories when discussing their effect on health. These categories are (a) odour and sensory effects, (b) mucosal irritation and other morbidity due to system toxicity, and (c) genotoxicity or carcinogenic effects. Much of the work around VOCs has focused on indoor and enclosed exposure as evidence of health effects from open sources such as landfills and incinerators open to atmosphere is regarded as 'inadequate'.

1.4.2.1 Sensory Effects

Sensory effects can be regarded as the 'mildest' effects of VOC exposure. This classification covers a range of effects which includes such things as strong odours / nasal irritation, and irritation of the eyes and skin. The difficulty in assessing sensory effects is that they are very much dependent on an individual's perception and as such are hard to quantify. It has been stated, for example, that irritation of the skin/mucus membranes may account for up to 30% of what an individual regards as 'odour'[71].

One way to quantify this is to look at the derived effects from sensory exposure which may be less subjective. These include the onset of conjunctivitis, sneezing, coughing, hoarseness, dryness of the mucus membranes, skin erythema, and other physiological changes brought about by contact with the VOC.

1.4.2.2 System Toxicity, Genotoxins and Carcinogens

More easily identifiable are the toxic effects of VOCs. These effects include, but are not limited to, haematological, neuro-, hepatic, renal, and mucosal toxicitity. Many of these effects can be caused by known industrial chemicals and solvents: toluene is a neurotoxin[72], dichloromethane produces carboxyhaemoglobin[73], and it is well known that chronic exposure to methanol vapours can severely impair vision[74]. Many solvents, such as dichloroethane and benzene, are also known carcinogens[70]. While most people

encounter these solvents in levels which pose no risk, industrial exposure can lead to chronic effects if not carefully handled.

1.4.3 Sensors for VOCs

Given the many and varied sources of VOCs available it is important that viable methods are found for their detection and measurement. Many of the publications on VOCs referred to above discuss the methods used[55, 75-99], these range from electronic devices based on polymers and carbon nanotubes to colorimetric systems. Many of these are based on standard analytical techniques using expensive and sometimes unique pieces of equipment. For example, in the work of Lee et. al.[55] the detection of VOCs and particulates from everyday photocopiers requires a custom built, stainless steel environment chamber to capture vapours which are then fed into a gas chromatography mass selective detector (GC-MSD). In another paper by Dechow[59] the detection and analysis of VOCs within aircraft cabins requires a series of laser optic particle detectors, pressure transducers and power supplies to be built into the aircraft themselves.

Other methods may not be as highly specialised, but may still be regarded as too expensive or technically complex to be suitable for widespread use. Kanda et. al.[79], for example, developed an electrode based on WO_3 films.

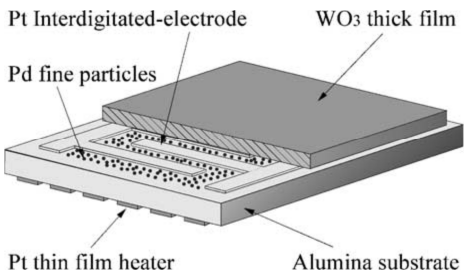

Figure 1-13 – a schematic of the WO_3 sensor as reported by Kanda et. al.

This system heats the WO_3 film to 400°C and uses a potentiostat to measure the change in resistance of the WO_3 when exposed to various VOCs. Kanda's system calls for 32 of these electrodes to allow for measurement of concentrations in the parts per billion

Of particular interest are those systems described as 'vapochromic'[88, 93, 100, 101]. These are sensors which change their optical properties when exposed to different vapours. Daws, for example, studied the spectral properties of $[Pt(arylisocyanide)_4][Pt(CN)_4]$ compounds when exposed to a variety of solvent vapours[101] and found distinct changes in their IR profiles (figure 1-14).

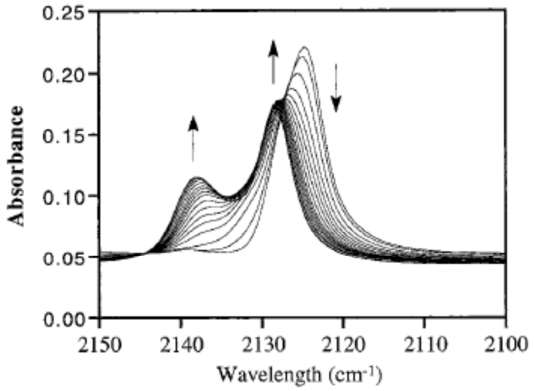

Figure 1-14 – changes in the spectra of $[Pt(CNC_6H_4C_{10}H_{21})_4][Pt(CN)_4]$ as the air around it is saturated with methanol vapour, as reported by Daws et. al.[101]

A team led by Bailey[100] demonstrated the changes in the visible spectrum of the same compound: when exposed to trichloro-methane, the λ_{max} of a film of $[Pt(CNC_6H_4C_{10}H_{21})_4][Pt(CN)_4]$ shifts from 578 to 592 nm. This type of change is of most interest as it raises the possibility of an indicator which could give a visual indication of VOC exposure, and perhaps levels of exposure, without the need for complex electronics.

It is proposed that an indicator will be developed which will provide a quick, clear indication of exposure to VOCs. Preferably this indicator will be small, portable, and also demonstrate a quantitative response.

1.5 Aims

In summary, the initial aims of this project were to develop optical sensors for two chosen analytes: UV light and VOCs. The exact nature of these devices should be as follows:

1. A dosimeter for UV. This device will comprise a viologen or tetrazolium species encapsulated within a solid support. The support should be transparent, or close to transparent, at UV wavelengths of 200 nm and above, ensuring that only the dye species absorbs any UV directed at the system. This dosimeter must display a reproducible response to UV light which varies with the intensity of light. Specifically this system must respond to erythemal levels of radiation and must have undergo an obvious colour change by the time 1 MED of light has been absorbed. For the purposes of this thesis this will amount to 1 MED for skin phototype II.
2. A sensor for VOCs. This will comprise the solvatochromic Reichardt's dye embedded in a solid support. This support must be a porous material to allow the exposure of the dye to various solvent vapours. The support material must be shown to allow a rapid change in colour of the dye upon exposure to these vapours and should be demonstrably faster than existing polymer supports. This sensor should be able to distinguish between different solvent vapours and it should also be possible to quantifiably determine the concentration of the vapour.

Finally, the last chapter provides the results of an indicating technology for revealing the presence and activity of self-cleaning films.

1.6 References

1. Wolfbeis, O. S., *Fiber Optic Chemical Sensors and Biosensors*. CRC Press: 1991; Vol. I.

2. Kautsky, H.; Hirsch, A., *Zeitschrift fur anorganische und allgemeine Chemie* **1935,** *222*, 126.

3. Bergman, I., *Nature* **1968,** *218*, 396.

4. Lubbers, D. W.; Opitz, N., *Zeitschrift fur Naturforschung C* **1975,** *30C*, 532.

5. Opitz, N.; Lubbers, D. W., *European Journal of Physiology* **1975,** (355), R120.

6. Diffey, B. L., *Methods* **2002,** *28*, 4

7. Skov, L.; Hansen, H.; Allen, M.; Villadsen, L.; Norval, M.; Barker, J. N. W. N.; Simon, J.; Baadsgaard, O., *British Journal of Dermatology* **1998,** *138*, 216

8. UVR from fluorescent lamps. http://www.hpa.org.uk/radiation/understand/radiation_topics/ultraviolet/uv_from_lamps.htm (accessed 27th June 2006).

9. Artifical Tanning Sunbeds: risks and guidance. http://www.who.int/uv/publications/en/sunbeds.pdf (accessed 15th November 2006).

10. Dixon, A. J.; Dixon, B. F., *Medical Journal of Australia* **2004,** *181*, 155

11. Grant, W. B.; deGruijl, F. R., *Photochemical and Photobiological Sciences* **2003,** *2*, 1307

12. Lips, P., *Biophysics & Molecular Biology* **2006,** *92*, 4

13. Global Solar UV Index: A Practical Guide. http://www.who.int/uv/publications/en/GlobalUVI.pdf (accessed 25th May 2005).

14. Matsumura, Y.; Ananthaswamy, H. N., *Toxicology and Applied Pharmacology* **2004,** *195*, 298

15. Harrison, G. I.; Young, A. R., *Methods* **2002,** *28*, 14

16. Hennessy, A.; Oh, C.; Rees, J.; Diffey, B.L, *Photodermatology Photoimmunology & Photomedicine* **2005,** *21*, 229

17. Slominski, A.; Pawelek, J., *Clinics in Dermatology* **1998,** *16*, 503

18. Urbach, F., *Journal of Photochemistry and Photobiology B* **1997,** *40*, 3

19. Edstrom, D. W.; Porwit, A.; Ros, A.-M., *Photodermatology Photoimmunology & Photomedicine* **2001,** *17*, 66

20. Glanz, K.; Mayer, J. A., *American Journal of Preventative Medicine* **2005,** *29*, 131

21. Ramirez, C. C.; Federman, D. G.; Kirsner, R. S., *Internation Journal of Dermatology* **2005,** *44*, 95

22. Saraiya, M., *American Journal of Preventative Medicine* **2004,** *27*, 467

23. Intersun, The Global UV Project: A Guide and Compendium. http://www.who.int/uv/publications/en/Intersunguide.pdf (accessed 15th November 2006).

24. Ponsonby, A.-L.; McMichael, A.; Mei, I. v. d., *Toxicology* **2002,** *181 - 182*, 71

25. MacKie, R. M., *Progress in Biophysics and Molecular Biology* **2006,** *92*, 92

26. McKinley, A. F.; Diffey, B. L., *CIE Journal* **1987**, *6,* 17

27. Diffey, B. L.; Farr, P. M., *Journal of Photochemistry and Photobiology B* **1991**, *8,* 219

28. Diffey, B. L.; Farr, P. M., *Clinical Physics and Physiological Measurement* **1991,** *12*, 311

29. Diffey, B. L.; Jansen, C. T.; Urbach, F.; Wulf, H. C., *Photodermatology Photoimmunology & Photomedicine* **1997,** *13*, 64

30. Fitzpatrick, T. B., *Archives of Dermatology* **1988,** *124*, 869

31. Davis, A.; Diffey, B. L.; Deane, G. H. W., *Nature* **1976,** *261*, 169

32. Davis, A.; Diffey, B. L.; Tate, T. K., *Photochemistry and Photobiology* **1981,** *34*, 283

33. Diffey, B. L., *Photodermatology* **1984,** *1*, 151

34. Diffey, B. L., Ultraviolet radiation dosimetry with polysulphone film. In *Radiation Measurement in Photobiology*, Diffey, B. L., Ed. Academic Press, New York: 1989; pp 136

35. SolarSafe innovators in Sun Care. http://www.solarsafe.com/tradepack2007-english.pdf (accessed January 10th 2007).

36. Wang, T.C. V., *Biochemical and Biophysical Research Communications* **1991,** *177*, 48

37. Kerns, D., *Sensors and Actuators A* **1993,** *39*, 225

38. Horkay, I.; Wikonkal, N.; Patko, J.; Bazsa, G.; Beck, M.; Ferenczi, A.; Nagy, Z.; Racz, M.; Szalay, T., *Journal of Photochemistry and Photobiology B* **1995,** *31*, 19

39. Naggar, S. E.; Gustat, H.; Magister, H.; Rochlitzer, R., *Journal of Photochemistry and Photobiology B* **1995,** *31*, 83

40. Abu-Jarad, F.; Hadidy, M. E.; Al-Jarallah, M. I., *Radiation Measurements* **1997,** *28*, 409

41. Rahn, R.; Lee, M. A., *Photochemistry and Photobiology* **1998,** *68*, 173

42. Ramirez-Nino, J.; Mendoza, D.; Castano, V. M., *Radiation Measurements* **1999,** *30*, 181

43. Garcia-Guinea, J., *Journal of Materials Science Letters* **1999,** *18*, 1263

44. Ishigaki, Y.; Takayama, A.; Yamashita, S.; Nikaido, O., *Journal of Photochemistry and Photobiology B* **1999,** *50*, 184

45. Terenetskaya, I., *Agricultural and Forest Meteorology* **2003,** *120*, 45

46. Sandby-Moller, J.; Theiden, E.; Philipsen, P. A.; Heydenreich, J.; Wulf, H. C., *Photodermatology Photoimmunology & Photomedicine* **2004,** *20*, 33

47. Mills, A.; Lee, S.-K.; Sheridan, M., *Analyst* **2005,** *130*, 1046

48. Abdel-Fattah, A. A.; Hegazy, E.S. A.; El-Din, H. E., *Journal of Photochemistry and Photobiology A* **2000,** *137*, 37

49. Webb, A. R., *Journal of Photochemistry and Photobiology B* **1995,** *31*, 9

50. Rothweiler, H.; Wager, P. A.; Schlatter, C., *Environmental Technology* **1992,** *13*, 891.

51. Schaeffer, V. H.; Bhooshan, B.; Chen, S. B.; Sonenthal, J. S.; Hodgson, A. T., *Journal of the Air & Waste Management Association* **1996,** *46*, 813.

52. Sundell, J., *Indoor Air-International Journal of Indoor Air Quality and Climate* **1994**, *2,* 7.

53. James, K. J.; Cherry, M.; Stack, M. A., *Chemosphere* **1995,** *31*, 3741.

54. Rothweiler, H.; Wager, P. A.; Schlatter, C., *Atmospheric Environment Part a-General Topics* **1992,** *26*, 2219.

55. Lee, S. C.; Lam, S.; Fai, H. K., *Building and Environment* **2001,** *36*, 837.

56. Kagi, N.; Fujii, S.; Horiba, Y.; Namiki, N.; Ohtani, Y.; Emi, H.; Tamura, H.; Kim, Y. S., *Building and Environment* **2007,** *42*, 1949.

57. Leahey, D. M.; Hansen, M. C.; Schroeder, M. B., *Journal of the Air & Waste Management Association* **1993,** *43*, 341.

58. Fromme, H., *Zentralblatt Fur Hygiene Und Umweltmedizin* **1995,** *196*, 481.

59. Dechow, M.; Sohn, H.; Steinhanses, J., *Chemosphere* **1997,** *35*, 21.

60. Norback, D.; Wieslander, G.; Strom, G.; Edling, C., *Indoor Air-International Journal of Indoor Air Quality and Climate* **1995,** *5*, 166.

61. Wieslander, G.; Norback, D.; Bjornsson, E.; Janson, C.; Boman, G., *International Archives of Occupational and Environmental Health* **1997,** *69*, 115.

62. Wolkoff, P.; Schneider, T.; Kildeso, J.; Degerth, R.; Jaroszewski, M.; Schunk, H., *Science of the Total Environment* **1998,** *215*, 135.

63. Brosseau, J.; Heitz, M., *Atmospheric Environment* **1994,** *28*, 285.

64. Deloraine, A.; Zmirou, D.; Tillier, C.; Boucharlat, A.; Bouti, H., *Environmental Research* **1995,** *68*, 124.

65. Bukowski, J. A.; Meyer, L. W., *Environmental Science & Technology* **1995,** *29*, 673.

66. Bukowski, J. A.; Robson, M. G.; Buckley, B. T.; Russell, D. W.; Meyer, L. W., *Environmental Science & Technology* **1996,** *30*, 2543.

67. Wilson, S. C.; Burnett, V.; Waterhouse, K. S.; Jones, K. C., *Environmental Science & Technology* **1994,** *28*, 259.

68. Rothweiler, H.; Schlatter, C., *Toxicological and Environmental Chemistry* **1993,** *40*, 93.

69. Schleibinger, H. W.; Wurm, D.; Moritz, M.; Bock, R.; Ruden, H., *Zentralblatt Fur Hygiene Und Umweltmedizin* **1997,** *200*, 137.

70. Sheppard, S. E., *Reviews of Modern Physics* **1942,** *14*, 303

71. Cain, W. S., *Annals of the New York Academy of Science* **1974,** *237*, 28

72. Cintra, A.; Andbjer, B.; Finnman, U. B.; Hagman, M.; Agnate, L. F.; Hoglund, G.; Fuxe, K., *Neuroscience Letters* **1996,** *217*, 61

73. Roth, R. P.; Drew, R. T.; Lo, R. J.; Fouts, J. R., *Toxicology and Applied Pharmacology* **1975,** *33*, 427

74. Becker, C. E., *The Journal of Emergency Medicine* **1983,** *1*, 51

75. Cusano, A.; Pisco, M.; Consales, M.; Cutolo, A.; Giordano, M.; Penza, M.; Aversa, P.; Capodieci, L.; Campopiano, S., *IEEE Photonics Technology Letters* **2006,** *18*, 2431.

76. Groves, W. A.; Grey, A. B.; O'Shaughnessy, P. T., *Journal of Environmental Monitoring* **2006,** *8*, 932.

77. Hamilton, S.; Hepher, M.; Sommerville, J., *Sensors and Actuators B-Chemical* **2005,** *107*, 424.

78. Han, L.; Shi, X. J.; Wu, W.; Kirk, F. L.; Luo, J.; Wang, L. Y.; Mott, D.; Cousineau, L.; Lim, S. I. I.; Lu, S.; Zhong, C. J., *Sensors and Actuators B-Chemical* **2005,** *106*, 431.

79. Kanda, K.; Maekawa, T., *Sensors and Actuators B-Chemical* **2005,** *108*, 97.

80. Kim, S.; Kim, H. J.; Moon, S. J., *Indoor and Built Environment* **2006,** *15*, 511.

81. Kim, S.; Kim, J. A.; An, J. Y.; Kim, H. J.; Moon, S. J., *Journal of Adhesion Science and Technology* **2006,** *20*, 1783.

82. Li, B.; Sauve, G.; Iovu, M. C.; Jeffries-El, M.; Zhang, R.; Cooper, J.; Santhanam, S.; Schultz, L.; Revelli, J. C.; Kusne, A. G.; Kowalewski, T.; Snyder, J. L.; Weiss, L. E.; Fedder, G. K.; McCullough, R. D.; Lambeth, D. N., *Nano Letters* **2006,** *6*, 1598.

83. Sanchez, J. B.; Berger, F.; Fromm, M.; Nadal, M. H., *Sensors and Actuators B-Chemical* **2006,** *119*, 227.

84. Shin, S.; Paik, J. K.; Lee, N. E.; Park, J. S.; Park, H. D.; Lee, J., *Ferroelectrics* **2005,** *328*, 59.

85. Sobanski, T.; Szczurek, A.; Nitsch, K.; Licznerski, B. W.; Radwan, W., *Sensors and Actuators B-Chemical* **2006,** *116*, 207.

86. Suslick, K. S.; Rakow, N. A.; Sen, A., *Tetrahedron* **2004,** *60*, 11133.

87. Szczurek, A.; Maciejewska, M., *Talanta* **2004,** *64*, 609.

88. Terrones, S. C.; Aguado, C. E.; Bariain, C.; Carretero, A. S.; Maestro, I. R. M.; Gutierrez, A. F.; Luquin, A.; Garrido, J.; Laguna, M., *Optical Engineering* **2006,** *45,* 1

89. Vaishanv, V. S.; Patel, P. D.; Patel, N. G., *Materials and Manufacturing Processes* **2006,** *21*, 257.

90. Wanekaya, A. K.; Uematsu, M.; Breimer, M.; Sadik, O. A., *Sensors and Actuators B-Chemical* **2005,** *110*, 41.

91. Wolfrum, E. J.; Meglen, R. M.; Peterson, D.; Sluiter, J., *Sensors and Actuators B-Chemical* **2006,** *115*, 322.

92. Athawale, A. A.; Kulkarni, M. V., *Sensors and Actuators B* **2000,** *67*, 173

93. Bariain, C.; Matias, I. R.; Romeo, I.; Garrido, J.; Laguna, M., *Sensors and Actuators B* **2001,** *76*, 25

94. Linert, W.; Gutmann, V., *Coordination Chemistry Reviews* **1992,** *117*, 159

95. Mohr, G. J.; Citterio, D.; Spichiger-Keller, U. E., *Sensors and Actuators B* **1998,** *49*, 226

96. Mohr, G. J.; Spichiger-Keller, U. E., *Analytica Chimica Acta* **1997,** *351*, 189

97. Posch, H. E.; Wolfbeis, O. S., *Talanta* **1988,** *35*, 89

98. Simon, D. N.; Czolk, R.; Ache, H. J., *Thin Solid Films* **1995,** *260*, 107

99. Soukup, R. W.; Schmid, R., *Journal of Chemical Education* **1985,** *62*, 459

100. Bailey, R. C.; Hupp, J. T., *J. Am. Chem. Soc.* **2002,** *124*, 6767.

101. Daws, C. A.; Exstrom, C. L.; Sowa, J. R.; Mann, K. R., *Chem. Mat.* **1997,** *9*, 363

2 Experimental

2.1 Materials Preparation

The chemicals used during the course of this work were purchased from Sigma-Aldrich, Alfa Aesar and Merck. All materials were used as purchased and without further purification. The water used as a solvent was double distilled and de-ionised within the department.

2.1.1 Polymer Solutions

All of the stock polymer solutions were prepared using a similar method: typically, 10 g of polymer would be dissolved in 90 g of solvent to give a 10 % w/w solution.

Table 2-1 –A list of polymers used throughout the bulk of the thesis.

Polymer	Mass (amu.)	Solvent
Poly(vinyl Alcohol) (PVA)	146 – 186,000	Water
Poly(vinyl pyrrolidone) (PVP)	~ 160,000	Water
Hydroxy ethylcellulose (HEC)	~ 90,000	Water
Poly(vinyl chloride)	~ 97,000	THF
Poly(acrylonitrile)	~ 150,000	DMF

The dye polymer solutions described in were turned into films via a spin coating process. A few drops of any solution were placed onto a substrate (glass or quartz) and spun at a set rpm for 15 seconds. Spin-coating details are shown in table 2-2.

Table 2-2 – Spin speeds required to give 2.5 μm thick films of different polymer solutions

Polymer	Spin Speed (rpm)
PVA (10 %)	1200
HEC (10 %)	700
PVP (20 %)	2400

The thickness of the polymer films was measured using a dektak profilometer. This machine drags a small diamond tip over a set distance, detecting and measuring any variation in the vertical axis of the tip. By coating a polymer film onto half of a quartz/glass substrate it is possible to drag the tip across a distance which includes the blank substrate and the coated film. The film will lift the tip and thus the machine records the thickness of the film.

Figure 2-1 – the dektak profilometer used for measuring the thickness of thin polymer films.

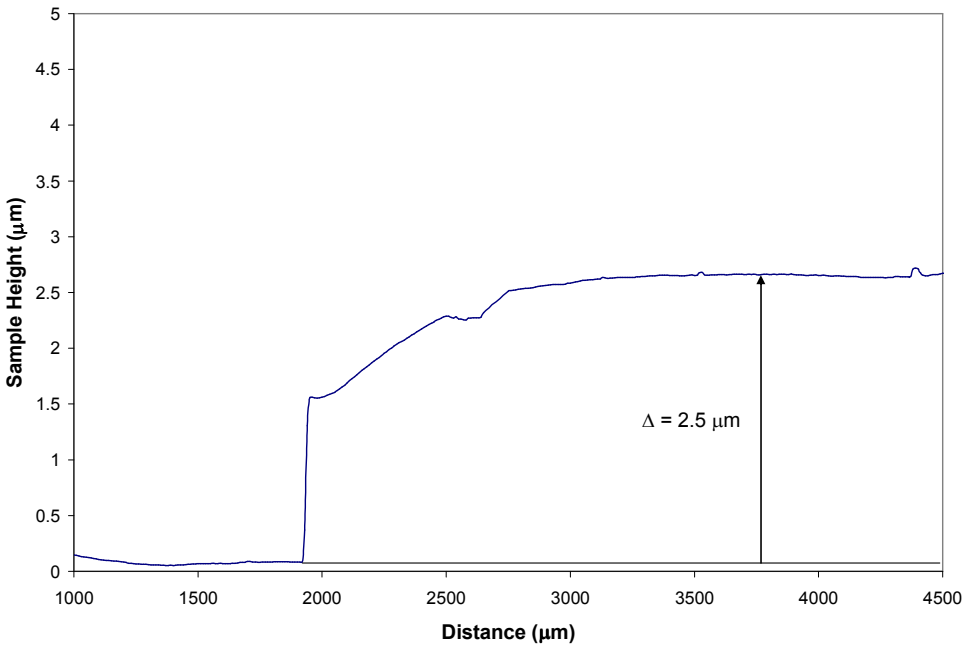

Figure 2-2 – Above: The dektak profilometer. The height profile of a 10% w/w HEC solution spun onto quartz at 700 rpm

The dektak profiler can only measure variations of 50mm, so in instances when films were thicker than this, a Mitutoyo micrometer was used to provide accurate measurement.

Figure 2-3 – A mitutoyo micrometer, used for measuring the thickness of some polymer films.

2.1.2 Dye solutions

To prepare the stock dye solutions for the UV dosimeter, 50 mg of the dye were placed in 10 g of stock 10 % w/w polymer solution and stirred vigorously to ensure complete dissolution. This gave a standard mixture containing 5 parts dye per hundred resin (5 phr). Unless stated otherwise all experiments using these materials were carried out using films prepared from this solution.

2.1.3 Silica coated with Reichardt's dye

1.9 g of the fumed silica were placed into ca 125 ml of methanol in a round bottomed flask, which were continuously stirred. 0.1 g of Reichardt's dye were dissolved in small volume of methanol – typically 10 to 20 ml – which was then added to the silica suspension. The resultant mixture was left to stir for 30 minutes before being placed under rotary evaporation, leading to the generation of silica coated with Reichardt's dye.

For the solvatochromic work the fumed silica coated with Reichardt's dye was converted into a thin, transparent, coloured layer on glass by placing a glass cover slip on top of the first stainless steel die in a standard IR press, evenly spreading 50 mg of the dye-impregnated silica over this disc, sandwiching the powder with a second stainless steel die, and then applying 2000 kg of pressure for 30 minutes. After this time the pressure was *slowly* released and the glass cover slip, now bonded with a thin layer of the impregnated silica, was removed. A full schematic of this set-up is shown in figure 3-3.

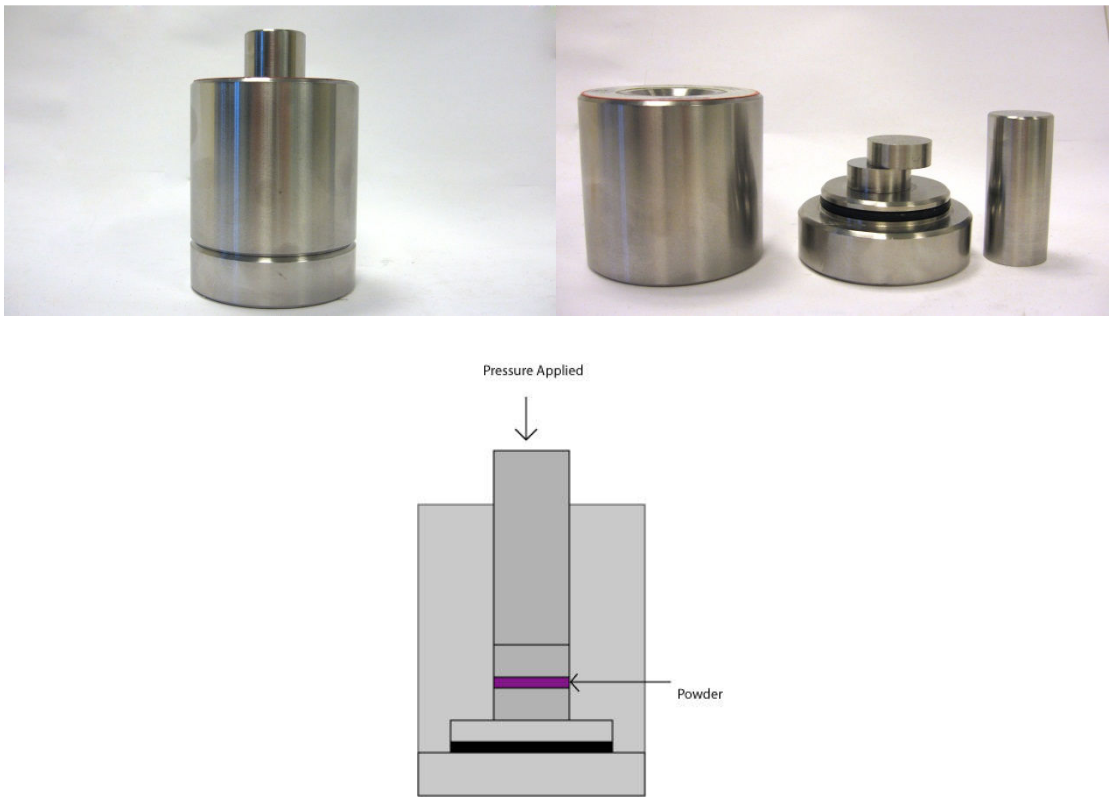

Figure 2-4 – Pictures of the IR press used for compressing dye impregnated powders into solid discs. The lower illustration shows a cutaway diagram of the press when in use.

2.2 Spectroscopic Analysis

All spectroscopic analysis during the course of this work was carried out using UV-Vis spectrometers. The machines used for the UV dosimeter work were a Varian Cary 50 and a Perkin-Elmer Lambda 20. Most of the analysis for the solvatochromic work was performed using a Unicam Helios Beta spectrometer.

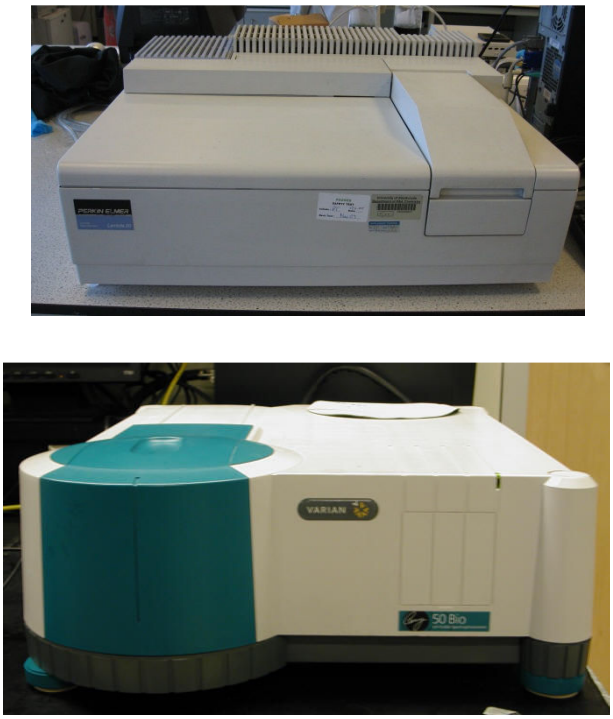

Figure 2-5 – Top: Perkin-Elmer lambda 20 spectrometer. Bottom: Varian Cary 50 spectrometer.

The samples to be tested were held within a specially designed brass cell (figure 2-6). The cell consists of three brass plates, each with a 25mm diameter circular window, fixed together with screws. All the plates have circular grooves on either side which accommodate either glass or quartz cover slips as windows and allow the placement of O-rings into the apparatus, creating a gas-tight chamber for experiments in which the atmosphere varies from ambient conditions. In this work one of the cover slip windows of the cell acts as the substrate for the sample film under test; the other was simply a clear window to allow absorbance measurements to be made.

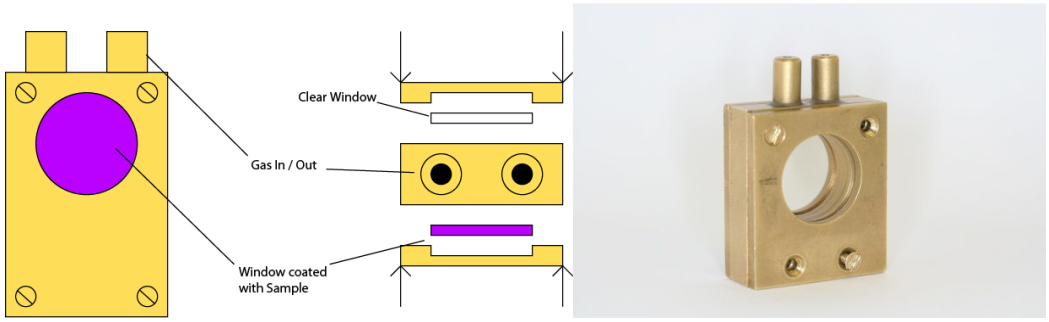

Figure 2-6 – A schematic showing the basic setup of the brass cell used for most spectroscopic analysis.

In spectroscopic analysis a beam of light of fixed intensity, I_0, and wavelength, λ, is passed through a transparent cell containing a light-absorbing species, which is usually dissolved in a solvent. As the light passes through the sample some of it will be absorbed, resulting in a reduction in the intensity of the beam. Thus the transmitted light intensity, I, is usually less than the incident light intensity, I_0. Both I_0 and I are measured by a photo-detector. The basic setup of a spectrometer is shown in figure 2-7.

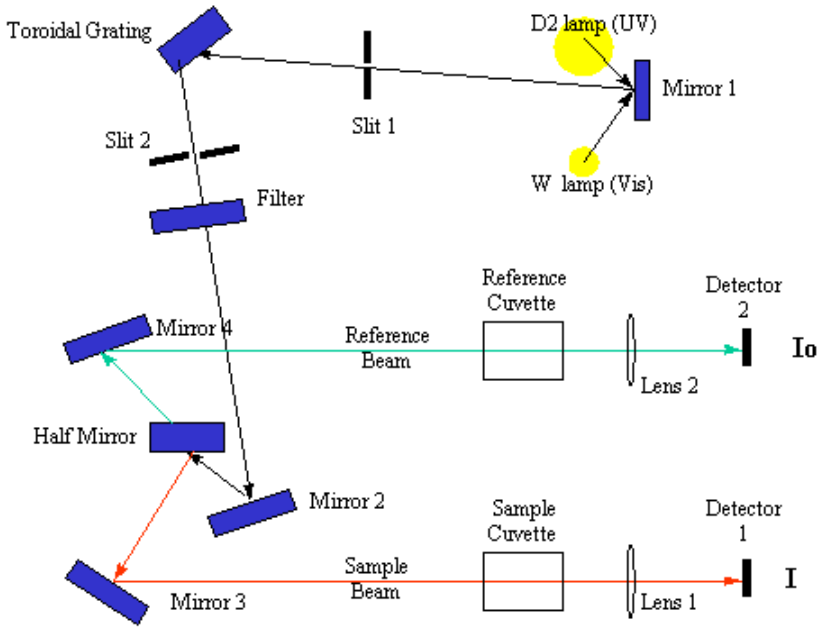

Figure 2-7 – Schematic of a typical UV-Vis spectrometer. The example given is a double-beam spectrometer which allows for measurement of the sample and a blank reference at the same time.

The data collected is commonly calculated as a percentage of transmitted light, %T, which is related to I_o and I as follows:

$$\%T = \frac{I}{I_O} x100 \qquad (2.1)$$

This value is often converted to an absorbance value, A, using the following relationship:

$$A = -\log_{10}\left(\frac{I}{I_O}\right) \qquad (2.2)$$

As the absorbance is calculated on a log scale a value of 1 corresponds to 90% light absorbed, an absorbance of 2 equals 99% absorption, 3 corresponds to 99.9% and so on.

2.2.1 Beer's Law

It is known that the reduction in intensity, *dI*, that occurs when light passes through a layer of thickness *dl* containing an absorbing species at a molar concentration *c* is proportional to the thickness of the layer, the concentration, and the intensity, *I*, incident on the layer.

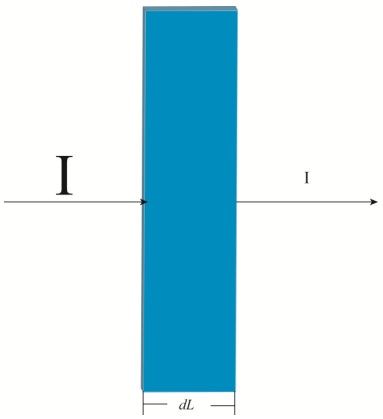

Figure 2-8 – Light of intensity, I, being adsorbed by a species of thickness dL

We can therefore write:

$$dI = -kcIdl \tag{2.3}$$

where *k* is a proportionality coefficient. This is equivalent to:

$$\frac{dI}{I} = -kcdl \tag{2.4}$$

Equation 2.4 can be applied to each successive layer into which the sample is divided. Therefore, to obtain the intensity that emerges from a sample of thickness l when the incident intensity is I_0, we sum all the successive changes:

$$\int_{I_0}^{I} \frac{dI}{I} = -k\int_0^l c dl \tag{2.5}$$

If the concentration is constant throughout the sample then the above equation integrates to:

$$\ln \frac{I}{I_0} = -kcl \tag{2.6}$$

Which is equivalent to:

$$\log_{10} \frac{I}{I_0} = \frac{-k}{2.303} cl \tag{2.7}$$

$$\Rightarrow \log_{10} \frac{I}{I_0} = -\varepsilon cl \tag{2.8}$$

$$\Rightarrow -\log_{10} \frac{I}{I_0} = \varepsilon cl \tag{2.9}$$

where $\varepsilon = \kappa/2.303$. Following on from equation (2.2) we can then simply say that:

$$A = \varepsilon cl \tag{2.10}$$

Where ε is the absorptivity coefficient, c is the concentration, and l is the sample thickness. This is Beer's law, otherwise known as the Beer-Lambert or Beer-Lambert-Bougouer law, and can be used to calculate the absorbance of a species at λ_{max} if the other three variables are known.

2.3 Gas Blending

Some experiments, especially those relating to the solvatochromic work, required that the atmosphere in the gas sample cell be modified so as to contain specific vapour concentrations. This was achieved by using a gas blender purchased from Cole-Parmer, comprising two direct reading, 500 ml min^{-1} flowmeters (cat. N^o A-32047-76) as input, as illustrated in figure 2-9. Each of the flowmeters could be individually adjusted to allow various blends of two gas streams to be created.

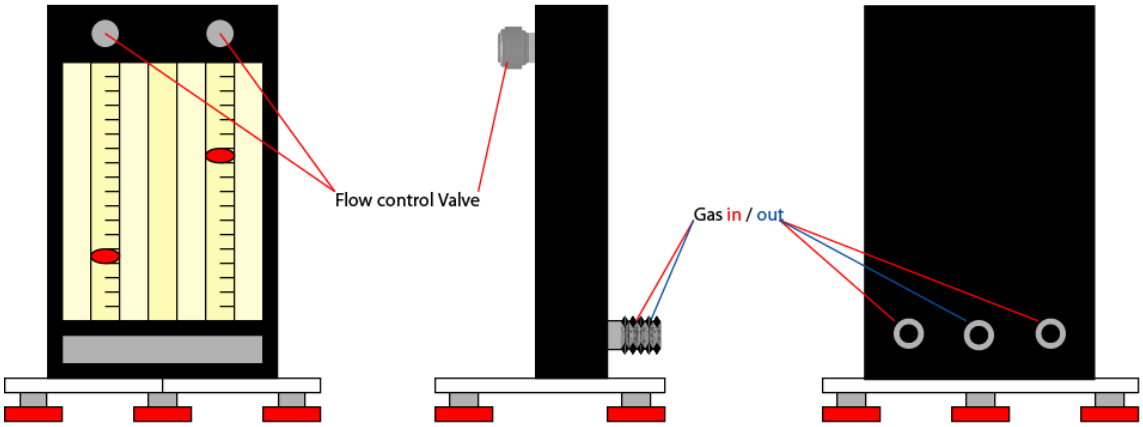

Figure 2-9 – A diagram of the gas-blender used during the course of this work.

2.4 Sample Irradiation

Many of the experiments required irradiation with a UV source (UVA, B or C). This often simply involved placing the sample at a fixed distance from the light source so as to exposed to known irradiance. In this regime, the samples would then be irradiated for a fixed period of time before being subjected to analysis using a UV-Vis spectrometer.

2.4.1 Instruments

UV irradiances were measured with two instruments. The first was an UltraViolet Products (UVP) MS-100 multi-sense optical radiometer fitted with an appropriate light sensor. A MP-136 UVA sensor, a MP-131 UVB sensor, and a MP-125 UVC sensor for measuring irradiance levels during the course of this work. The performances of these sensor heads are outlined in table 2-3 and they are shown, along with the radiometer, in figure 2-10.

Table 2-3 – Performance data of the different sensor heads for the MS-100 radiometer

Sensor	Operational Range (nm)	Maximum response (nm)
MP-136 UVA	315 – 400	370
MP-131 UVB	280 – 360	320
MP-125 UVC	200 - 300	260

Figure 2-10 – UVP MS-100 multi-sense optical radiometer with sensor head.

The second instrument used was a SafeSun solar meter, designed to measure the current UV index and the cumulative erythemal dose that the user has been exposed to.

Figure 2-11 – SafeSun Solar Meter used for measuring the UVI index and Erythemal Dose.

2.4.2 UV Light Sources

The light sources used for the UV dosimeter work were standard Vilber-Lourmat lamp housings designed to hold two 8W bulbs. These lamps were fitted with bulbs designed to act as UVA and UVB sources. The UVB bulbs were purchased from Cole Parmer. The emission spectra for the different lamps are shown in the figure below. The intensity of these bulbs was measured at a fixed distance every 2 weeks to ensure that irradiation was carried out consistently.

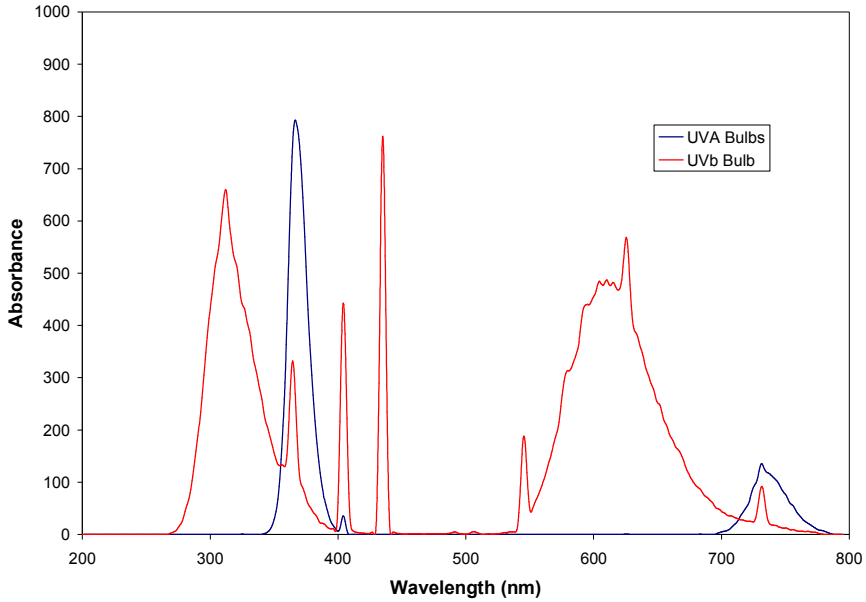

Figure 2-12 – Emission spectra profiles of UVA and UVB fluorescent tubes.

2.4.3 Solar Simulation

Some of the UV dosimeter work required the use of a solar simulator. The solar simulator used comprised a 150 W xenon arc lamp fitted with UG5 and WG320 filters from Präzisions Glas & Optik (PGO). These filters are used to minimise emitted light and the UVC and visible regions of the spectrum. The absorbance spectra of these filters are shown in figure 2-13, while the emission spectrum of the filtered lamp is shown in figure 2-14.

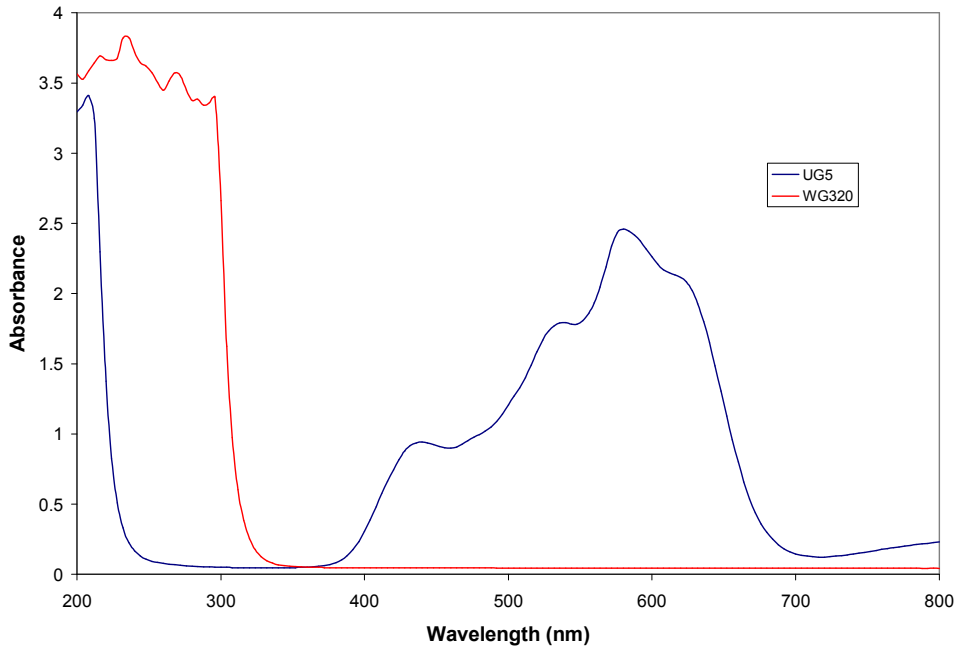

Figure 2-13 – the absorbance spectra of the UG5 and WG320 filters used to turn a xenon arc lamp into a solar simulator.

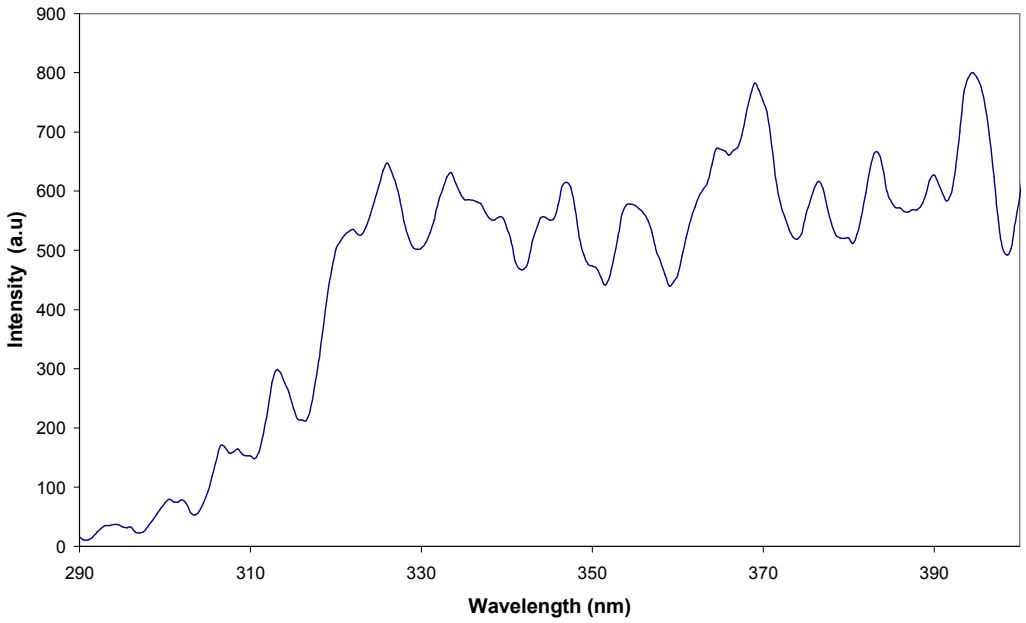

Figure 2-14 – Shown above are the absorbance spectra of two filters placed in front of a xenon lamp. These filters caused the lamp to give the emission spectrum shown at the bottom, which approximates to the solar UV spectrum.

3 A Viologen based UV dosimeter

Methyl viologen and its analogues can be reduced to form a coloured radical species as shown in figure 3-1.

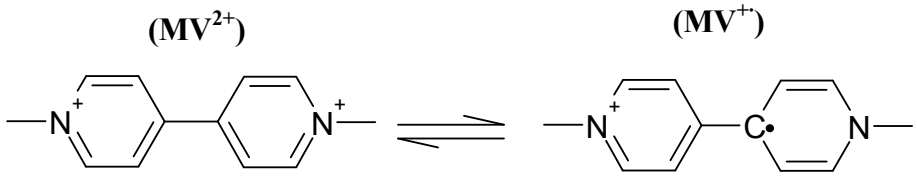

Figure 3-1 – The reduction of methyl viologen (MV^{2+}) to a coloured radical cation ($MV^{+\cdot}$).

This reaction has been studied extensively over the years and the viologens have been used as indicators in many redox reactions[1-7], as well as forming the base of an oxygen indicator[8]. In 1980 Kamogawa and his team demonstrated that the photochemical reduction of viologen could occur in a solid polymer matrix, with no other species present[9]. This followed work by Simon and Moore on polyviologens as novel redox polymers with film forming properties[10]. Kamogawa's first paper demonstrated that the rate of photoreduction of a low molecular weight viologen in a polymer matrix could be affected by factors including the aryl / alkyl groups on the viologen moiety and the polymer matrix itself[9]. It is stated for example that a polyvinyl pyrrolidone (PVP) - viologen film changes colour at a higher rate than a polyvinyl alcohol (PVA) - viologen film, with the offset being that the PVP film also loses colour quicker as well i.e. the reverse reaction occurs at a higher rate. This was attributed to the PVA acting as an oxygen barrier, slowing the oxidation of the reduced $MV^{+\cdot}$. Later work attributes the faster rate of reaction in PVP and other polar aprotic polymers to poor solvation of the viologen dication and its anionic component[11-17]. The suggestion is that they appear to exist as "naked" ion pairs in these matrix films, accelerating the photoreduction process indicated in equation 3.1.

$$MV^{2+} + 2X^{-} \overset{h\nu}{\leftrightarrow} [V^{2+}]^{*} + 2X^{-} \leftrightarrow V^{+\cdot} + X\cdot + X^{-} \qquad (3.1)$$

where MV^{2+} is the viologen, $[V^{2+}]^*$ refers to an excited state, and X^- is the counterion. However, some argument is made against this idea by Chen and his team[18]. Their study of the rate of colouration of butylviologen bromide in PVA and PVP has led them to suggest that the reaction may occur via a mechanism proposed by Ledwith et al[19] (equations 3.2 and 3.3). From this they suggest that the function of the polymer matrix as an electron donor to the reaction system must be considered.

$$MV^{2+} \xrightarrow{h\upsilon} \left[MV^{2+}\right]^* \xrightarrow{RCH_2OH} \left[MV^{+\bullet}, \dot{O}CH_2R, H^+\right] \tag{3.2}$$

$$\left[MV^{+\bullet}, \dot{O}CH_2R, H^+\right] \xrightarrow{MV^{2+}} 2MV^{+\bullet} + RCHO + 2H^+ \tag{3.3}$$

It is surprising that, despite disagreement over the mechanism of the reaction, more hasn't been made of the possible use of these systems as UV dosimeters. As of writing there are only a few sensors which use the viologen moiety, including a glucose sensor developed by Jyh-Myng Zen and Chin-Wen Lo[20], and a humidity sensor developed by Myoung-Seon Gong et al[21]. However these systems are more dependent on the electrical properties of the system rather than the optical. Of considerably more interest is the dosimeter proposed by Taichi Ogawa and his group[22]. In their study they looked at the possible use of methyl viologen in PVA as a highly sensitive dosimeter for ionizing radiation such as gamma- or electron-beam radiation.

The aim of this project was to use the redox properties of the viologens to develop a UV dosimeter, based on a viologen trapped in a polymer support, for identifying the point at which a minimum erythemal dose (MED) has been reached.

3.1 Methyl viologen in polymer (MV^{2+}-Polym.)

Methyl viologen was encapsulated within a film of polyvinyl alcohol by dissolving 5 phr of the dye in a 10 wt % aqueous solution of the polymer. This solution was then spun onto a glass disc at 1200 rpm, making a 2.5 μm thick film. The UV-Vis absorbance spectrum of the methyl viologen/PVA film, hereafter referred to as MV^{2+}-PVA, was recorded and compared to the spectra of PVA. The aim of this was to demonstrate that the only species absorbing any UV light in this system was the viologen. Figure 3-2 illustrates the recorded absorbance spectra of the different components of a typical MV^{2+}/PVA film.

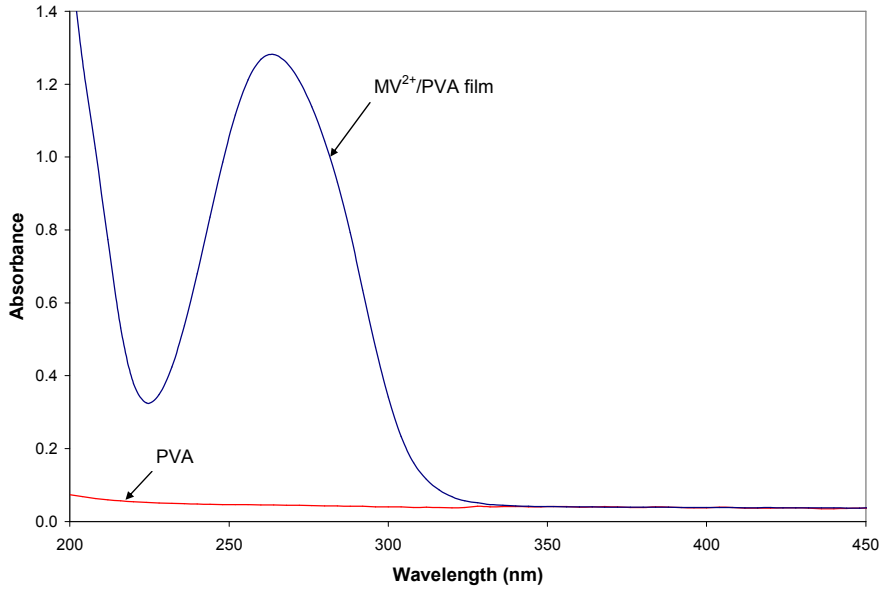

Figure 3-2 – A plot showing the absorbance spectrum of a PVA film on quartz and a 5 phr MV^{2+}/PVA film.

Figure 3-2 clearly shows it is only when MV^{2+} is added to the polymer that the system exhibits an absorbance in the UV region. Thus any change in the properties of the film brought about by exposure to UV can only be due to the MV^{2+}.

3.1.1 MV^{2+}/PVA film's response to UV

Having established that only the MV^{2+} in a MV^{2+}/PVA films is able to absorb any incident UV light, the next step was to test the response of the system to UV light. Ideally, the effect of the back reaction (i.e. $MV^{+\bullet} + O_2 \rightarrow MV^{2+}$) should be minimal, although the blue semi-reduced radical of MV^{2+}, $MV^{+\bullet}$, is usually very oxygen sensitive. In order to establish if one or more different encapsulation polymers would act as a barrier to O_2 diffusion into the film, spin-coated films of PVA, polyvinyl pyrrolidone (PVP) and hydroxyethyl cellulose (HEC) containing 5phr MV^{2+} were irradiated using 4 mW cm^{-2} UVB light, with their UV-Vis spectra being recorded every 60 seconds. Pictures of the observed colour change are shown in figure 3-3, while the recorded spectra follow after.

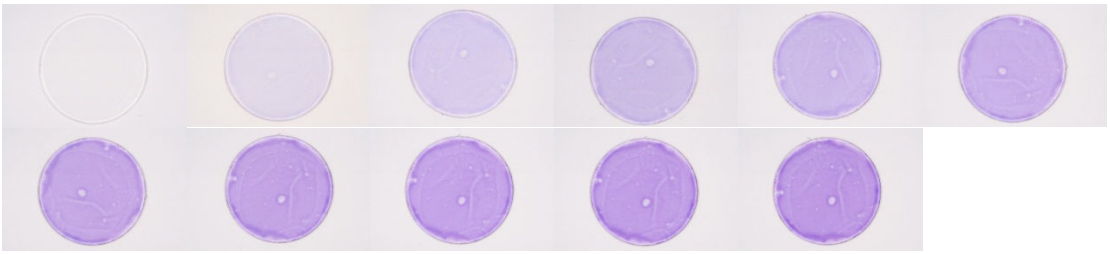

Figure 3-3 – Shown are images of a MV^{2+}-PVA as it is irradiated with 4 mW cm^{-2} UVB light. The images show, in increasing order from left to right, the film every minute from 0 to 10 minutes of irradiation.

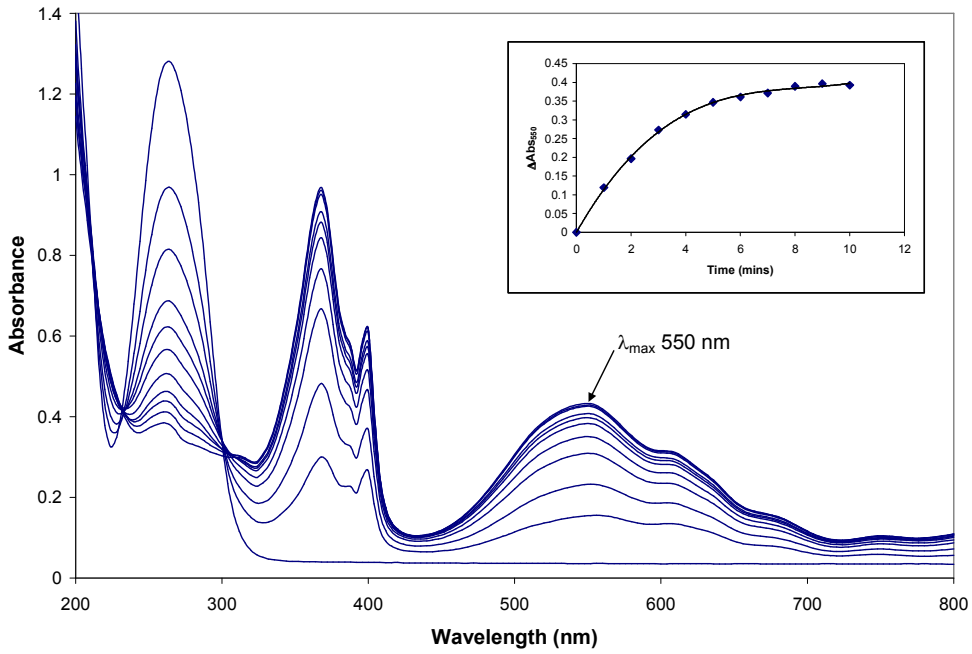

Figure 3-4 – The UV-Vis spectra of a MV^{2+}-PVA film after irradiation with 4 mW cm^{-2} UVB light. The inset shows the change in absorbance at λ_{max} (550 nm) with time.

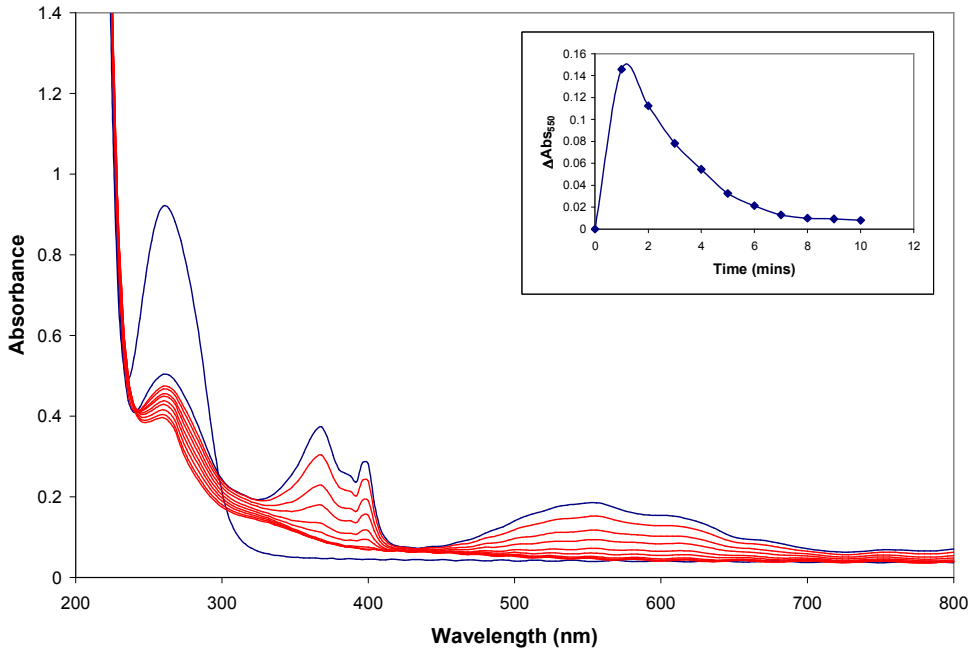

Figure 3-5 – The UV-Vis spectra of a MV^{2+}-PVP film after irradiation with 4 mW cm^{-2} UVB light. Some spectra are red to indicate a decrease in absorbance. The insert shows the change in absorbance at λ_{max} (550 nm) with time.

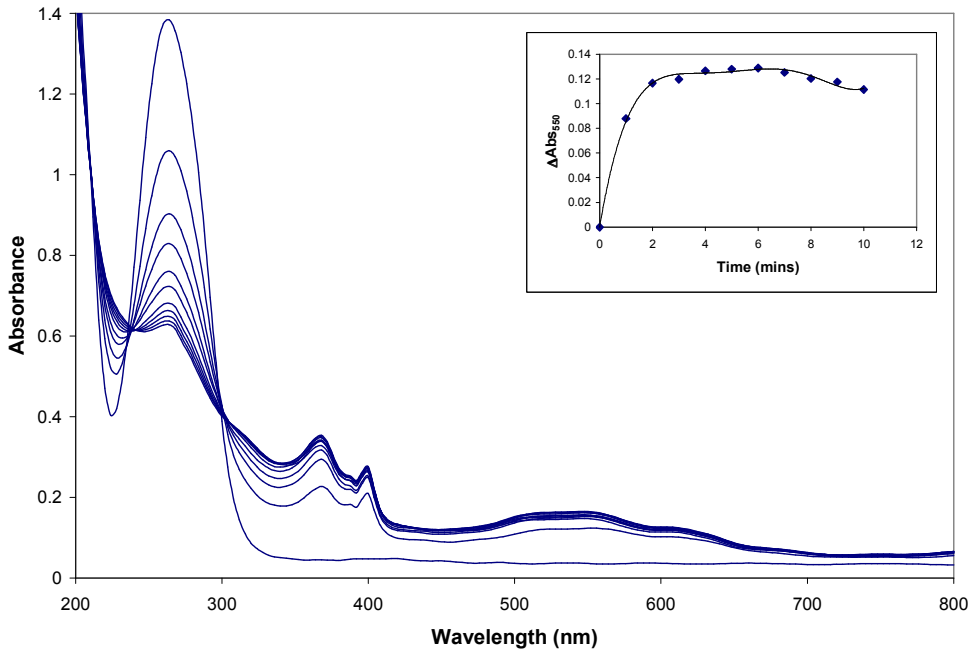

Figure 3-6 – The UV-Vis spectra of a MV^{2+}-HEC film after irradiation with 4 mW cm^{-2} UVB light. The inset shows the change in absorbance at λ_{max} (550 nm) with time.

The absorbance spectra obtained after irradiation has a λ_{max} in the visible region of approximately 550 nm, which differs from the stated literature value of 610 nm used by Kamogawa and other groups. This is probably due to the formation of a dimer species as the spectra matches very well with those reported for viologen dimers by Chongmok Lee et al[23].

As can be seen from the previous figures, the MV^{2+} reaches a higher absorbance value in PVA than it does in the other two polymers, while the MV^{2+}-PVP film fails to retain its colour and actually loses colour with continued irradiation. In this work, PVA is much more effective as an encapsulating medium as it is less permeable to oxygen than either PVP or HEC. As such the greater increase in colour, and therefore concentration of the $MV^{+\bullet}$ species, is assumed to be because of the lack of oxygen in the system. To test this each film was irradiated for long enough to give maximum absorbance, as indicated in figures 3-3 to 3-6 and summarised in table 3-1, then the UV lamp was

switched off. The spectra of the films were then recorded every minute for a period of 25 minutes. The change in absorbance at λ_{max} is shown in figure 3-7.

Table 3-1 – Time required for max absorbance as taken from figures 4-4 to 4-6.

Encapsulating Medium	Time required for max absorbance (mins)
PVA	8
PVP	1
HEC	4

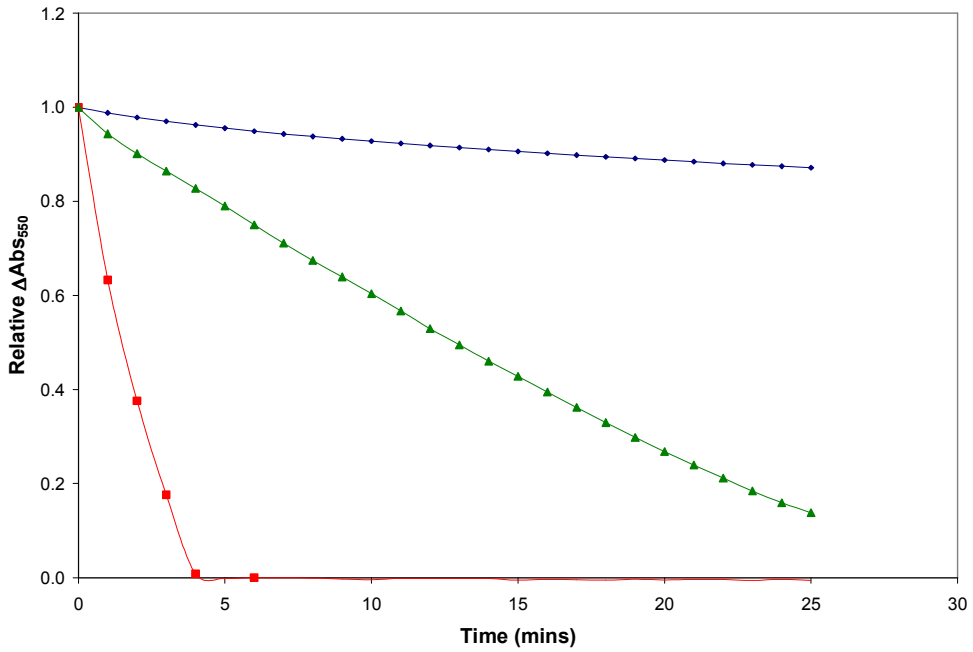

Figure 3-7 – A plot showing the change in absorbance at 550 nm of PVA, HEC and PVP films containing 5 phr methyl viologen.

Figure 3-7 suggests that the HEC and PVP films may lose colour at a much greater rate than the MV^{2+}-PVA film. If this loss of absorbance is due to the presence of oxygen in the system it should be possible to lessen or stop the effect by repeating the experiment

in an oxygen free environment. The experiment was repeated with the MV^{2+}-PVP film under nitrogen in one instance and coated with an oxygen barrier in another. The oxygen barrier used for these experiments was Sellotape™, which comprises a layer of adhesive of a film of regenerated cellulose[24]. Each film was irradiated for the same amount of time listed previously and the spectra recorded every minute after the lamp was switched off. The resultant spectra are shown in figure 3-8.

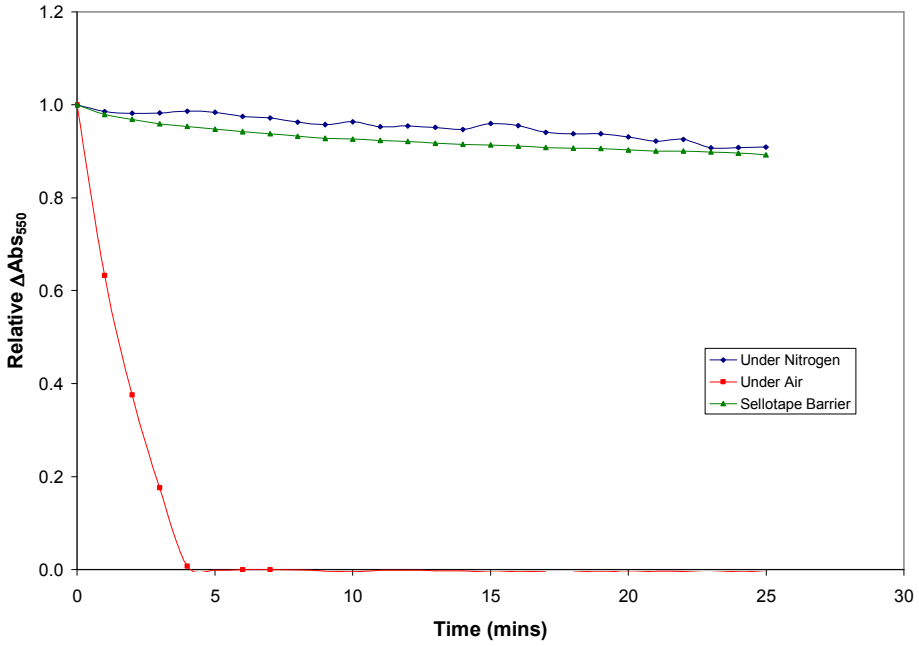

Figure 3-8 – A plot showing the relative change in absorbance of three MV^{2+}-PVP films after irradiation with a 4 mW cm^{-2} UVB lamp has stopped. The curves shown are for films allowed to recover in air, nitrogen and under a Sellotape™ barrier.

It may be assumed from figure 3-8 that MV^{2+}-PVP films which are kept in oxygen free environment are able to retain their colour. Repetition of this experiment with HEC yielded similar results. Thus MV^{2+}-PVA films demonstrate the ability to retain their colour (due to $MV^{+\bullet}$ production) without the need for an oxygen free environment. As an illustration of this feature, a standard MV^{2+}-PVA film was monitored for several hours after UV irradiation, and its absorbance at 550 nm (due to $MV^{+\bullet}$) recorded every 15 minutes. The results of this work are illustrated in figure 3-9 and reveal the UV-photogenerated $MV^{+\bullet}$ radical to be stable in the PVA film in the dark over 8 hours.

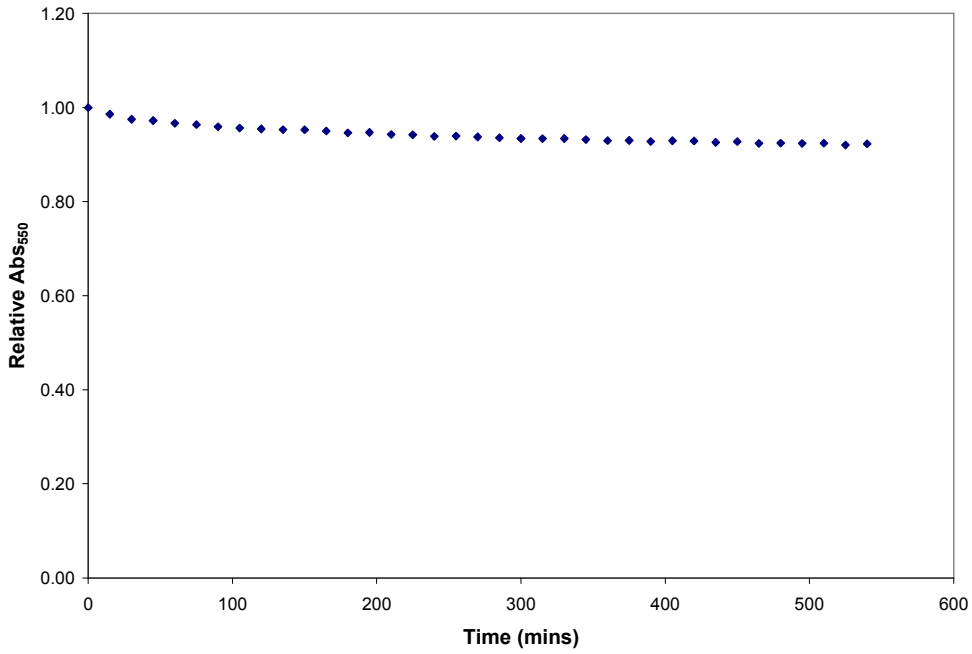

Figure 3-9 – The relative absorbance of a MV^{2+}-PVA film several hours after a 10 minute irradiation with 4 mW cm^{-2} UVB light. The absorbance values were taken at λ_{max} (550 nm) and were recorded every 15 minutes.

The PVA polymer is therefore an ideal support medium for a UV dosimeter: it does not absorb UV light and acts as an oxygen barrier, allowing the reduction reaction to proceed unhindered.

3.1.2 Response to different UV wavelengths

Having chosen the support medium the next step was to discover how the system responded to the different wavelengths of light. To accomplish this the MV^{2+}-PVA films were subjected to UVA, UVB and UVC radiation at 4 mW cm^{-2}, and the absorbance at 550 nm monitored with time. Ideally the system should respond very well to UVB, which is the wavelength region of greatest interest, but not as well to UVA (due to poor overlap between the emission spectrum of the lamp and the absorption spectrum of MV^{2+}). UVC light is of little concern for most terrestrial uses of

a UV dosimeter for erythema but is included for completeness. The results are shown in figure 3-10.

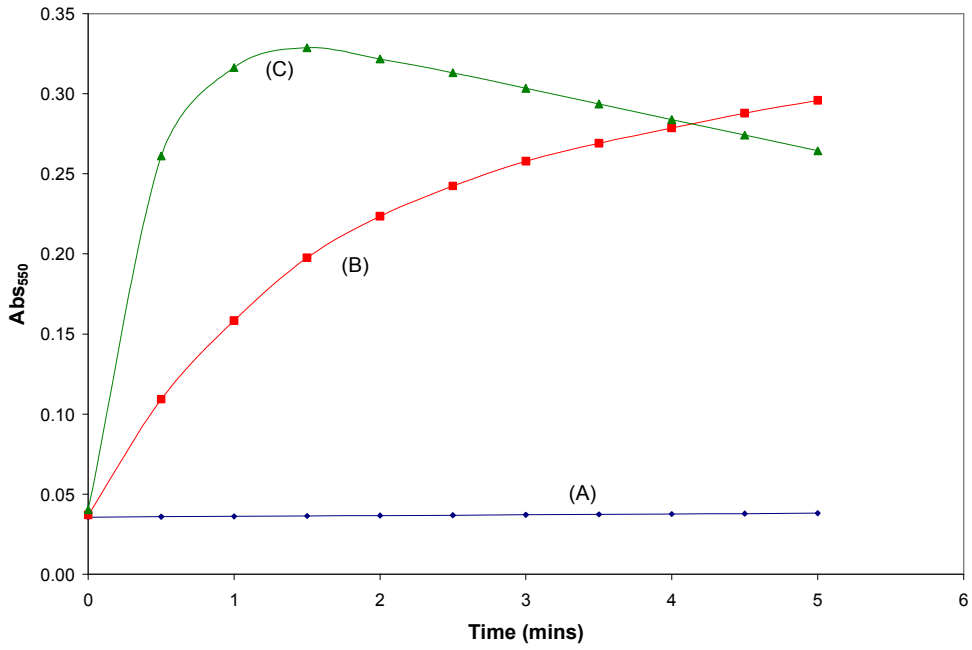

Figure 3-10 – The change in absorbance at 550 nm of MV^{2+}-PVA film subjected to different wavelength regions of UV light. The curves shown are for 4 mW cm^{-2} UV(A), UV(B) and UV(C) respectively.

From the results shown in figure 3-10 it can be seen that the MV^{2+}/PVA films did not respond to UVA illumination. On the other hand the system responds very well to UVB and UVC irradiation, reaching Δabs values of 0.187 and 0.281 respectively after only 2 minutes. It is worth noting, however, that after reaching its maximum absorbance value the film exposed to UVC quickly begins to lose its colour with continued exposure, presumably due to UV-induced photolysis of the dye.

In the context of a UV dosimeter for erythema, of greater importance is the response of the MV^{2+}/PVA film to UVB irradiation.

3.1.3 Response to light intensity

MV^{2+}/PVA films were prepared and exposed to intensities of UVB light from 1 to 5 mW cm^{-2} of UVB and the results are shown in figure 3-11.

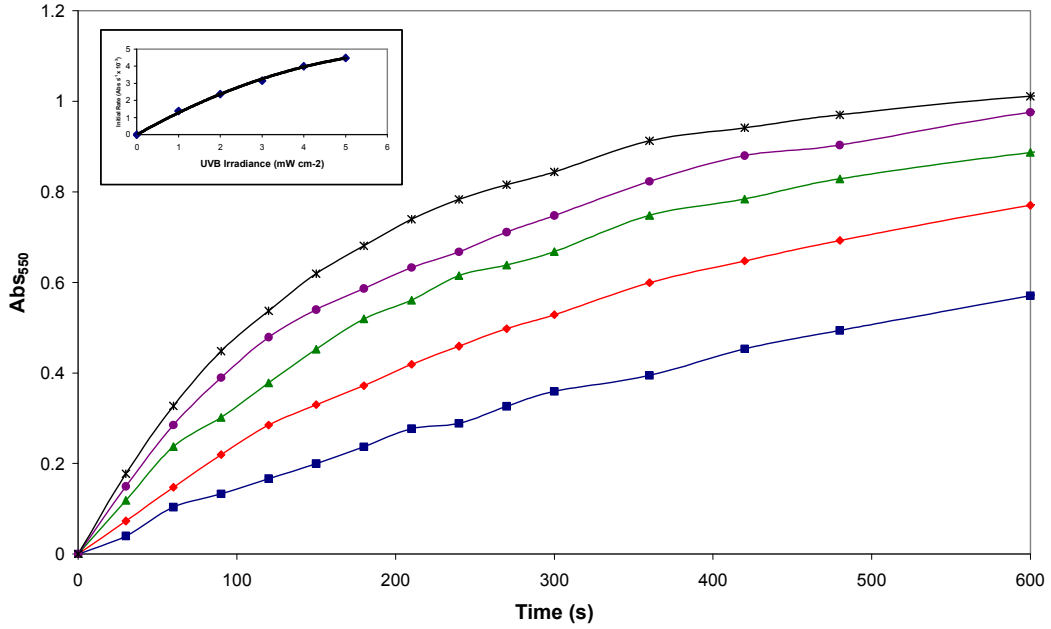

Figure 3-11 – Curves showing the change in Absorbance at 550 nm of MV^{2+}-PVA films exposed to, in increasing order, 1, 2, 3, 4, and 5 mW cm^{-2} UVB light. The inset shows the change in the rate of reaction of the system with varying irradiance.

3.1.4 Concentration Study

The simplest method of controlling the extent of the colour change is to alter the concentration of the viologen within the system. The Beer-Lambert Law states that absorbance is directly proportional to concentration, so it can be assumed that increasing the concentration will increase the fraction of UV absorbed. PVA films were prepared containing 0.5, 1, 5, 7.5, 10, 15, 20, 30 and 60 phr MV^{2+} and their UV/Vis absorption spectra are shown in figure 3-12.

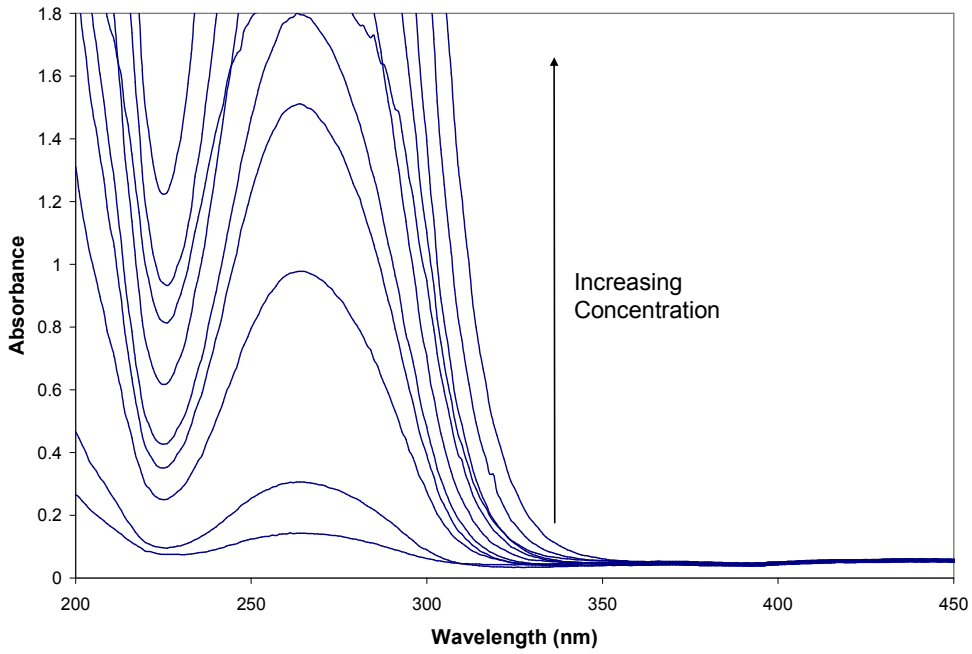

Figure 3-12 – The UV absorbance spectra of PVA films containing various concentrations of MV^{2+}. The concentrations used were, in increasing order, 0.5, 1, 5, 7.5, 10, 15, 20, 30 and 40 phr.

Figure 3-12 clearly shows the absorption in the UV region of the spectrum increasing as the concentration of viologen in the PVA is increased. These films were then irradiated for 5 minutes each with 4 mW cm^{-2} of UVB. The resulting spectra for this experiment, and a plot of ΔAbs at 550 nm as a function of concentration, are shown in figures 3-13 and 3-14.

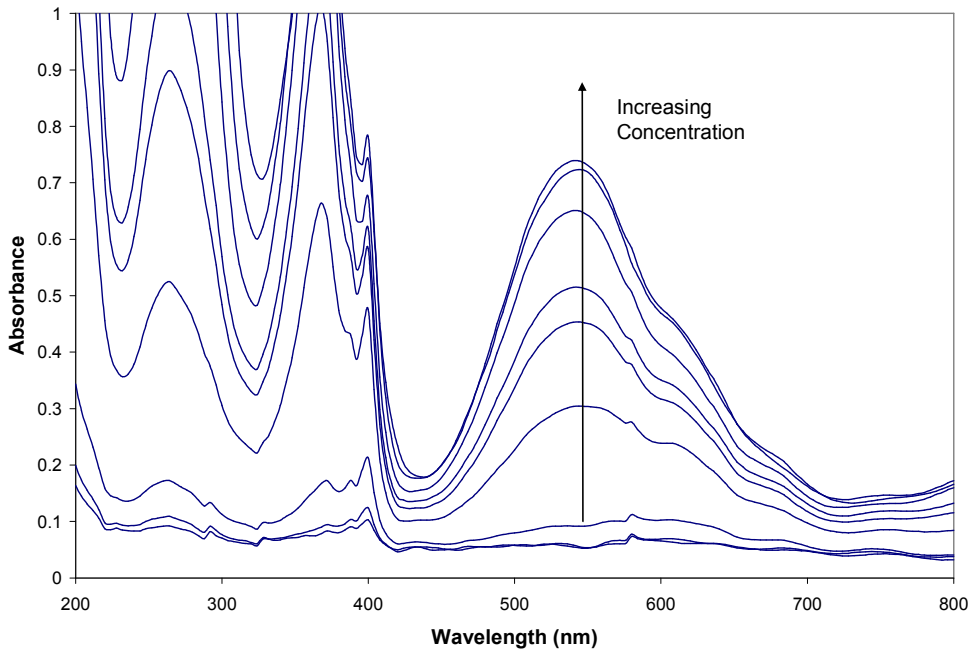

Figure 3-13 – UV-Vis spectra of the PVA films shown in figure 14 after 5 minutes of irradiation with 4 mW cm^{-2} UVB.

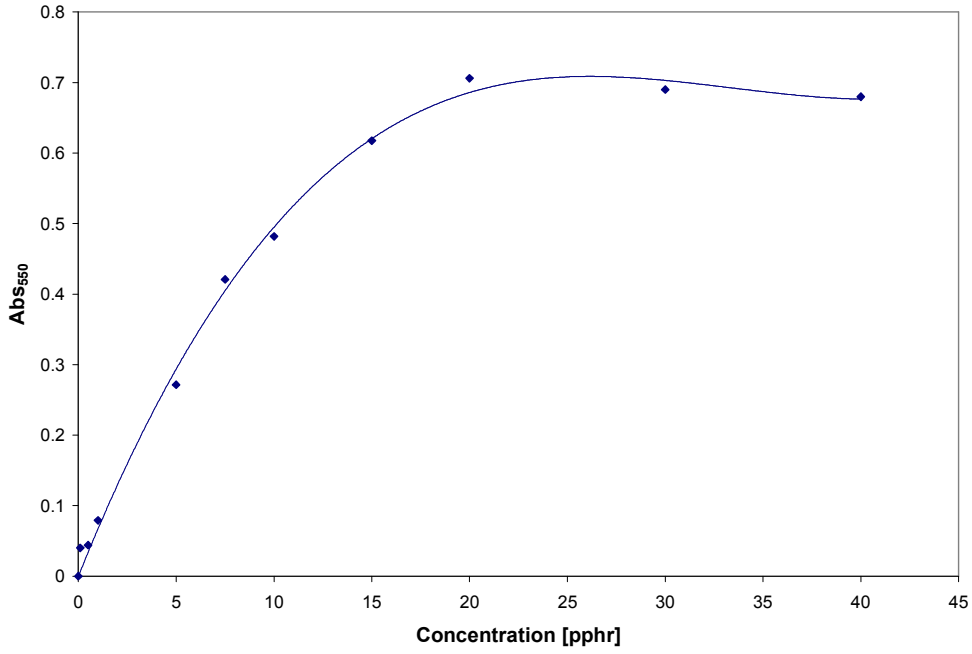

Figure 3-14 – A plot showing ΔAbs at 550 nm as a function of MV^{2+} concentration after 5 minutes irradiation with 4 mW cm^{-2} UVB.

It is clear from the above figures that, as expected, an increase in concentration causes a subsequent increase in the UV absorption of the film and the observed colour change after irradiation. It is worth noting that ΔAbs appears to reach a maximum as the higher concentrations are reached. It is assumed that this is due to viologen molecules at the surface of the film absorbing all the available light and preventing the remainder from being converted to the radical species. The following factors can be used to calculate the concentration in moles dm^{-3} of each films and, using the absorbance values, show the percentage of the MV^{2+} species being converted to $MV^{+\bullet}$

3.1.5 Film Thickness

A series of MV^{2+}/PVA films of different thicknesses were prepared by spinning a standard PVA-5 phr MV^{2+} coating solution at the following different spin speeds: 1200, 900, 600, and 300 rpm. A particularly thick film was coated by spreading a fixed amount of solution – 0.45 g – over a quartz disc and allowing it to dry in air. These films were then irradiated over ten minutes with 4 mW cm^{-2} UVB and their spectra recorded every minute. The ΔAbs profiles are shown in figure 3-15.

Table 3-2 – The film thicknesses of MV^{2+}-PVA solutions coated at different spin speeds

Spin Speed (rpm)	**Film thickness** (μm)
1200	2.3
900	3.0
600	4.6
300	13
N/A*	40

Hand coated film

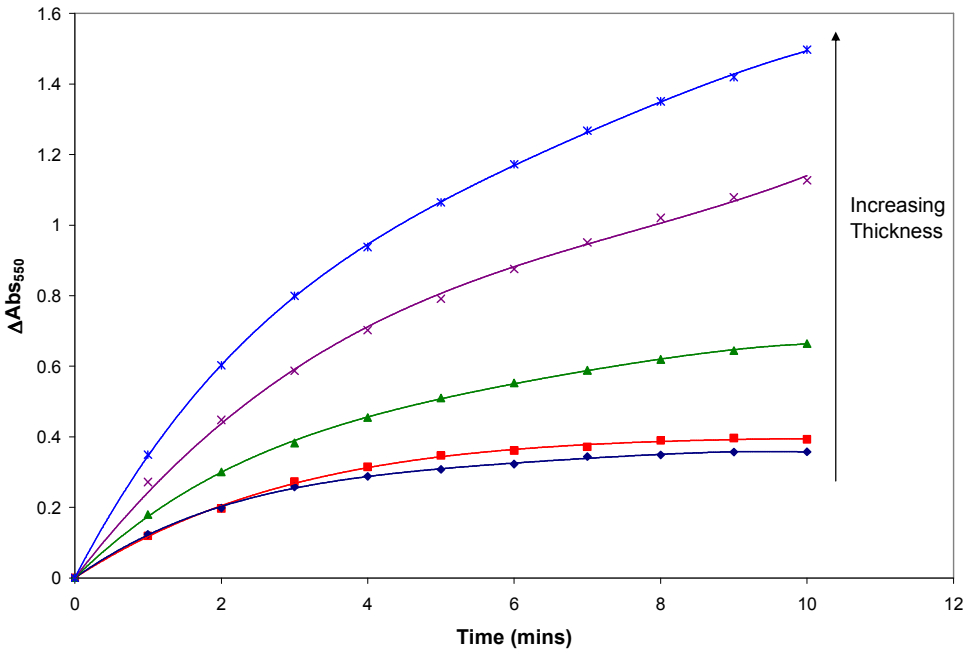

Figure 3-15 – A plot of the ΔAbs profiles, at 550 nm, of various thicknesses of PVA film containing 5 phr MV^{2+}. The profiles shown are for films 2.3, 3.0, 4.6, 13, and 40 µm thick.

There are some problems with this method of controlling the colour change however. By increasing the thickness of the film the overall absorbance of the system is increased, including the UVA region of the spectrum. While this is only a small increase it has to be remembered that UVA makes up the bulk of solar light and, if the focus is on an erythemal UVB dosimeter, any increase in UVA absorbance will have some effect on the results.

3.1.6 Salt Concentration

It is suggested by Kamogawa et al that the electron donor for the reduction of the viologen species, when present in a polymer matrix is the associated halide[9, 14, 16, 17]. The proposed reaction is outlined below:

$$MV^{2+} + 2X^- \overset{h\nu}{\leftrightarrow} [MV^{2+}]^* + 2X^- \leftrightarrow MV^{+\cdot} + X\cdot + X^- \quad (3.4)$$

Ledwith et al. on the other hand suggested that in aqueous and alcoholic solutions that the solvent itself acts as the electron donor[19]. Their proposed scheme is shown in equations 3.5 and 3.6

$$MV^{2+} \xrightarrow{h\upsilon} \left[MV^{2+}\right]^* \xrightarrow{RCH_2OH} \left[MV^{+\bullet}, \dot{O}CH_2R, H^+\right] \quad (3.5)$$

$$\left[MV^{+\bullet}, \dot{O}CH_2R, H^+\right] \xrightarrow{MV^{2+}} 2MV^{+\bullet} + RCHO + 2H^+ \quad (3.6)$$

We have seen that it has been suggested by one group that the $MV^{+\bullet}$ radical is formed due to the electronically excited state of MV^{2+} reacting with Cl^- to produce a $Cl^\bullet$ radical. This mechanism would suggest that the addition of more halide to the system, via the addition of a salt such as sodium chloride, might well increase the observed rate of $MV^{+\bullet}$ photoproduction. Similarly, if the chloride were to be replaced with a less electronegative halide, easier to oxidise, such as iodide then there should be a subsequent increase in the rate of radical photoproduction. In either case this would give another method of controlling the extent of colour change, which in turn would present the opportunity for creating UV dosimeters with different UV sensitivities (for specific skin types etc.).

Thus, a standard mixture of 4 g PVA solution (10% w/w) and 20 mg of MV^{2+} was mixed with 90 mg of NaCl, increasing the number of chloride ions in the system by a factor of 10. This film was then irradiated with 4 mW cm^{-2} UVB and its absorbance at λ_{max} recorded with time. The results of this work are shown in figure 3-16 alongside a plot of a film containing no excess salt.

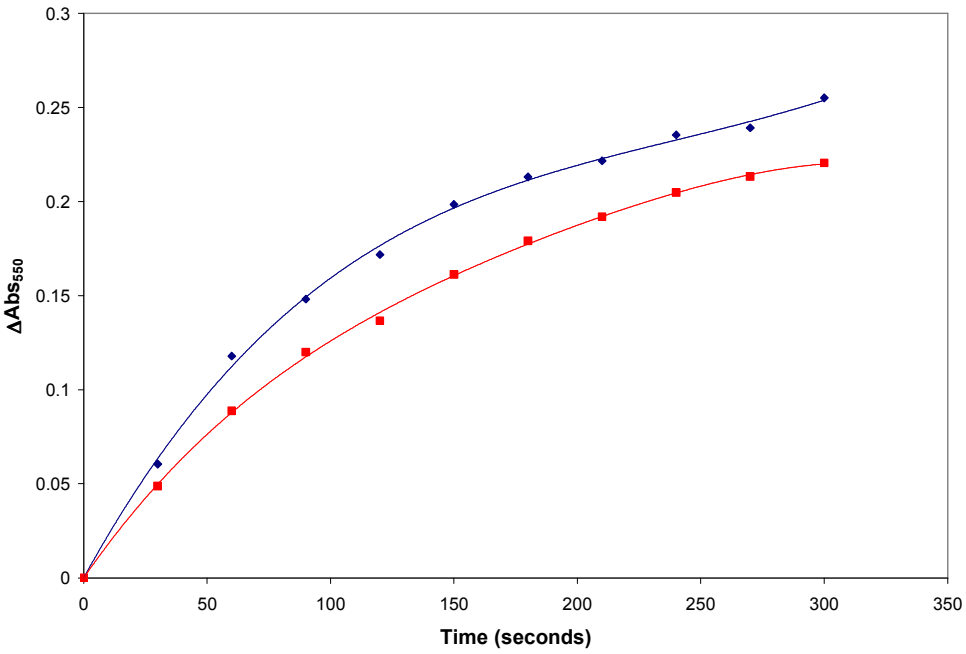

Figure 3-16 – The ΔAbs vs time plots of 2 sample MV^{2+}-PVA films. The first curve shows the response of a film containing an excess of NaCl. The second curve shows the response of a standard film with no additives.

The results shown in figure 3-16 suggest that the addition of a 10-fold excess of Cl^- to the system does produce an increase (albeit small) in the rate of reaction. These results lend some support for the suggestion that the key photochemical process is the photo-oxidation of Cl^- to $Cl^\bullet$ by $[MV^{2+}]^*$.

In order to test this mechanism further the Cl^- in $MVCl_2$ was substituted with iodide as follows: 0.15 g of methyl viologen were dissolved in 50 ml of methanol, 1.9 g of potassium iodide were then added and the solution stirred vigorously for 120 minutes. The KI was added in excess (20 molar equivalents) to drive the following reaction.

$$MV^{2+}.2Cl^-_{(Solv.)} + 2K^+I^-_{(Solid)} \leftrightarrow MV^{2+}.2I^-_{(Solv.)} + 2K^+Cl^-_{(Solid)} \quad (3.7)$$

After 120 minutes the solution was filtered to remove the insoluble KCl and any undissolved KI. The solvent was then removed and the crystals collected. The crystals were then placed into 50 ml of acetone and, after another 10 minutes, this solution was then filtered. The crystals were then washed through with acetone several times. This procedure was to ensure that all the KI had been removed. The dried crystals were then collected and a small quantity used to prepare a MV^{2+}/PVA/I^- solution as outlined previously. The spectra of a film prepared using this solution are shown in figure 3-17.

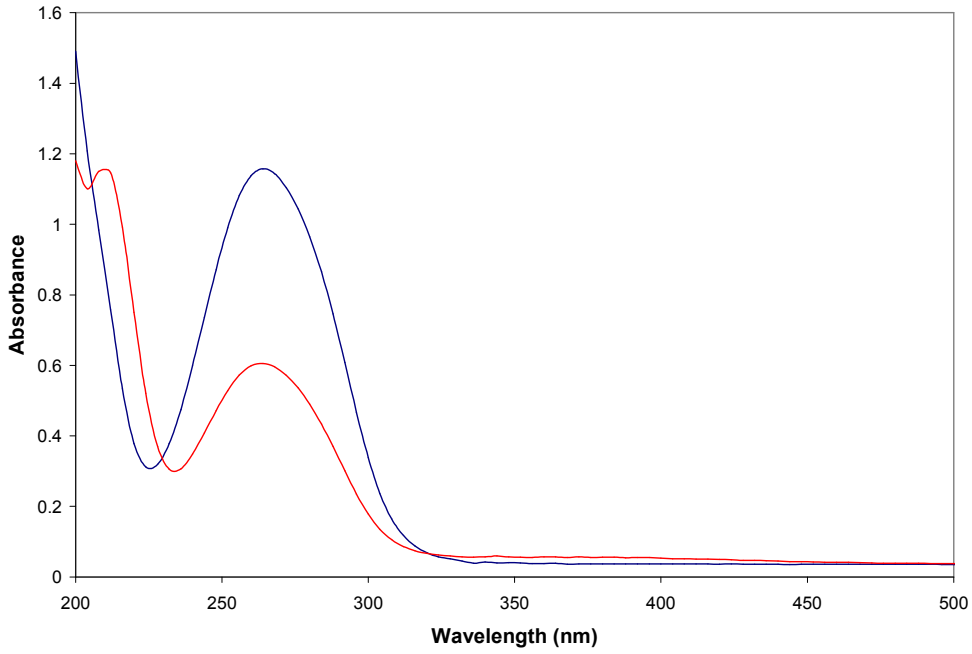

Figure 3-17 – UV/Vis spectra of 2 MV-PVA films. The spectra shown are for methyl viologen chloride and methyl viologen iodide.

Figure 3-17 shows that replacement of the chloride in $MV^{2+}Cl_2$ with iodide has produced a molecule that is less absorbing in the UVB to UVA regions, and has a peak at approximately 210 nm. The film also absorbs slightly in the visible region, giving the salt a noticeable yellowish colouration. Irradiation of this film with 4 mW cm^{-2} UVB leads to the ΔAbs curve shown in figure 3-18.

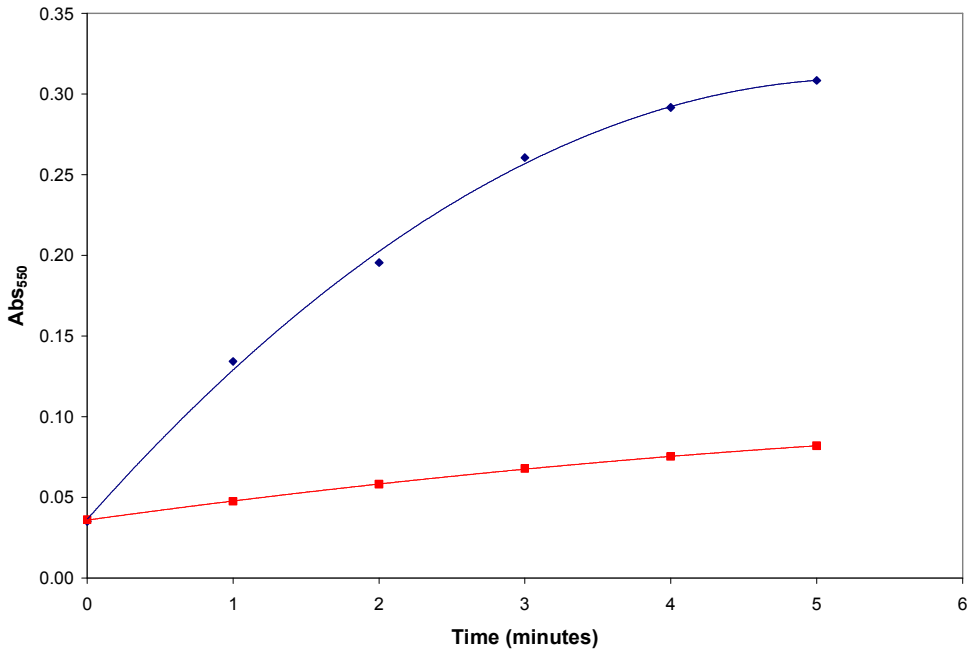

Figure 3-18 – A plot showing the Δabs curves at 550 nm of two different PVA films. The first contains methyl viologen chloride, and the second contains methyl viologen iodide. Both these films contain 5 phr of the respective dye and were irradiated using 4 mW cm^{-2} UVB light.

Examination of figure 3-18 reveals that the addition of iodide to the system, in place of the chloride already present, actually retards the UV absorbance and subsequent colour change of our PVA film. This is in agreement with some photolysis work carried out by Ebbesen[25]. The results of this work suggest that the substitution of the halide provides another method of controlling the rate of colouration.

3.1.7 Other Electron Donors

In another set of experiments, electron donors other than halides were added to the system to promote the reduction of the MV^{2+}. Thus, MV^{2+}/PVA films were prepared containing 5 molar equivalents of EDTA or TEOA and figure 3-19 illustrates the effect on the UV-induced colour change for these films.

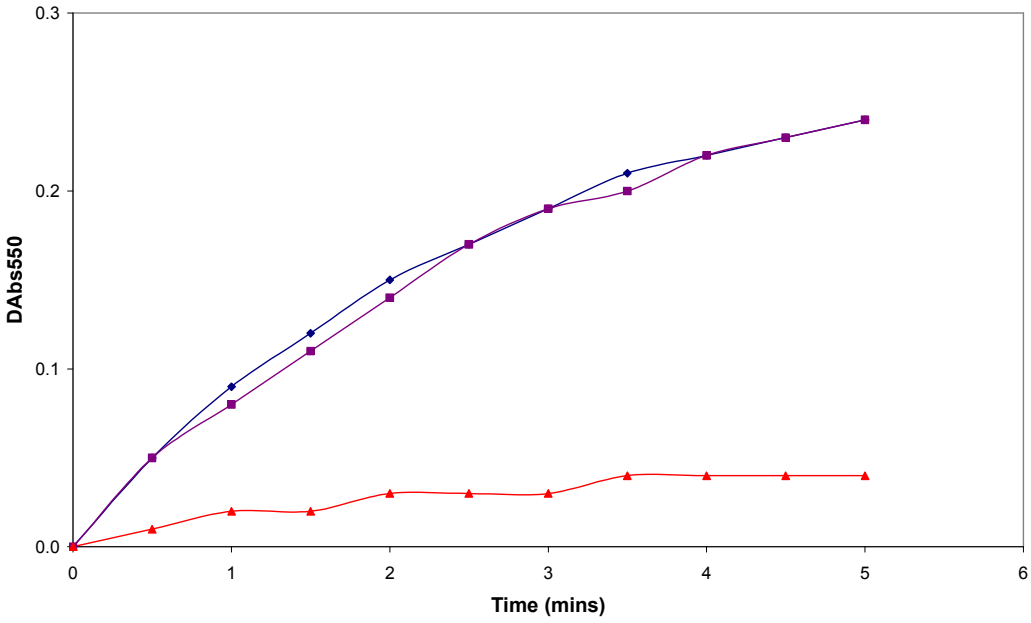

Figure 3-19 – ΔAbs plots, at 550 nm, of MV^{2+}-PVA films irradiated with 4 mW cm^{-2} UVB light. The responses shown are for a standard film, a film containing 25 phr EDTA, and a film containing 25 phr TEOA.

The addition of excess EDTA to the PVA film causes no change in the observed response whereas TEOA appears to actually retard the rate of reaction. However, TEOA is a liquid and may serve as a plasticizer for the film, allowing oxygen to enter more freely and thus promote the reaction of $MV^{+\bullet}$ with environmental oxygen. To test this theory the experiment was repeated for a MV^{2+}/PVA/TEOA film but after 5 minutes the UVB lamp was switched off and the spectrometer left to record the observed spectra. Figure 3-20 shows the variation in ΔAbs_{550} as a function of time and reveals that a MV^{2+}/PVA film containing TEOA quickly loses its colour after irradiation with UV is stopped. This contrasts quite sharply with what has been observed in MV^{2+}/PVA-only films and indicates that TEOA does indeed act as plasticiser, allowing oxygen into the film to react with any photogenerated $MV^{+\bullet}$.

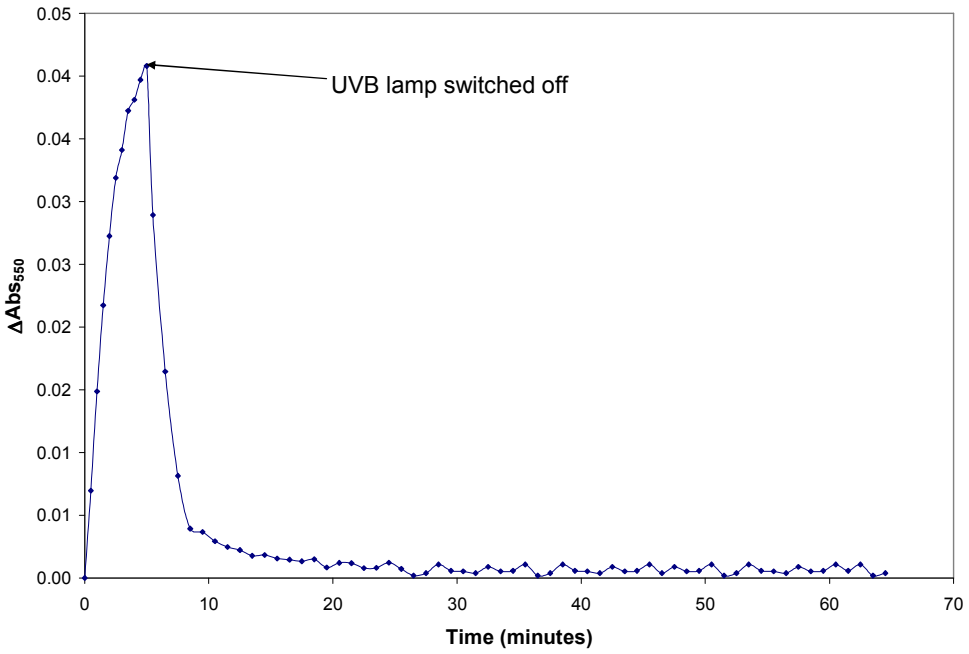

Figure 3-20 – A plot showing the change in absorbance, at 550 nm, of a MV^{2+}-PVA film containing 25 phr TEOA. The film was irradiated for 5 minutes with 4 mW cm^{-2} UVB and then the lamp was switched off.

3.2 Benzyl Viologen

3.2.1 Spectral Properties

According to Kamogawa[9], it is easier to convert benzyl viologen (BV^{2+}) to the reduced radical by UV irradiation than it is with MV^{2+}. This may be expected as BV^{2+} has a higher redox potential (-0.359V) than MV^{2+} (-0.446V). This suggests that the BV^{2+} will be easier to reduce and thus harder to oxidise. The decision was made to assess the spectral properties of BV^{2+} and, if it behaved in a similar fashion to MV^{2+} and proved to be more stable, it would be used as the bases of an erythemal sensor. Thus a comparison was made of the absorbance spectra of both MV^{2+} and BV^{2+} in PVA at 5 phr, the results of which are shown in figure 3-21.

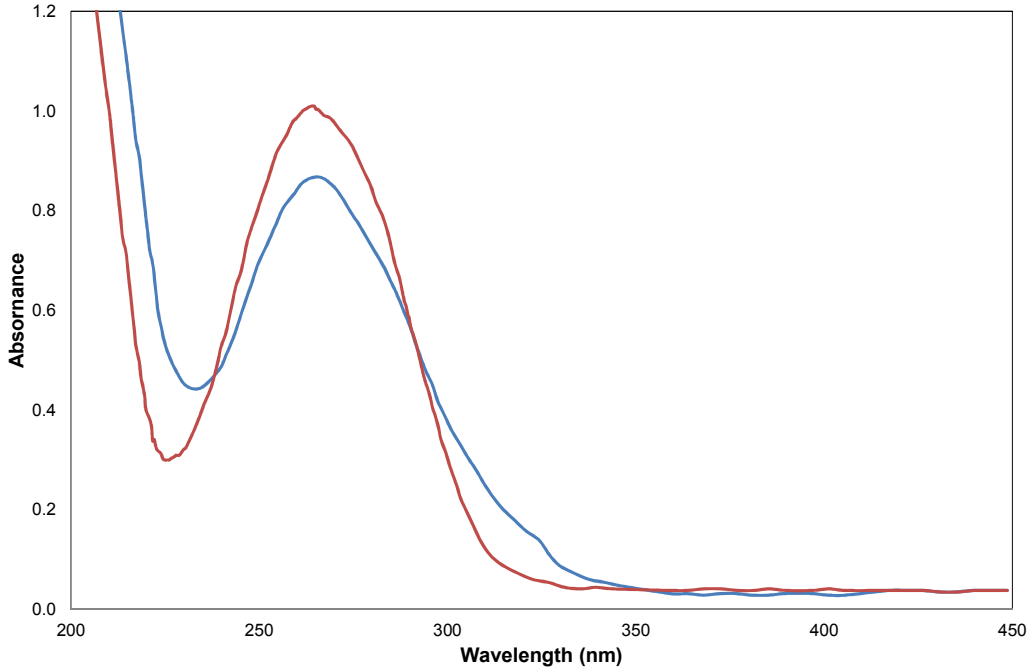

Figure 3-21 – A plot showing the absorbance spectra of methyl viologen (MV^{2+}) and benzyl viologen (BV^{2+}) in a PVA film. Both species are present at 5 phr. λ_{max} in PVA is 263nm for MV^{2+} and 266nm for BV^{2+}. The extinction coefficient for MV^{2+} at λ_{max} is ~16,000 cm^2 mol^{-1}, while the value for BV^{2+} is ~18,000 cm^2 mol^{-1}.

At this concentration the spectra of MV^{2+} and BV^{2+} are reasonably similar to one another. It may be reasoned then, assuming they both respond in the same way to UV, that the performance of the two systems will be very similar.

3.2.2 Response and Recovery

Having established that the BV^{2+} system had similar spectral characteristics to a MV^{2+}/PVA film the next step was to study its response to UV and ensure that it did indeed behave in a similar manner. To do this the same procedure as used previously was followed: a PVA film containing 5 phr BV^{2+} was exposed to 4 mW cm^{-2} UVB light and its spectrum recorded every 60 seconds. Irradiation with the UVB was then stopped and the spectrometer continued to record the absorbance spectra every 60 seconds. The results of this work are shown in figures 3-22 and 3-23.

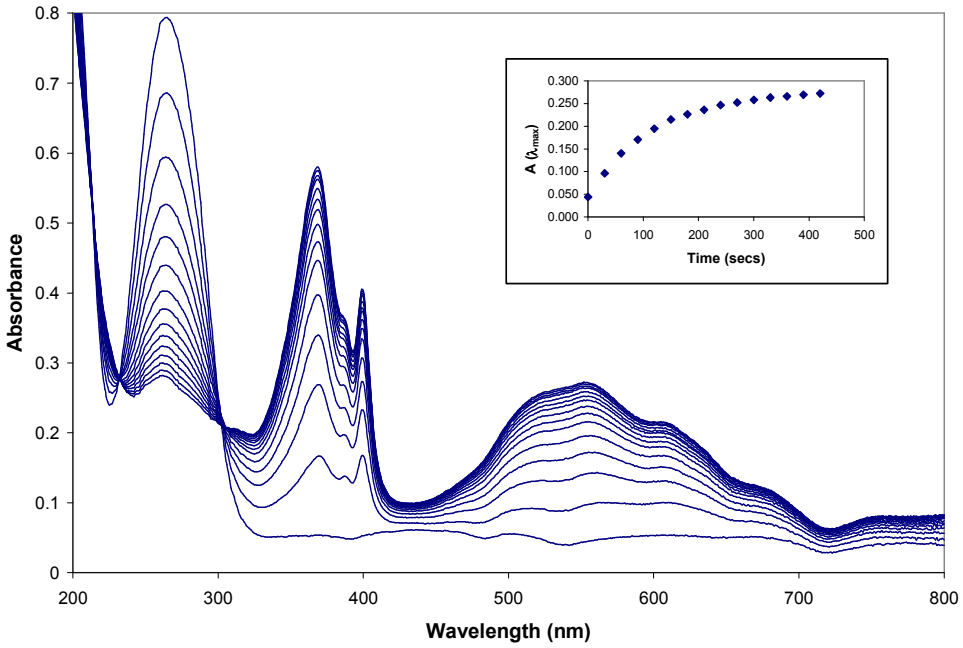

Figure 3-22 – The UV-Vis spectra of a BV^{2+}-PVA film after irradiation with 4 mW cm^{-2} UVB light. The inset shows the change in absorbance at λ_{max} with time.

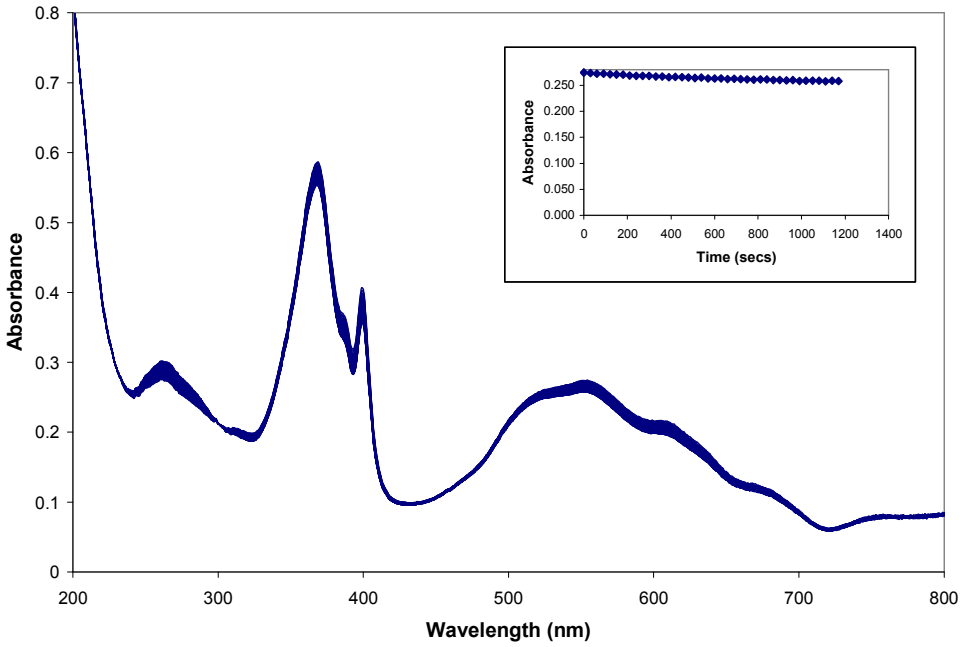

Figure 3-23 – The UV-Vis spectra of a BV^{2+}-PVA film after irradiation with 4 mW cm^{-2} UVB light has ended. The inset shows the change in absorbance at λ_{max} with time.

Examination of figures 3-22 and 3-23 shows that the BV^{2+} system does appear to respond in a similar manner to MV^{2+} i.e. a similar absorbance change after 10 minutes and is shown to be stable for at least 20 minutes in the dark under ambient conditions. In fact, if anything, the BV^{2+}/PVA system seems to be more stable than the MV^{2+}/PVA films.

3.2.3 An Erythemal sensor

Having shown that a viologen based system could be successfully used as a dosimeter for UV the next step was to prove that the same films could be used to measure erythemal levels of radiation. It was thought that the type of sensor being developed would be well suited to this task as it responds very well to UVB, the major source of erythemal harm, with little or no response to UVA.

A brief study of the UVB output of the UVB light sources used in this work, measured using a power meter, and the UV index values associated with the sun (1-10) – measured using a SolarMeter – revealed a direct a relationship between the two (see figure 3-24). However, the UVB irradiance values are typically 20 times lower than used in the characterisation study of these films. Thus, in order to ensure a clear and rapid colour change at a typical UVI value of 5 (a UK summer's day), a thicker (40mm) BV^{2+}/PVA film was used. The variation in Δabs_{550} vs time profile for this thick BV^{2+}/PVA films as a function of UVI is illustrated in figure 3-25.

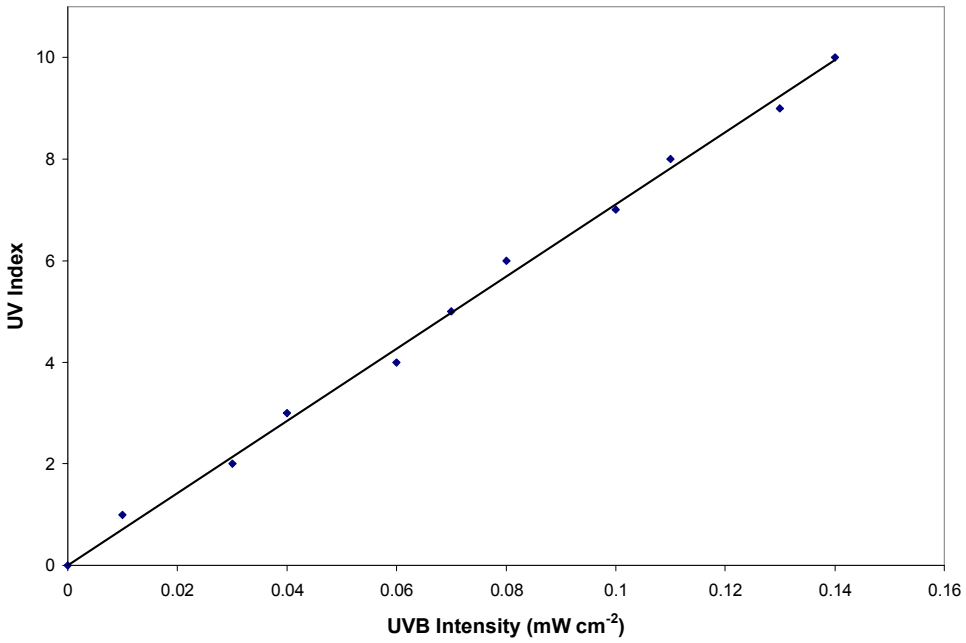

Figure 3-24 – A plot showing the relationship between UV index and UV-B intensity. UVI measurements were made with an Optix SafeSun UV meter. UV-B measurements were made with a Ultra-Violet Products UV-B sensor.

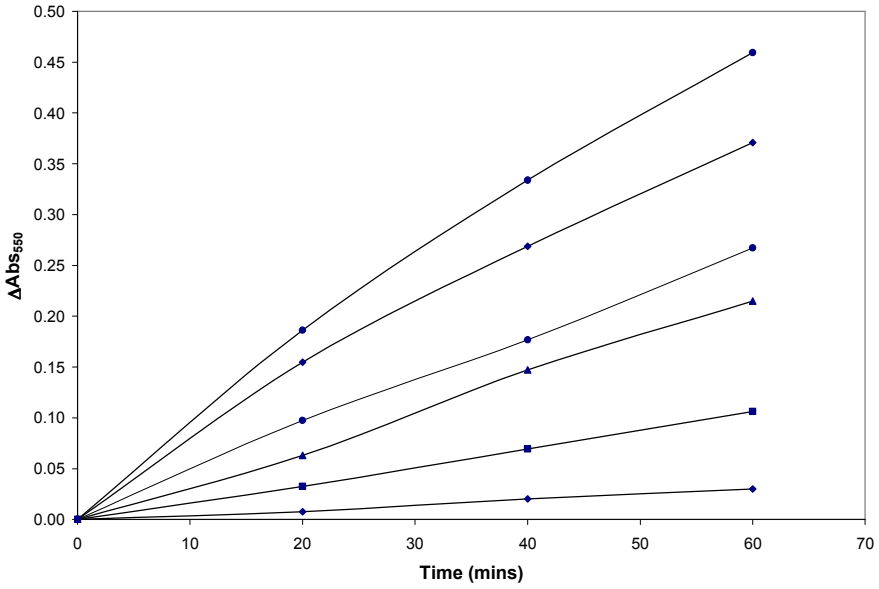

Figure 3-25 – A plot showing the change in absorbance of a 40 μm BV^{2+}-PVA film on exposure to UVB light at, in ascending order, UVI 1, 2, 4, 6, 8, and 10.

Samples of this thick BV^{2+}/PVA film were exposed to UVI 5 and 10 using a solar simulator and their absorbances at 550 nm measured when the SafeSun meter recorded that the MED value increased by 0.1. The results of this work are illustrated in figures 3-26 and 3-27.

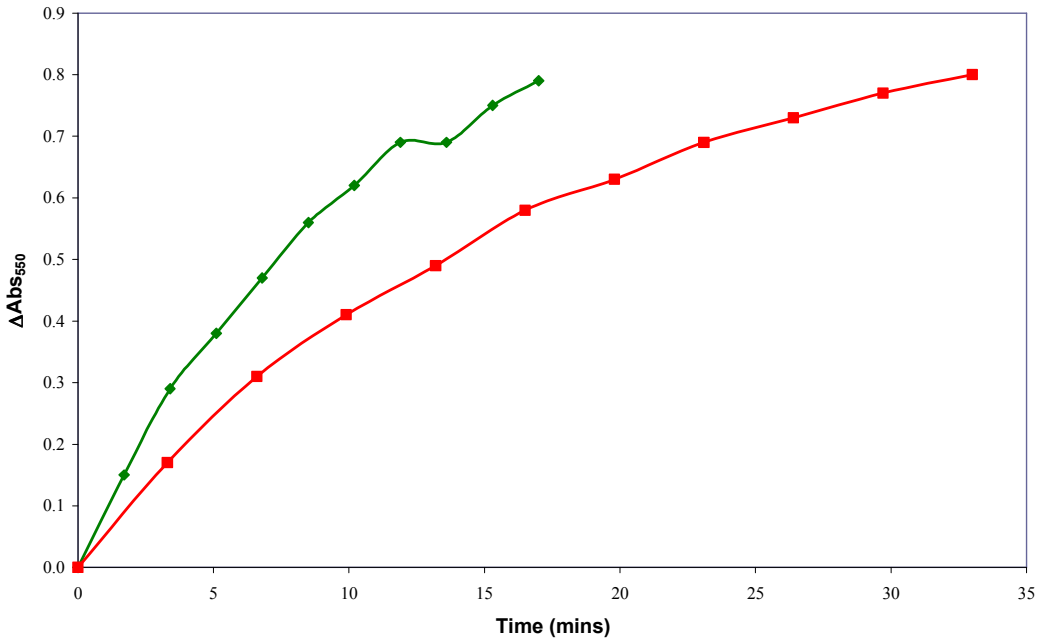

Figure 3-26 – A plot showing the change in absorbance at λ_{max} (550 nm) of BV^{2+}-PVA films with time. The curves shown were obtained when films were exposed to UVI 5 solar simulator light, and UVI 10 light also from a solar simulator.

As expected, from the data in figure 3-26, the observed colour change associated with each film increased with increased exposure to UV light and the plot of data in the form of ΔAbs vs MED for each of the samples, alongside the same curve for a MV^{2+}-PVA film in figure 3-27, yield a common curve. While the MV^{2+}-PVA film yields a slightly higher colour change (and does so consistently) it is felt the BV^{2+}-PVA film is still the better option due to its higher resistance to oxidation.

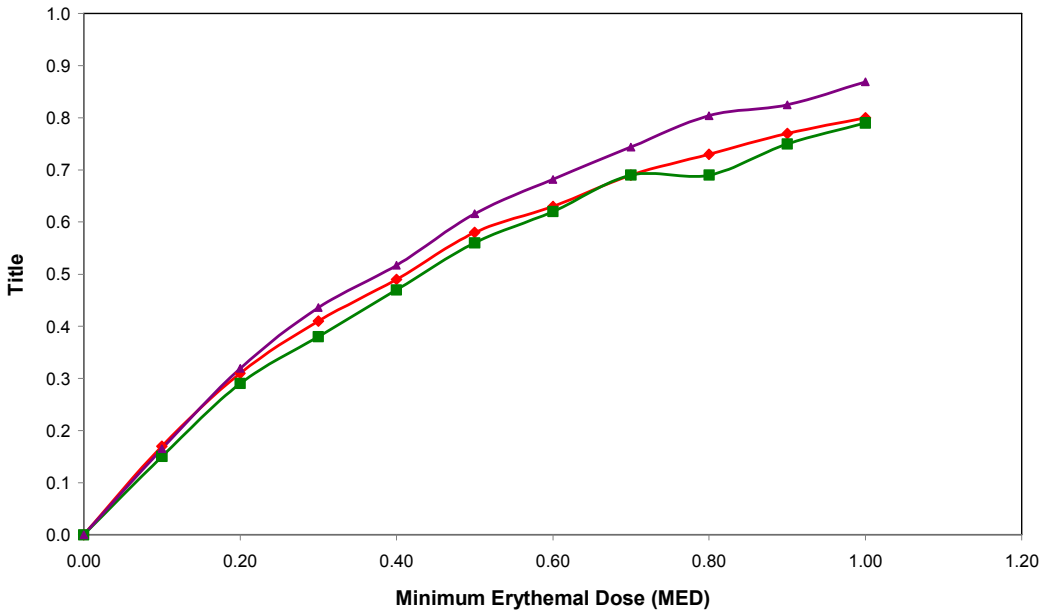

Figure 3-27 – A diagram showing the response of 40 µm BV^{2+}-PVA films. The plot shows the change in absorbance at 550 nm with MED for three different films. The plotted lines show films that were exposed to UVI 5 solar simulator light, and UVI 10 solar simulator light. Also shown is the same curve obtained for a 40 µm MV^{2+}-PVA film.

Finally, the response (ΔAbs_{550}) of the thick (40 mm) BV^{2+}/PVA film were tested as a function of MED from solar UV light (1st Sept 2005; Glasgow 12:00 – 13:30) and the results of this work are illustrated in figure 3-28. The variation observed is identical to that observed in the lab using UVB lamps (see figure 3-27). These results indicate these films have potential as UV dosimeters for indicating the onset of erythema.

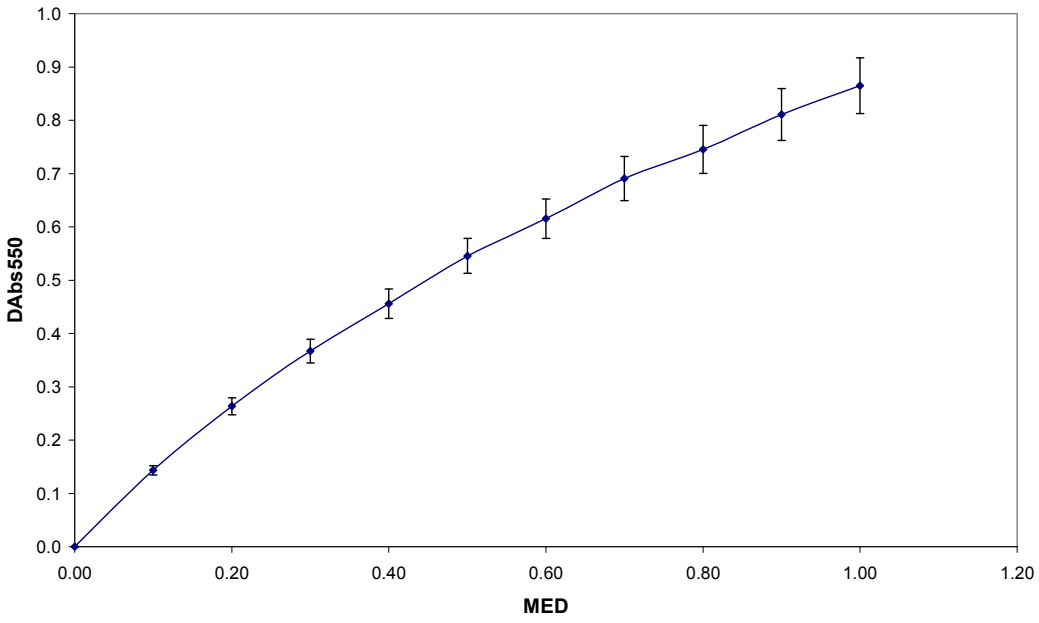

Figure 3-28 – A plot showing the average change in absorbance as a function of the erythemal dose received from sunlight of a 40 μm BV^{2+}-PVA film.

The experiment shown above was performed on the 1st of September 2005, between 12:00 and 13:30 in the afternoon. During this period the UVI remained fairly constant at 3, with an increase to 4 towards the end of the run. The total exposure time was 53 minutes, which lies well within the 56 – 42 minutes suggested for these UVI values in chapter 1. As can be seen the average ΔAbs value reached after an MED of 1 was approximately 0.8.

3.3 Conclusions

It has been shown that a UV and erythemal dosimeter can be developed using the viologens in a water soluble polymer system. This system responds uniformly to differing intensities of solar UV and is stable in the absence of oxygen.

Problems faced by the system are caused largely by the encapsulating medium. Permeability to oxygen ensures that there is little to no observable reaction. Solubility in water also makes the system impractical for real world use.

Attempts to place the viologen species into a non-aqueous environment were unsuccessful and generated no useful data.

To improve this system it is recommended to find a method of encapsulating the viologens in a non-aqueous, oxygen impermeable system which is transparent to UV light.

It is also suggested that more work is required to make this a practical device. At the moment colour is monitored by a spectrometer and the endpoint can easily be identified once defined. Monitoring a gradual colour change like this by eye, on the other hand, leaves interpretation of the end point up to the user. One suggestion is a "traffic-light" system in which different materials provide different colour changes at set points during a period of exposure.

3.4 References

1. Darwent, J. R.; Kalyanasundaram, K.; Porter, G., *Proceeds of the Royal Society of London* **1980,** *373*, 179

2. Holton, D.; Windsor, M. W.; Parson, W. H.; Gouterman, M., *Photochemistry and Photobiology* **1978,** *28*, 951

3. Gurunathan, K.; Maruthamuthu, P.; Sastri, M. V. C., *Internation Journal of Hydrogen Energy* **1997,** *22* (1), 57

4. Noyori, R.; Kurimoto, I., *Journal of the Chemical Society: Chemical Communications* **1986**, 1425

5. Rieger, A. L.; Edwards, J. O.; Levey, G., *Photochemistry and Photobiology* **1983,** *38*, 123

6. Johansen, O.; Launikonis, A.; Loder, J. W.; Mau, A. W.; Sasse, W. H. F.; Swift, J. D.; Wells, D., *Australian Journal of Chemistry* **1981,** *34*, 2347

7. Czege, J.; Bagyinka, C. S.; Kovacs, K. L., *Photochemistry and Photobiology* **1989,** *50*, 697

8. Sweetser, P. B., *Analytical Chemistry* **1967,** *39*, 979

9. Kamogawa, H.; Masui, T.; Nanasawa, M., *Chemistry Letters* **1980**, 1145

10. Simon, M. S.; Moore, P. T., *Journal of Polymer Science: Part A: Polymer Chemistry* **1975,** *13*, 1

11. Kamogawa, H.; Amemiya, S., *Journal of Polymer Science: Part A: Polymer Chemistry* **1985,** *23*, 2413

12. Kamogawa, H.; Kato, A.; Mizuno, J., *Bulletin of the Chemical Society of Japan* **1992,** *65*, 623

13. Kamogawa, H.; Kikushima, K.; Nanasawa, M., *Journal of Polymer Science: Part A: Polymer Chemistry* **1989,** *27*, 393

14. Kamogawa, H.; Masui, T.; Amemiya, S., *Journal of Polymer Science: Part A: Polymer Chemistry* **1984,** *22*, 383

15. Kamogawa, H.; Satoh, S., *Journal of Polymer Science: Part A: Polymer Chemistry* **1988,** *26*, 653

16. Kamogawa, H.; Sugiyama, M., *Bulletin of the Chemical Society of Japan* **1985,** *58*, 2443

17. Kamogawa, H.; Suzuki, T., *Journal of the Chemical Society: Chemical Communications* **1985**, 525

18. Chen, Y. L.; Guan, Y. J.; Mai, Y. L.; Li, W.; Liang, Z. X., *Journal of Macromolecular Science* **1988,** *A25*, 201

19. Ledwith, A.; Russell, P. J.; Sutcliffe, L. H., *Proceeds of the Royal Society of London* **1973,** *332*, 151

20. Zen, J.-M.; Lo, C.-W., *Analytical Chemistry* **1996,** *68*, 2635

21. Gong, M.-S.; Lee, M.-H.; Rhee, H.-W., *Sensors and Actuators B* **2001,** *73*, 185

22. Ogawa, T.; Nishikawa, H.; Nishimoto, S.-I.; Kagiya, T., *Radiation Physics and Chemistry* **1987,** *29* (5), 353

23. Chongmok, L.; Young Mi, L.; Myung Sun, M.; Sang Hee, P.; Joon Woo, P.; Kyung Gon, K.; Jeon, S.-J., *Journal of Electroanalytical Chemistry* **1996,** *416*, 139

24. Pauly, S., In *Polymer Handbook*, 3rd ed.; Brandrup, J.A.I., E H, Ed. Wiley Interscience: New York, 1989; pp 435

25. Ebbesen, T. W.; Manring, L. E.; Peters, K. S., *Journal of the American Chemical Society* **1984,** *106*, 7400

4 A tetrazolium based UV dosimeter

The tetrazolium salts are organic heterocycles with the basic structure shown below.

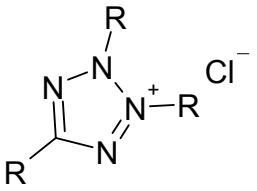

Figure 4-1 – The structure of the tetrazolium salts, where R = Me, or another organic group.

These water soluble salts have been show to undergo ready reduction to form partially soluble formazans. The tetrazolium salts are generally colourless to pale yellow in solution and the formazans are mostly coloured species. This reaction is outlined in figure 4-2.

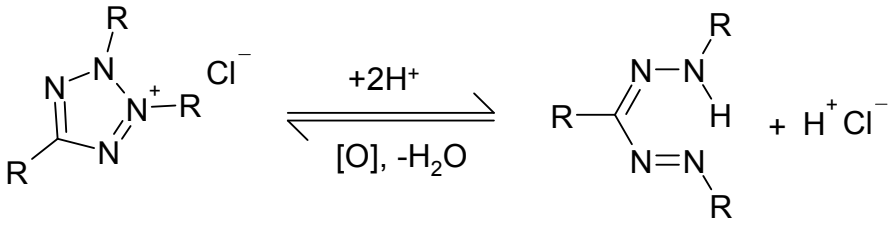

Figure 4-2 – Reduction of a tetrazolium salt to the equivalent coloured formazan.

This colour changing reaction has made the tetrazolium salts a popular choice as indicators for the evaluation of bacterial metabolic activity[1] as well as the detection of diseases such as tuberculosis[2]. A look through the literature finds numerous references to the "Tetrazolium Test" or the "Nitro Blue Test"[3-7]. More often than not these tests involve the addition of a tetrazolium salt to a cell culture, with the premise being that the dye will change colour if specific circumstances are met within the cell. Assuming

that nothing else in the cell under study affects the salt, this gives a quick visual indication of cell activity.

As well as occurring via electron transfer in chemical and biological environments, the tetrazoluims can also be reduced to formazans with radiation. Much work in this area has been carried out using triphenyl tetrazolium chloride (TTC)[8-10]. Dosimeters for radiation monitoring have been proposed as aqueous solutions and agar gels of TCC[8]. Polymeric films containing TTC have also been investigated specifically for ultraviolet applications[10]. The doismetery characteristics of nitro blue tetrazolium solutions and films have also been characterised for high dose and pulsed radiation sources.

4.1 Neotetrazolium Chloride

As stated many of these salts are used as redox indicators, with no real preference seeming to be given to any. The first step in the work therefore was to test each of the commercially available tetrazoliums and determine which displayed the greatest response to UV. The best of these would be compared against tetraphenyl tetrazolium chloride (TTC); a material which has already been described as a dosimeter, although with some unusual behaviour. The materials to be tested were neotetrazolium (NTC), tetrazolium blue (TB), tetrazolium violet (TV) and iodotetrazolium (ITC) – all chloride salts, the structures of which are shown in figure 4-3. Films of each salt in PVA were prepared as outlined previously and then exposed to 4 mW cm^{-2} UVB. Each film was exposed for 30 minutes and their spectra recorded every 5. The obtained are shown in figures 4-4 to 4-7, with a direct comparison plotted in figure 4-8.

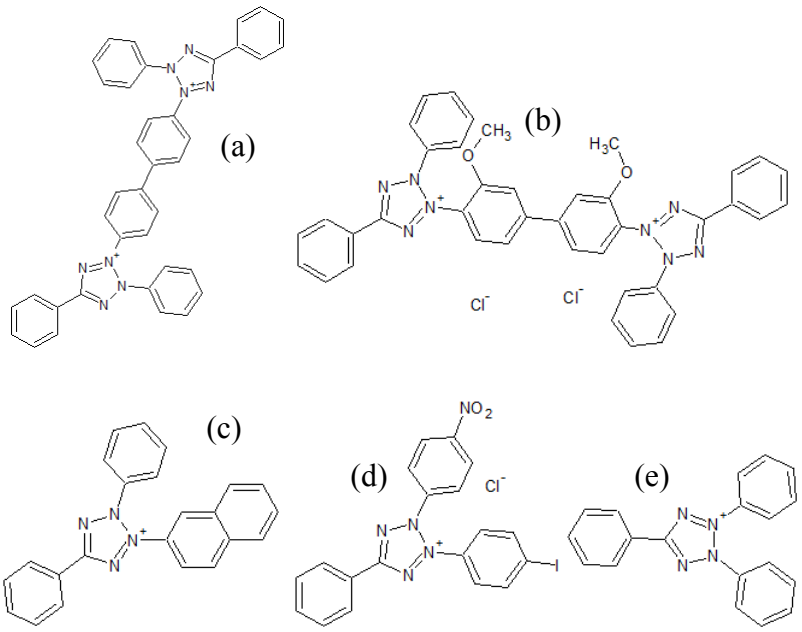

Figure 4-3 – The structures of the tetrazolium salts compared in this study. These are (a) neotetrazolium chloride, (b) tetrazolium blue, (c) tetrazolium violet, (d), iodotetrazonium chloride, and (e) triphenyl tetrazolium chloride.

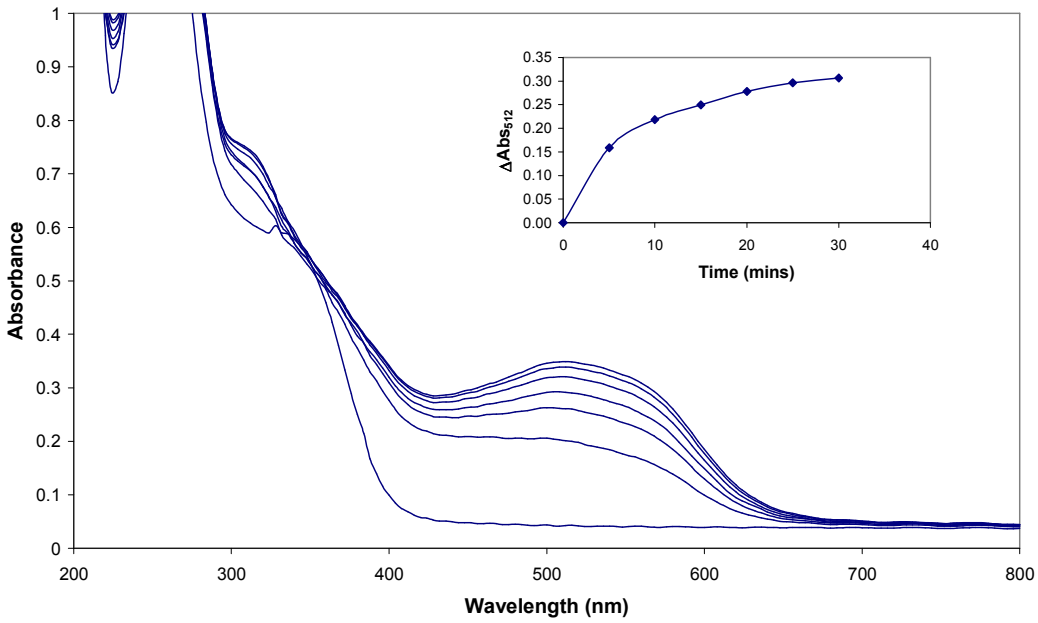

Figure 4-4 – The response profile of a PVA film containing 5phr neotetrazolium chloride after exposure to 4 mW cm^{-2} light.

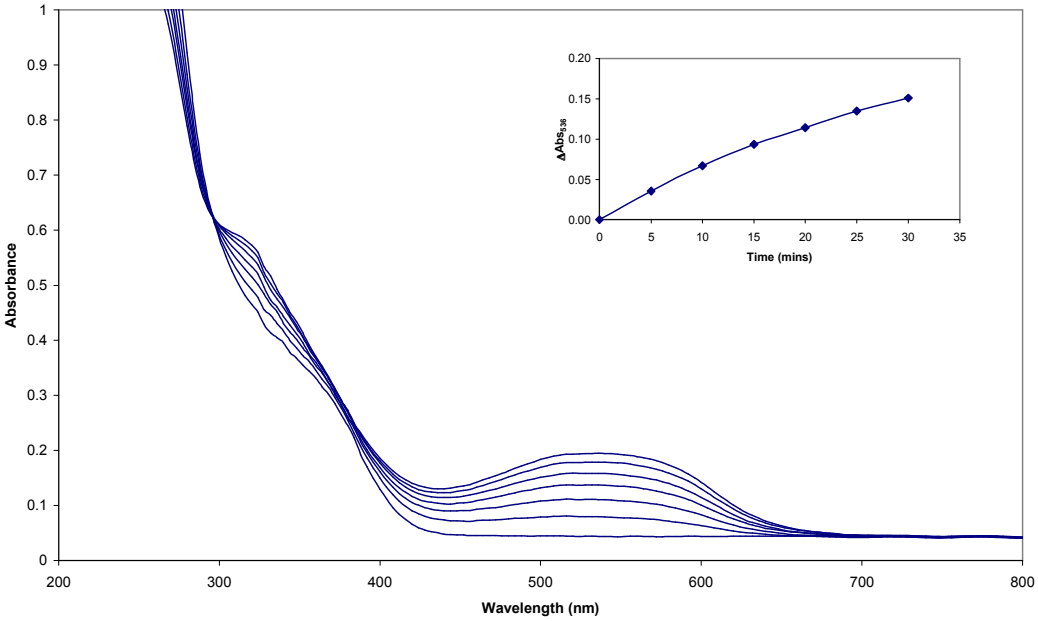

Figure 4-5 – The response of a PVA film containing 5phr tetrazolium blue after exposure to 4 mW cm^{-2} light.

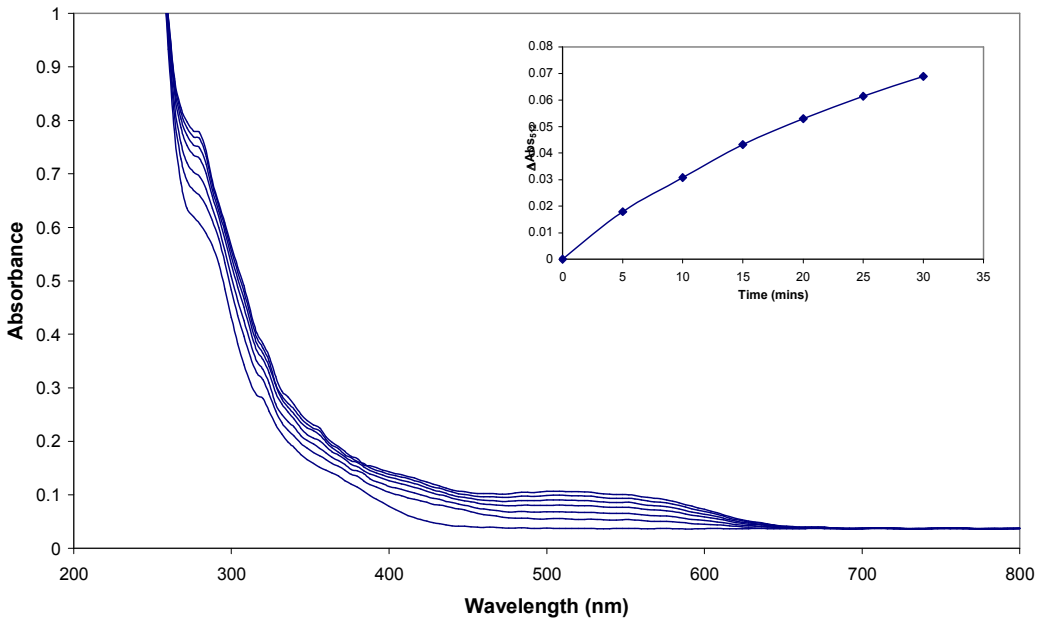

Figure 4-6 – The response of a PVA film containing 5phr tetrazolium violet after exposure to 4 mW cm^{-2} light.

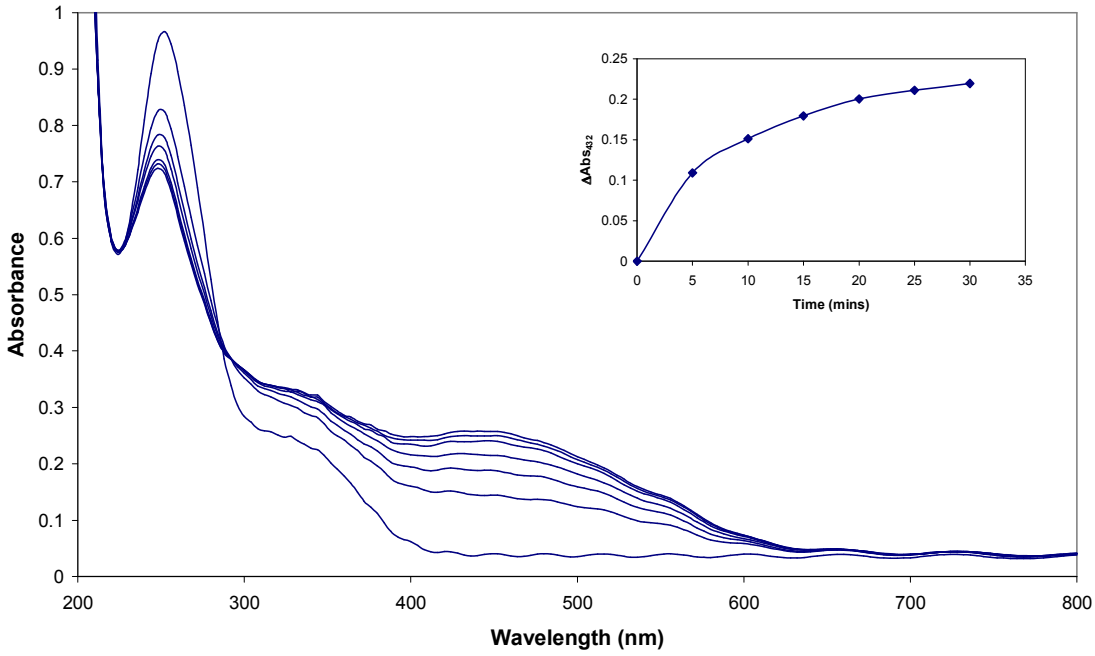

Figure 4-7 - The response of a PVA film containing 5phr iodotetrazolium chloride after exposure to 4 mW cm^{-2} light.

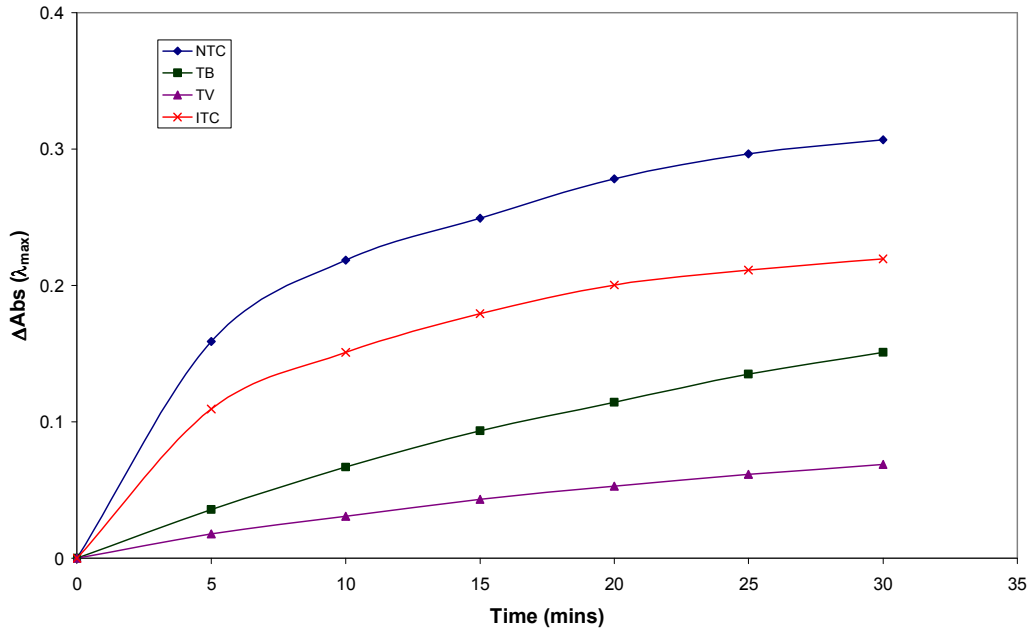

Figure 4-8 – A plot comparing the ΔAbs vs Time profiles of 4 different tetrazolium salts when irradiated with 4 mW cm^{-2} UVB light.

4.1.1 Comparison with TTC

Of the materials outlined above the neotetrazolium chloride (NTC) clearly displays the greatest response to UVB. This material was therefore chosen as the basis for the development of a dosimeter, the first of which was the comparison with an existing dosimeter material in tetraphenyl tetrazolium chloride (TTC). Each of these materials was dissolved at 5 phr in 10 % PVA and spun at 1200 rpm. Each was then exposed to 4 mW cm^{-2} UVB as before. The results are shown in figure 4-9.

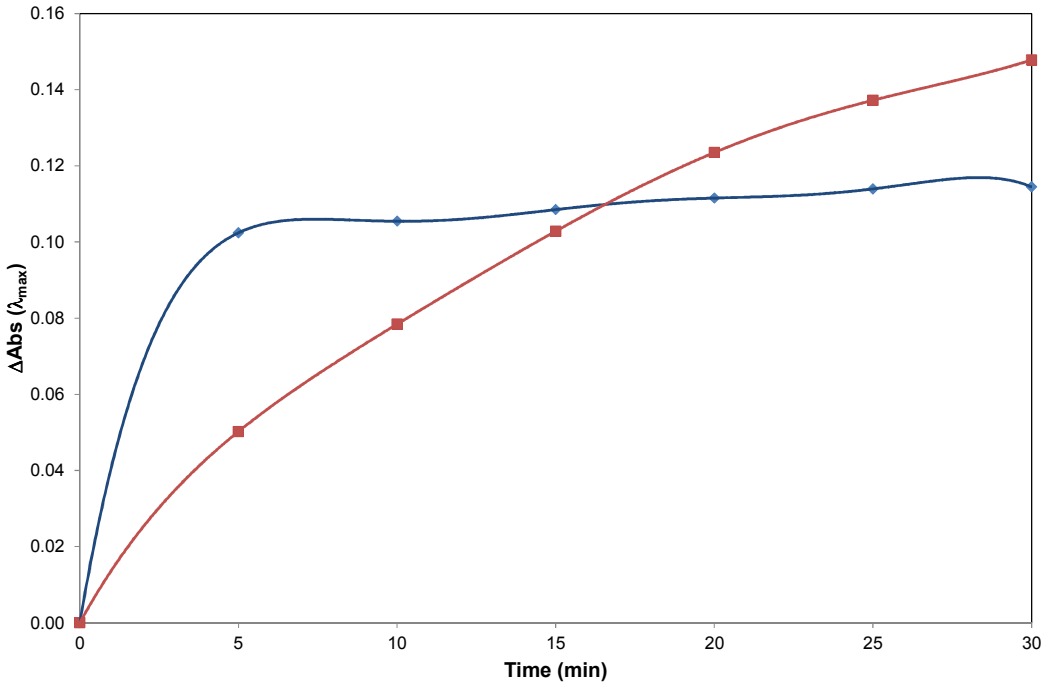

Figure 4-9 – The response curves of 5 phr TTC and NTC in PVA under 4 mW cm^{-2} UVB light. The curves shown are for TTC and NTC respectively.

Examination of figure 4-9 reveals that the NTC is slower to react than the TTC, which reaches maximum absorbance in 5 minutes or less (This is also slower than the viologen system which reached max absorbance in approx 10 minutes). However we can see that the NTC reaches a higher absorbance at the end of the irradiation period and still does not appear to have reached its maximum. This is seen as preferable as it may allow us a greater deal of control over the system (the suggestion being that we have more options to increase the observed colour change than we have of decreasing it).

4.1.2 Oxygen Sensitivity

One of the important problems associated with the viologen sensors is their sensitivity to oxygen. Placement in an oxygen permeable polymer led to almost no colour change upon exposure to UV, or a rapid loss of colour once irradiation had finished. If the tetrazolium systems are to be shown to be better they must show a greater ability to keep their colour. As a quick test of this we made 5 phr solutions of NTC in PVA and

HEC. PVA is known to be a good oxygen barrier, while HEC has been shown to be oxygen permeable. If oxygen is going to be a problem it is expected that the HEC film will show almost no colour change or show a greater decrease in colour over time when compared to the PVA film. These films were irradiated for half an hour under 4 mW cm^{-2} UVB then placed in a spectrometer. Their absorbance at 550 nm was monitored over 12 hours after irradiation.

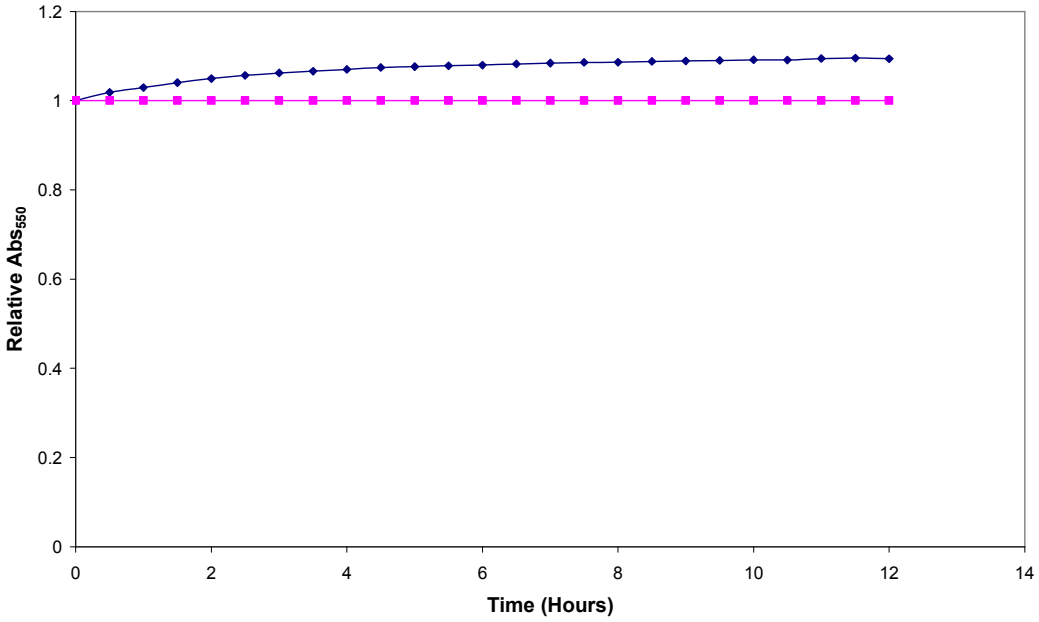

Figure 4-10 – The absorbance at 550 nm of PVA and HEC films containing 5 phr NTC over 12 hours. The films had previously been irradiated with 4 mW cm^{-2} UVB for 30 minutes.

Figure 4-10 shows that neither HEC or PVA films shows any significant decrease in the colour of the system with time, which would seem to suggest that the oxygen in air is having little effect on this system. What is strange to note is that the PVA film seems to *increase* in colour over time, a phenomenon that hasn't been reported before.

4.2 Response to UV light

Having chosen our dye the next step was to evaluate its behaviour in response to UV light. First would be a test of its response to different wavelength regions of light, specifically UVA, UVB and UVC (all at 4 mW cm^{-2}). Once this was completed we then tested the sample under different intensities of light at each wavelength, in order to ensure there was a notable difference in the colour change with changing intensity. The results obtained are shown in the following diagrams.

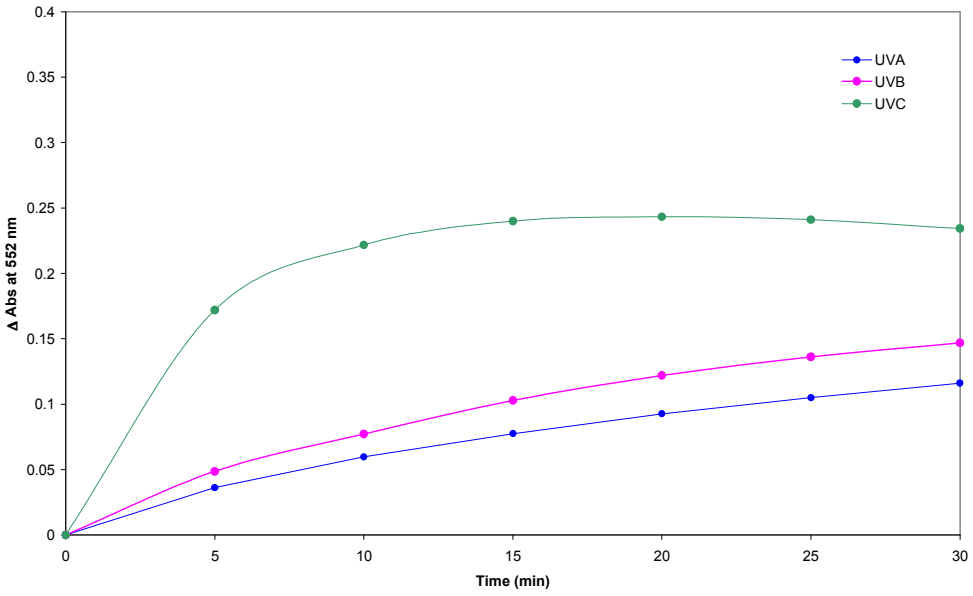

Figure 4-11 – A comparison of the response of the 5 phr NTC film to the different wavelength regions of UV. Response shown are those at 552 nm.

Figure 4-11 shows a clear trend in the response of these dyes to the different wavelengths of UV. As we move from UVA to UVC we see an increase in the extent of colouration. This is to be expected as we can see, from a sample spectrum, that the NTC absorbs more light in the UVC than in any other region.

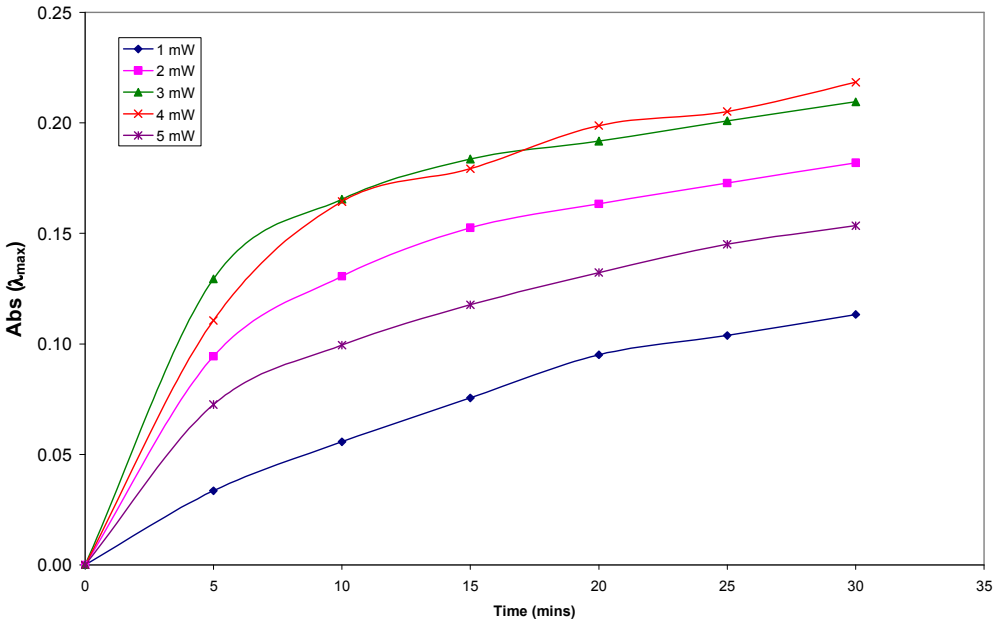

Figure 4-12 – A plot showing the change in absorbance at λ_{max} (550 nm) of a 5 phr NTC film under varying intensities of UVA light.

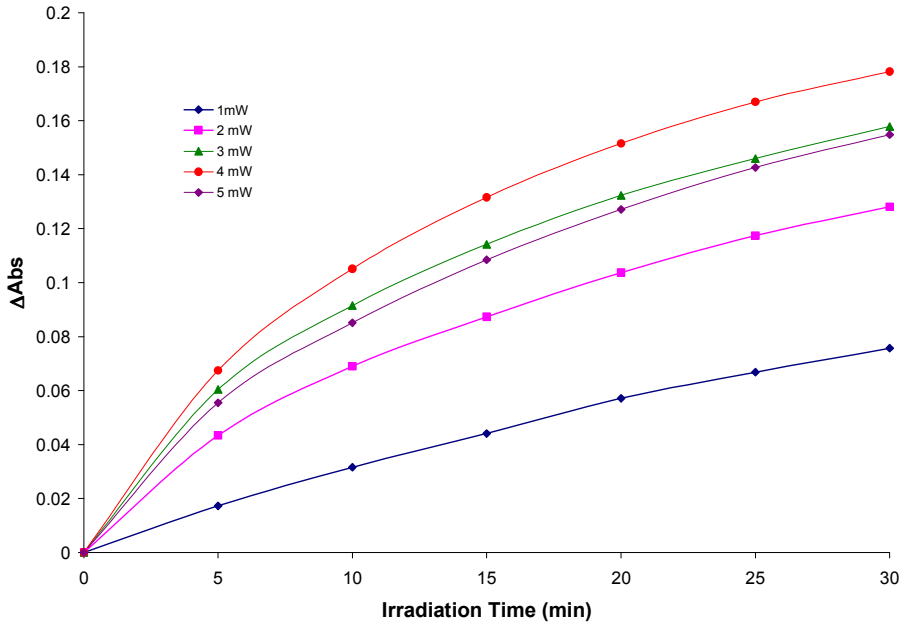

Figure 4-13 – A plot showing the change in absorbance at l_{max} (550 nm) of a 5 phr NTC film under varying intensities of UVB light.

Looking at figures 4-12 and 4-13 we can see that the response of the NTC definitely changes with varying intensity of incident light. There are some anomalous results, however. Under UVA and UVB light for example we see an overall decrease in the rate when the sample is exposed to 5 mW cm^{-2} light. UVC on the other hand shows a general decrease in the maximum absorbance value reached at intensities above 2 mW cm^{-2} (not shown). These experiments have been repeated and, as of current writing, have been shown to be reasonably consistent. The reason for this drop in observed absorbance at high intensities of all UV regions is not yet understood. It is worth noting that UVC is not of immediate concern and that the UVB intensities used are very high when compared to the erythemal levels we wish to detect.

4.2.1 Dye Concentration and Film Thickness

We have established that NTC in PVA changes colour under UV light and its response depends on the wavelength and intensity of the incident light. The next step is to determine how we can control the extent of colour change, as some degree of control will be required if we are to develop dosimeters for specific skin types. The easiest ways of doing this involve altering the dye concentration and the film thickness.

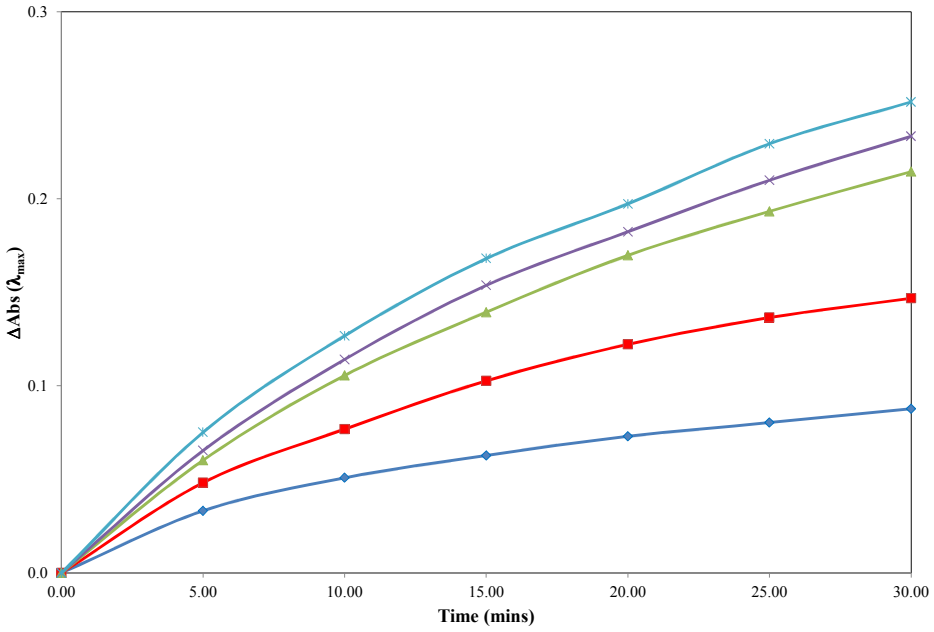

Figure 4-14 – A plot showing the change in absorbance of PVA films containing varying concentrations of NTC under 4 mW cm^{-2} UVB light. The plots shown are for – in increasing order – 2.5, 5, 10, 15 and 20 phr NTC in PVA.

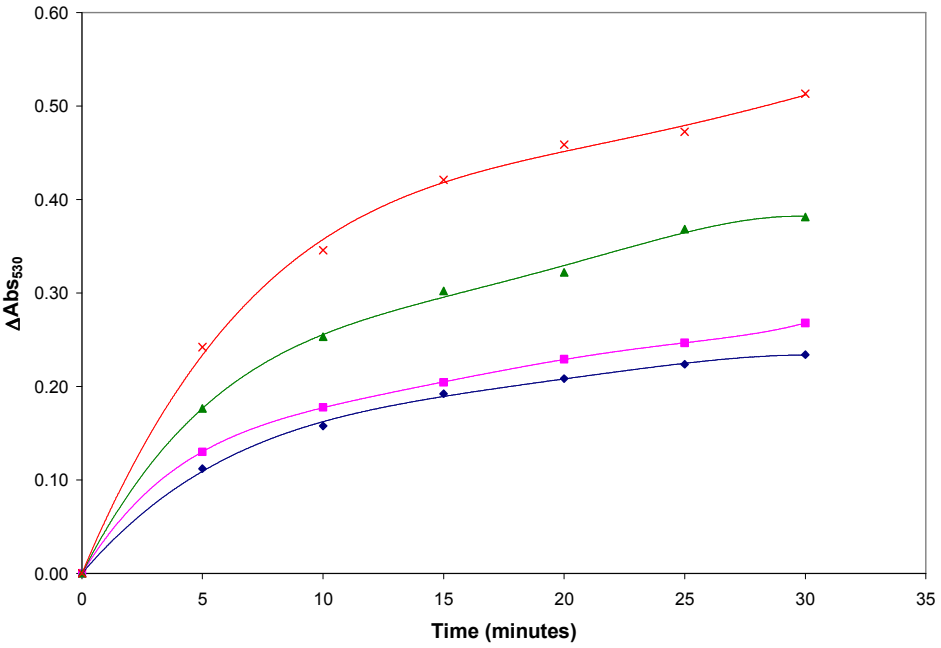

Figure 4-15 – The response curves of 5 phr NTC films of differing thickness under 4 mW cm^{-2} UVB light. The curves shown are for films spun at 1200, 900, 600, and 300 rpm.

Figures 4-14 and 4-15 show that even very simple changes to the system can alter the extent of the observed colour change considerably. By spinning the films at 300 rpm rather than 1200 rpm, for example, results in a ΔAbs at λ_{max} of 0.5 rather than 0.2.

4.3 An erythemal sensor

As one last piece of the current work we had to show a good response of these films to solar light. We established the same criteria as before: the sample must obtain a ΔAbs at λ_{max} of approximately 1 after 1 MED has been reached. We set the xenon-arc solar simulator so that our SafeSun meter registered a UVI. This would mean that 1 MED had been reached in approximately half an hour. A 5 phr solution of NTC in PVA was then prepared and coated at 300 rpm. This film was then exposed to the UVI 5 solar light. The results are shown in the following diagram:

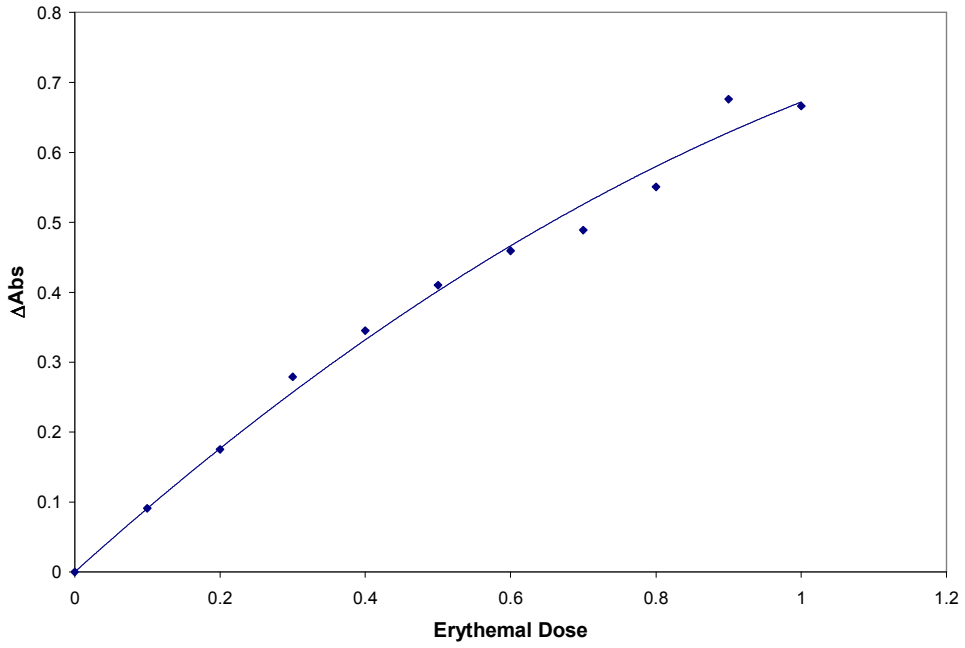

Figure 4-16 – The response curve of a 5 phr NTC film exposed to solar simulating light of UVI =5.

After 1 MED has been reached our NTC film had reached a ΔAbs of approx 0.7. While not quite the value of 1 we were hoping for it is close to the results shown by the viologens and it is firmly believed that this value can easily be increased.

4.4 Conclusions

It has been shown that a UV and erythemal dosimeter can be developed using the tetrazolium salts, of which neotetrazolium shows the greatest response, in a water soluble polymer system. This system responds uniformly to differing intensities of solar UV and is stable in the presence of oxygen.

Altering the concentration of the dye in the polymer, as well as altering the thickness of the polymer film has a direct effect on the colour response of the film when exposed to UV light.

More work is required to show that the response of this dosimeter is 'tuneable' out with changing physical characteristics and altering Beer-Lambert parameters. For example, as in the viologen work, electron donors could be added to the system to assess whether they could be used to increase the rate of reaction. These would not suffer from the same oxygen sensitivity as the viologen system.

Work is also required to fully explore the solar dosimeter characteristics of the films, using reaction promotors or UV attenuators to determine whether response is uniform at different UVI values.

NB: at time of publication some of this work has been carried on and completed by Pauline Grosshans (see Appendix).

4.5 References

1. Creach, J.; Baudoux, A.; Bertru, G.; Le Rouzic, B., *Journal of Microbiological Methods* **2003,** *52*, 19
2. Mshana, R. N.; Tadesse, G.; Abate, G.; Miorner, H., *Journal of Clinical Microbiology* **1998,** *36*, 1214
3. Gordon, A. M.; Rowan, R. M.; Brown, T.; Carsgon, H. G., *Journal of Clinical Pathology* **1974,** *26*, 52
4. Gordon, A. M.; Briggs, J. D.; Bell, P. R. F., *Journal of Clinical Pathology* **1974,** *27*, 734
5. Beveridge, M. V.; Herst, P. M.; Tan, A. S., *Biotechnology Annual Review* **2005,** *11*, 127
6. Meerhof, L. J.; Roos, D., *Journal of Leukocyte Biology* **1986,** *39*, 669
7. Baehner, R. L.; Boxer, L. A.; Davis, J., *Blood* **1976,** *48*, 309.
8. Pikaev, A. K.; Kriminskaya, Z. K., *Radiation Physics and Chemistry* **1998,** *52*, 555
9. Kovacs, A.; Wojnarovits, L.; McLaughlin, W. L.; Ebrhaim Eid, S. E.; Miller, A., *Radiation Physics and Chemistry* **1996,** *47*, 483
10. Ebraheem, S.; Abdel-Fattah, A. A.; Said, F. I.; Ali, Z. I., *Radiation Physics and Chemistry* **2000,** *57*, 195

5 A Solvatochromic Sensor for VOCs

5.1 Solvatochromism

It has long been known that the UV/Vis absorption spectra may change depending on the solvent used[1, 2]. This change may be in the position, intensity, or even shape of the absorption band and is called *solvatochromism*. However the term is now most commonly used to describe a pronounced change in the position of a UV/Vis absorption band in response to a change in the polarity of the medium. A hypsochromic (or blue) shift with increasing solvent polarity is called *negative solvatochromism* and the corresponding bathochromic (or red) shift is *positive solvatochromism*.

5.1.1 The Franck-Condon Principle

The *Franck-Condon Principle* states that since the time required for a molecule to execute a vibration is much longer than that required for an electronic transition, the nuclei of a chromophore and any surrounding solvent molecules do not appreciably alter their position during an electronic transition. Thus, when a chromophore is excited by the absorption of a photon the excited state molecule is momentarily in a vibrational state surrounded by a solvent cage whose orientation is best suited to the ground state of the molecule. This is known as the Franck-Condon state. The Franck-Condon state is of a greater energy than the equilibrium excited state which is eventually reached through the process of relaxation (figure 5-1).

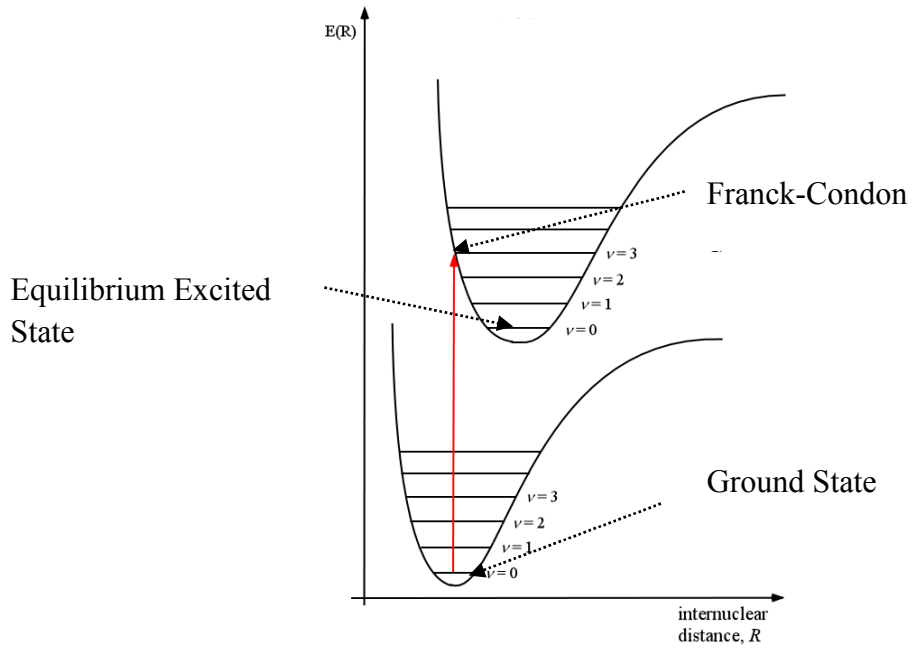

Figure 5-1 – An illustration of the excitation of an electron into the Franck-Condon vibrational state.

5.1.2 Negative and positive solvatochromism

In a system where the solute is a polar molecule in a polar solvent the solvation will result largely from dipole-dipole interactions. This results in an oriented solvent cage around the polar solute molecules, leading to a stabilization of the ground state. If the dipole moment increases during the electronic transition i.e. $\mu_g<\mu_e$, the Franck-Condon state will exist in a solvent cage of partially oriented solvent molecules. The stability of this state relative to the ground state will increase with increasing solvent polarity. As a consequence, as the polarity of the solvent is increased there will be a bathochromic shift in the absorption spectrum (or positive solvatochromism), the magnitude of which will depend on three factors; the extent of the change in the solute dipole moment, the value of the solvent dipole moment, and the extent of interaction between the dye molecule and the solvent.

If on the other hand the dipole moment decreases during the electronic transition ($\mu_g > \mu_e$), as it does for Reichardt's dye for instance (μ_g = 15 Debye, μ_e = 6 Debye), the Franck-Condon state will <u>not</u> be stabilised more than the ground state. The resulting effect is that, with increasing solvent polarity, there will be a hypsochromic shift (or negative solvatochromism). Thus, Reichardt's dye is a negatively solvatochromic dye.

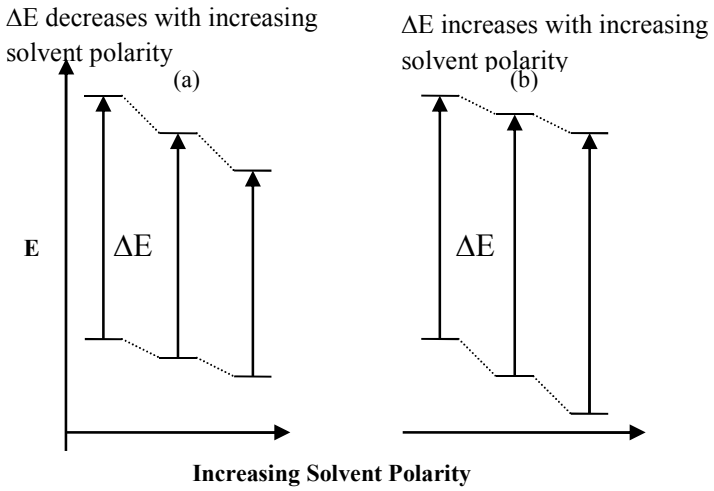

Figure 5-2 – A diagram illustrating solvent effects on the electronic transition energy of a polar solute in a polar solvent. (a) Demonstrates the behaviour of the system when the dipole moment of the Franck-Condon state is greater than that of the ground state ($\mu_g < \mu_e$). (b) Illustrates the opposite effect ($\mu_g > \mu_e$).

For either bathochromic or hypsochromic shifts the following equation applies:

$$\Delta E = h\Delta\upsilon = hc\frac{1}{\lambda_{max}} \qquad (5.1)$$

Where ΔE is the energy gap between the ground and excited states and λ_{max} is the wavelength of maximum absorbance. Thus, for negative solvatochromism, since ΔE increases with increasing solvent polarity, it follows from equation (5.1) that λ_{max} will

decrease, i.e. UV/Vis spectra will undergo a hypsochromic shift as the polarity of solvent increases.

5.1.3 Applications of Solvatochromism

Perhaps one of the first practical uses to be recommended for solvatochromism was to develop a solvent polarity scale. The idea was first suggested by Brooker et al. in 1951[3] and was first fully developed by Kosower in 1958[2]. These scales use the spectral data of a single probe molecule to establish the polarity of the solvent and are advantageous because they can be measured using equipment and chemicals found in most laboratories. These solvent polarity scales are dependent on the idea that the absorption spectra of a solvatochromic dye can be reliably used to record and determine the polarity of different solvents. This is most commonly achieved by establishing an *empirical solvent polarity parameter* using reference compounds and usually takes the form of a *linear free energy relationship* or LFER.

The basic assumption of an LFER is that, for a solvent-sensitive process, the process is representative of all the solute/solvent interactions that are present in the related solvent-influenced processes under study. This reference process can then be used to give an empirical measure of the solvation capability of a particular solvent for that process. Since these empirical parameters reflect all of the intermolecular forces acting within a given solution, it can be said to give a more reliable measure of the influence of a solvent on a solute than a single physical constant, such as solute dipole moment.

Since Brooker et al.[3] first made the suggestion that solvatochromic compounds could be used to develop solvent polarity scales, a large number of compounds have been studied as potential reference processes for establishing these scales[4-9]. One of the first was Kosower's *Z* scale[2] which is based on the intramolecular charge-transfer transition of 1-ethyl-4-(methoxycarbonyl)-pyridinium iodide (figure 5-3).

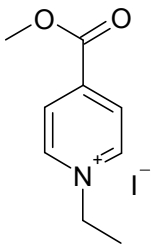

Figure 5-3 – 1-ethyl-4-(methoxycarbonyl)-pyridinium iodide

The factor Z is defined as the molar transition energy, E_T, in kcal/mol of the absorption band for the charge transfer in an appropriate solvent. This is calculated according to equation 5.2:

$$E_T\,/(kcal \cdot mol^{-1}) = h \cdot c \cdot \tilde{\upsilon} \cdot N_A = 2.859 \cdot 10^{-3} \cdot \tilde{\upsilon} / cm^{-1} \equiv Z \qquad (5.2)$$

where h is Planck's constant, c is the velocity of light, $\tilde{\upsilon}$ is the wavenumber of the photons that produce the electronic excitation under study, and N_A is Avogadro's number. Z values range from 94.6 kcal/mol for water (a very polar solvent) to about 60 kcal/mol for i-octane (a very non-polar solvent) and have been measured for a wide variety of solvents and binary mixtures. There are problems with the Z approach though. For example, Z values can only be calculated over the range 63.2 to 83.6 kcal/mol (trichloromethane and 70:30 ethanol:water respectively) i.e. from 452 nm to 342 nm. This is because the charge transfer band cannot be observed in highly polar solvents as it moves to such a short wavelength that the $\pi \rightarrow \pi^*$ absorption band of the pyridinium ion overshadows it. As a result, the Z values for highly polar solvents have to be extrapolated using the results obtained using other measurements. Also the pyridinium ion is insoluble in non-polar solvents, the outcome of which is that secondary standards must be used to determine values for non-polar solvents.

5.2 Reichardt's Dye

One way around the limitations of the pyridinium, as suggested by Dimroth and Reichardt[10], is to use *N*-phenolate betaine dyes such as shown in figure 5-4.

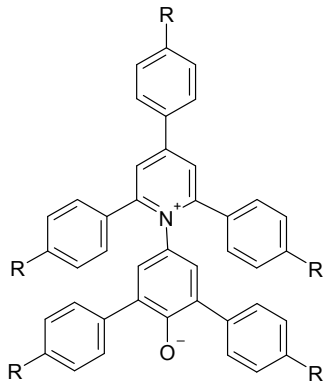

Figure 5-4 – The structure of 2,6-Diphenyl-4-(2,4,6-triphenylpyridinio)-phenolate, a solvatochromic dye. For this species R = -H.

Using this dye, now commonly known as Reichardt's dye, as a standard Dimroth and Reichardt proposed a new solvent polarity parameter, $E_T(30)$, which is based on the longest wavelength absorption band of the pyridinium *N*-phenolate dye. The nomenclature simply comes from the fact that this particular dye was dye number 30 in their study. The advantage this carries over Kosower's dye is that the absorption band in dye 30 (Reichardt's dye) lies at a much higher wavelength and gives a much larger range for solvatochromism, from approx 450 to 900 nm. As these are mostly visible wavelengths it is also possible to make a visual estimation of the solvent polarity. The only real problem with the Reichardt's dye approach is that the primary dye is only slightly soluble in water and other less polar solvents. It is also insoluble in non-polar solvents. This can be overcome by using dye variants where R = $-CF_3$ or $=C(CH_3)_3$ as secondary standards because there is an excellent correlation between E_T values of the dyes.

5.2.1 Reichardts dye-based Sensors

Various studies have now been performed in which Reichardt's dye (RD) is encapsulated within a polymer film with the intention of using it a sensor for various VOCs[11-15]. One of the earliest of these studies was the work of McGill et. al.[15] looking at the use of RD in various polymer films as optical sensors for water. This was followed by work from Fichou et. al.[13] placing RD in poly(methyl methacrylate) and using it to detect various solvents. Other studies have shown that RD can be used to detect alcohols and water in polysiloxane, nonadecane and poly(ethylene vinyl acetate)[12]. However, the most notable study to date was that carried out by Krech et. al.[14] who showed that RD could be encapsulated in a wide variety of polymers and responded with a measurable colour change when exposed to a variety of different VOC's including water, acetone, chloroform, carbon tetrachloride, dichloromethane, and various alcohols. The best of the optical sensors tested, in terms of optical response, was RD in poly(methyl methacrylate). In all of the above RD/polymer indicators the response times (where reported) were significant. The fastest of the RD/polymer indicators was that reported by Fichou and his coworkers, for RD in PMMA, which exhibited a response time of 50 s when exposed to ethanol vapour. These are summarised in table 5.1

Table 5.1 - A selection of optical sensors which have been developed using Reichardt's Dye

Matrix	Solvents Detected	Response Times	λ shifts
Polysiloxane[12]	Methanol, Ethanol, 2-Propanol, H_2O	Not Given	≤ 50 nm
Nonadecane[12]	H_2O, Ethanol	Sluggish	
PVP, PIB, PS, PECH, OV-1, FPOL[14]	H_2O, Methanol, Ethanol, Isopropanol, Acetone, Chloroform, Carbon Tetrachloride, DCM	Not Given	≤ 103 nm
PEVA copol. [11]	Ethanol	2-7 minutes	~ 50 nm
PMMA[13]	Methanol, TBA, TBME	Approx. 50s	≤ 112 nm
PMMA, PVP, PVAc, PVC[15]	H_2O	> 2 minutes	≤114 nm

Where: PVP = *Poly(vinyl pyrrolidone)*, PIB = *Poly(isobutylene)*, PS = *Poly(styrene)*, PECH = *Poly(epichlorohydrin)*, OV-1 = *Dimethylpolysiloxane*, FPOL = *Fluoropolyol*, PEVA = *Poly(ethylene vinylacetate) copolymer*, PMMA = *Poly(methyl methacrylate)*, TBA = *tert-butyl alcohol,* TBME = *tert-butyl methylether,* PVAc = *Poly(vinyl acetate)*, PVC = *Poly(vinyl chloride)*.

5.3 Riechardt's dye in Ethyl Cellulose (RD/EC)

Following on from the work of others, such as these references in table 3.1, the solvatochromic dye, Reichardt's dye, was encapsulated within a film of ethyl cellulose, by dissolving the dye in a 10 wt % toluene-ethanol solution of the polymer. This solvatochromic ink solution was then spun onto a glass disc and placed in a gas cell to allow it to be exposed to the solvent vapour under test. After 10 minutes exposure to the solvent vapour the UV-Vis absorbance spectrum of the Reichardts dye/EC film, hereafter referred to as RD/EC, was recorded and compared to the spectra of the original (air) film. The solvent vapours chosen for this study were as follows: methanol, ethanol, isopropanol (IPA), dichloromethane (DCM), acetone and water. The results of this work are illustrated in figure 5-5.

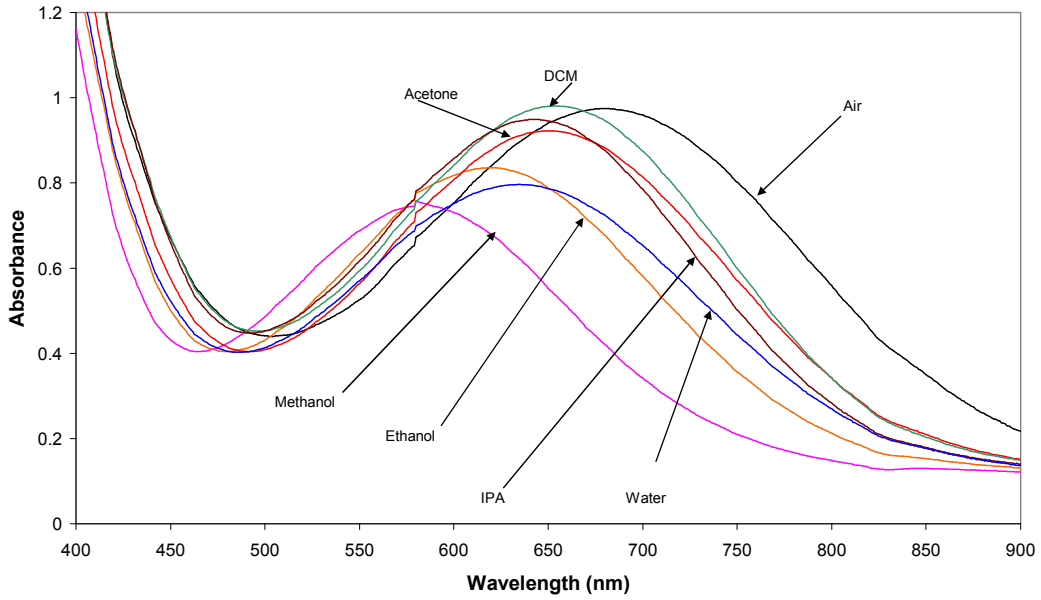

Figure 5-5 - The absorbance spectra of ethyl cellulose films containing Reichardt's dye after 10 minutes of exposure to various solvents. The spectra shown are for films exposed to methanol, ethanol, IPA, DCM, acetone and water.

From this spectral data it is clear there is a noticeable change in the position and intensity of the spectrum of a RD/EC film from each solvent vapour, including for the different alcohols tested. Table 5-2 outlines the changes in λ_{max} (and the related $E_T(30)$ value) for the RD/EC films. $E_T(30)$ values were calculated using the following equation[7, 8]:

$$E_T(30)/(kcal.mol^{-1}) = h \cdot c \cdot \tilde{\upsilon} \cdot N_A = 2.859 \cdot 10^{-3} \cdot \tilde{\upsilon} = \frac{2.859 \cdot 10^{-3}}{\lambda_{max}} \qquad (5.3)$$

where h is Planck's constant, c is the velocity of light, $\tilde{\upsilon}$ is the wavenumber of the photons associated with the maxiumum absorbance in the visible spectrum due to RD, and N_A is Avogadro's number.

Table 5-2 - λ_{max} and E_T30 values of RD/EC films after exposure to a variety of solvent vapours.

Solvent (BP ^oC)	λ_{max} (nm)	$\Delta\lambda_{max}$ (nm)	$E_T(30)$ (kcal mol^{-1})	$E_T(30)$ Literature†
Air	681	0	-	-
Water (100)	634	47	45.09	63.1
Methanol (64.7)	580	101	49.29	55.4
Ethanol (78.4)	621	60	46.04	51.9
IPA (82.3)	650	31	43.99	48.4
Acetone (56.3)	643	38	44.47	42.2
DCM (39.8)	654	27	43.72	40.7

† reported values for RD in the neat solvents[8, 9]

It might be expected that the λ_{max} and $E_T(30)$ values recorded for the RD/EC films exposed to different solvent vapours would simply be related to those, reported in the literature, for RD in the neat solvents themselves. However a comparison of the experimental and literature $E_T(30)$ values given in table 5-2 and illustrated in figure 5-6 reveals no such simple relationship. Thus these RD/EC films, whilst useful for detecting volatile organics, cannot be used to readily identify different vapours from the $E_T(30)$ values determined for RD in EC by simple comparison with the $E_T(30)$ values of RD in the neat solvents. It follows that, in order to use an RD/EC film for qualitative analysis, the indicator needs to be calibrated first with the vapour of interest in order to determine their λ_{max} (i.e. $E_T(30)$) values.

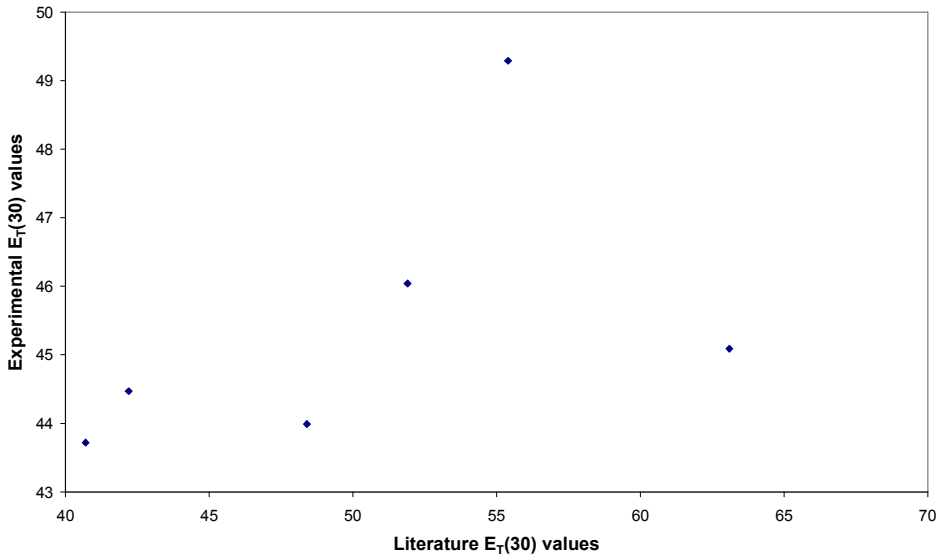

Figure 5-6 – a comparison of the $E_T(30)$ values obtained experimentally against those quoted for the dye in the neat solvent.

5.3.1 RD/EC films for quantitative analysis.

Although the work reported above has shown that RD/polymer films can be used for qualitative analysis (via the shift in λ_{max}) of VOC's, less effort has been directed at their use for quantitative analysis.

RD in a binary solvent mixture, such as MeOH/acetone, as shown in figure 3-3, gives a non-linear response as to the % composition of the mixture is raised. Suppan and others[16-21] have suggested that changes like this occur in many simple binary solvent mixtures because of preferential solvation of the dye by one of the solvents. It is not surprising to also note that the variation in the Abs (λ_{max}) for RD in methanol is not directly related to the % MeOH present in the mixture (see figure 5-8).

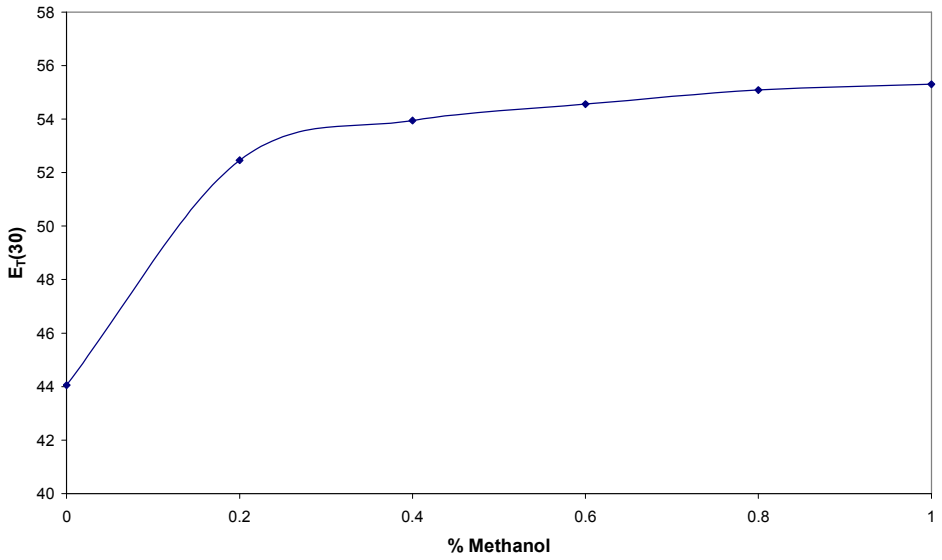

Figure 5-7 – A plot showing the shift in λ_{max} of a binary solvent system comprising methanol and acetone. The x axis of this plot shows the percentage of methanol present in the system.

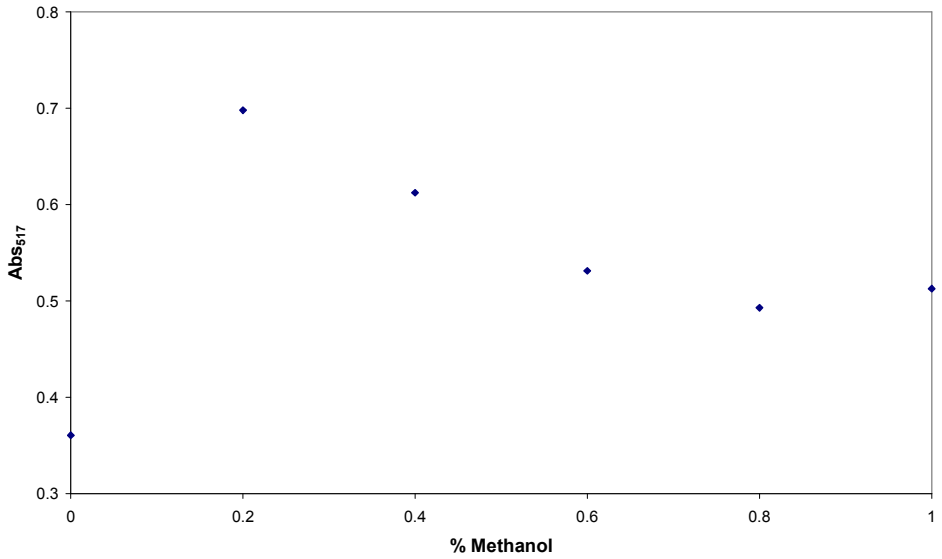

Figure 5-8 – A plot showing the change in absorbance at λ_{max} (methanol) for the same solvent mixtures shown in figure 5-7.

Interestingly the λ_{max} of RD in RD/EC film varies in a non-simple fashion as a function of % ethanol in the air, as illustrated by the results in figures 5-9 and 5-10, and yet the Abs (680nm) for the RD/EC indicator appears directly proportional to % ethanol (see figure 5-11.)

The calibration graph illustrated in figure 5-7 is approximately linear up to % ethanol levels of ≤ 90 % implying that the absorbance of a RD/EC film at 680 nm is, possibly fortuitously, directly related to the concentration of ethanol in the ethanol/air mixture it is exposed to. Although the colour change is striking (ca. 70 nm – see figs 5-9 and 5-10) the % change in absorbance (ca 40 %) is a little less so (fig 5-11), but still large enough to be used in quantitative analysis.

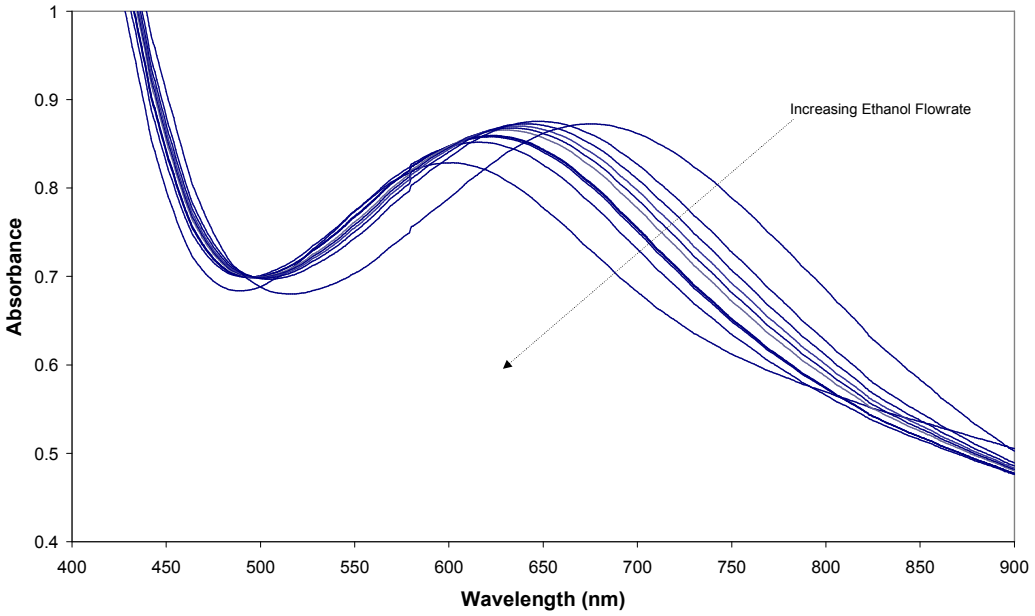

Figure 5-9 – The UV-Vis spectra of a RD/EC film. The spectra shown were obtained for the following % ethanol levels (from top to bottom): 0, 10, 20, 30, 40, 50, 60, 70, 80, 90 and 100 %.

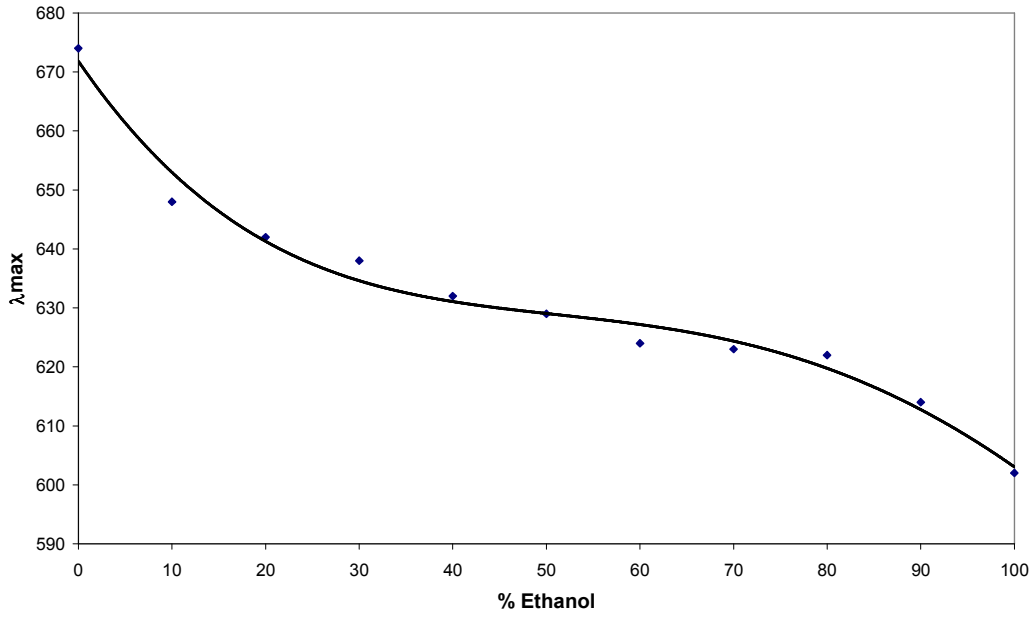

Figure 5-10 – A plot showing the change in λ_{max} with the change in % ethanol. A decrease in λ_{max} signifies an increase in the polarity of the system.

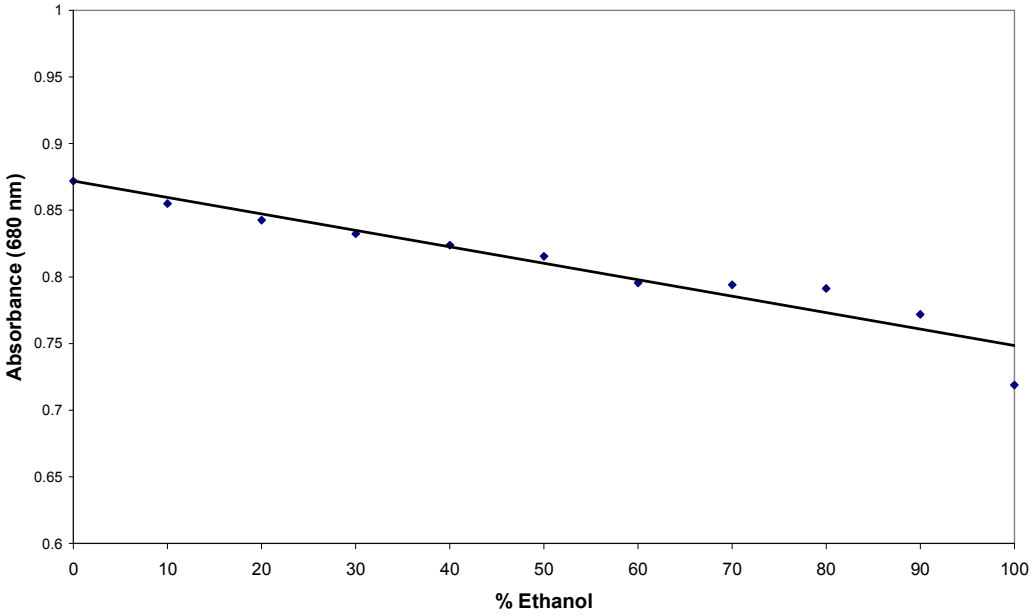

Figure 5-11 – A calibration curve of absorbance versus % ethanol for RD/EC film. The absorbance was measured at 680 nm as this showed a good distinction between each vapour concentration.

5.3.2 Response and recovery characteristics of a RD/EC film

An important characteristic of any optical sensor is how quickly the sensor responds to and recovers from exposure to the vapour under test. Thus, as part of the study being carried out the response and recovery times of the RD/EC indicators for the vapour of particular interest (ethanol) were determined by measuring the variation in the Abs(680nm), λ_{max} of an ethanol free film, as a function of time and the results of this work are illustrated in figure 5-12.

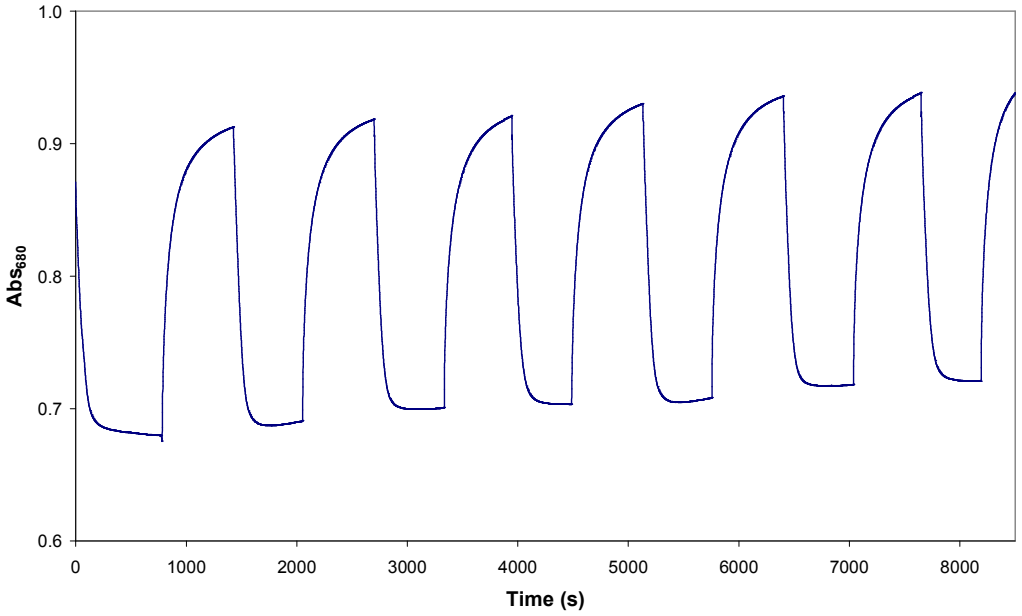

Figure 5-12 - The change in absorbance at 680 nm of a RD/EC film in response to ethanol vapour (decrease in absorbance) and on recovery from the vapour (increase in absorbance).

In figure 5-12 we can see that the change in absorbance is a largely reversible process and so a RD/EC film can be used many times over. Note also from this data that the ethyl cellulose film does not completely recover its initial absorbance within the selected time period (10 mins). The data presented in these plots was used to calculate the t_{50} and t_{90} values for response and recovery. These values represent the time taken to achieve 50% and 90% of the total change in absorbance in the system and are shown here.

Table 5-3 - Response and recovery times of an ethyl cellulose film doped with Reichardt's dye on exposure to ethanol.

Support	t_{50} Response (s)	t_{50} Recovery (s)	t_{90} Response (s)	t_{90} Recovery (s)
Ethyl Cellulose	34	43	98	278

It is clear from the data in figure 5-12 and table 5-3 that the ethyl cellulose sensors respond quickly (approximately 1½ minutes for t_{90}) but take slightly longer to recover from the vapour, with it taking almost 4½ minutes to achieve a 90 % change in absorbance. While these periods are by no means excessively long, they are not as fast as desired for an optical sensor. These values are not uncommon amongst polymer sensors[11-15] and are due to the solvent dissolving into and out of the polymer encapsulating media. In an attempt to produce faster acting films, an alternative inorganic encapsulating medium was explored; fumed silica.

5.4 Reichardt's dye on fumed silica films (RD/SiO_2)

Work by Demas et al[22] showed that fumed silica, as a support for luminescent transition metal complex oxygen indicators, proved very effective; it has a high surface area (approximately 200 m^2 g^{-1}), can be coated with a range of materials and forms "dense, very high surface area, optically transparent discs" when compressed. Demas and his team found that the luminescence of $Ru(L)_3$ adsorbed onto the silica, where L is an α-diimine, responded very quickly to any variation in the ambient level of O_2, due to the highly porous nature of the silica which is estimated to be 50 % for the pressed silica discs. Given the promise shown in his work as a potential dye support material for making clear, fast-acting films it was decided to test fumed silica as a support for a Reichardt's dye based indicator.

5.4.1 RD/SiO_2 films for qualitative analysis

The fumed silica discs were prepared using a similar technique to that outlined by Demas *et al*. Thus, 1.9 g of the fumed silica were placed into ca 125 ml of continually stirred methanol in a round bottomed flask. 0.1 g of Reichardt's dye were dissolved in small volume of methanol – typically 10 to 20 ml – which was then added to the silica suspension. The resultant mixture was left to stir for 30 minutes before being placed under rotary evaporation, leading to the generation of silica coated with Reichardt's dye. The RD/SiO_2 films were formed by placing a glass cover slip on top of the first stainless steel die in a standard IR press, evenly spreading 50 mg of the dye-impregnated silica over this disc, sandwiching the powder with a second stainless steel die, and then applying 2000 kg of pressure for 30 minutes. After this time the pressure was *slowly* released and the glass cover slip, now bonded with a thin layer of the impregnated silica, was removed. Thse RD/SiO_2 films were exposed to a variety of different solvent vapours and the UV/Vis spectral characteristics recorded. The solvents chosen for study were: methanol, ethanol, isopropanol (IPA), dichloromethane (DCM), acetone and water. As before each RD/SiO_2 film was exposed to each vapour for 10 minutes. The results of this work are illustrated in figure 5-13.

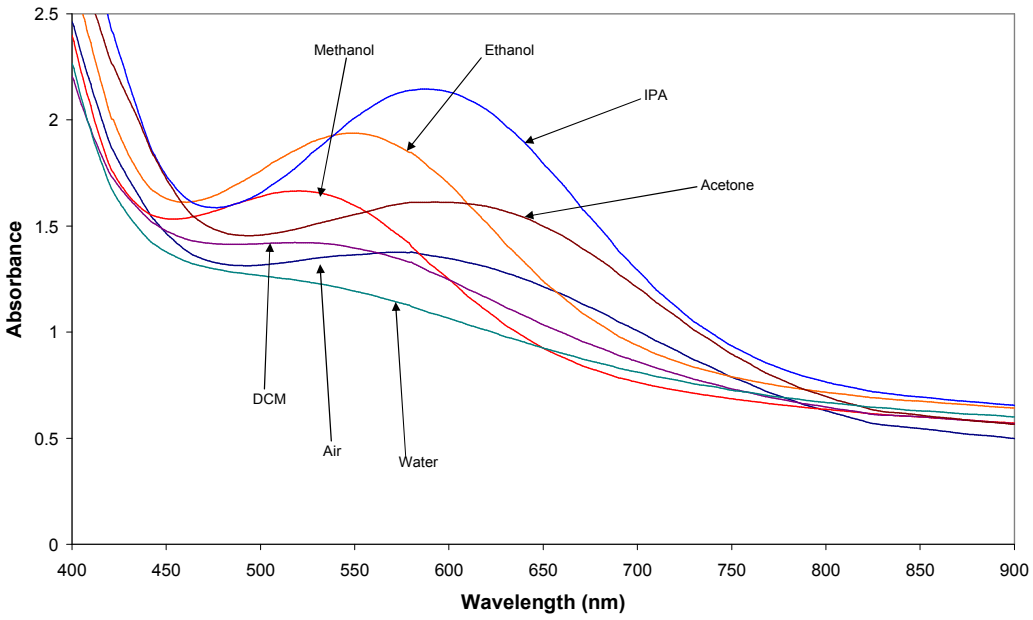

Figure 5-13 - The UV/Vis spectra of a RD/SiO_2 disc on exposure to various solvent vapours.

From these results it is clear that there is a notable difference between the spectra for each solvent vapour. However the RD molecules adsorbed onto the silica appear to be in a much more polar environment than when dissolved in ethyl cellulose, i.e. the λ_{max} in air for RD/SiO_2 films is lower, and the shifts in λ_{max} between solvent and air are much smaller, compared to an RD/EC film. The absorbance differences on the other hand are much larger, giving greater changes in the intensity of the colour. Also, it is noted that the spectrum for water vapour shows little evidence of an absorbance peak and so it is hard to assign a λ_{max} value in this case.

The spectral data in figure 5-13 were used to generate $E_T(30)$ values for the different solvent vapours and these were compared to those for RD in the neat solvents themselves, reported in the literature. As before, for RD/EC, the values of λ_{max} and $E_T(30)$ of the RD/SiO_2 films appear not to be correlated with those for RD in the neat solvents, except for the alcohols. More comment on this is given in a later section.

Table 5-4 - λ_{max} and $E_T(30)$ values for RD/SiO_2 films exposed to various solvent vapours.

Solvent (BP ^oC)	λ max (nm)	$E_T(30)$	$E_T(30)$ Literature
Air	580	-	-
Water (100)	-	-	63.1
Methanol (64.7)	520	55.0	55.4
Ethanol (78.4)	548	52.2	51.9
IPA (82.3)	587	48.7	48.4
Acetone (56.3)	594	48.1	42.2
DCM (39.8)	518	55.2	40.7

† reported values for RD in the neat solvents[8, 9]

5.4.2 Quantitative analysis

With the knowledge that the RD/fumed silica system could be used for qualitative analysis, the next step was to determine whether it could be used for quantitative analysis. The same procedure was followed as outlined for the RD/EC films; a gas blender was used to mix the solvent vapour under study with a flow of air at fixed percentages. Once again the solvent chosen for this work was ethanol. The results of this work are shown in figures 5-14 to 5-16

In this instance the very broad absorbance spectra shown in figure 5-14 make it difficult to pick out a definite λ_{max} and, as highlighted in figure 5-15, it is not clear if λ_{max} is related directly to % ethanol is linear. The best that can be said is that % ethanol and λ_{max} are correlated

The calibration graph illustrated in figure 5-16 on the other hand clearly shows that, unlike the RD/EC system, the relationship between Abs(λ_{max}) and % ethanol is not linear. Due to the differences in the polarity of the systems the colour change is also less striking (ca. 14 nm) than the RD/EC film (ca. 70 nm).

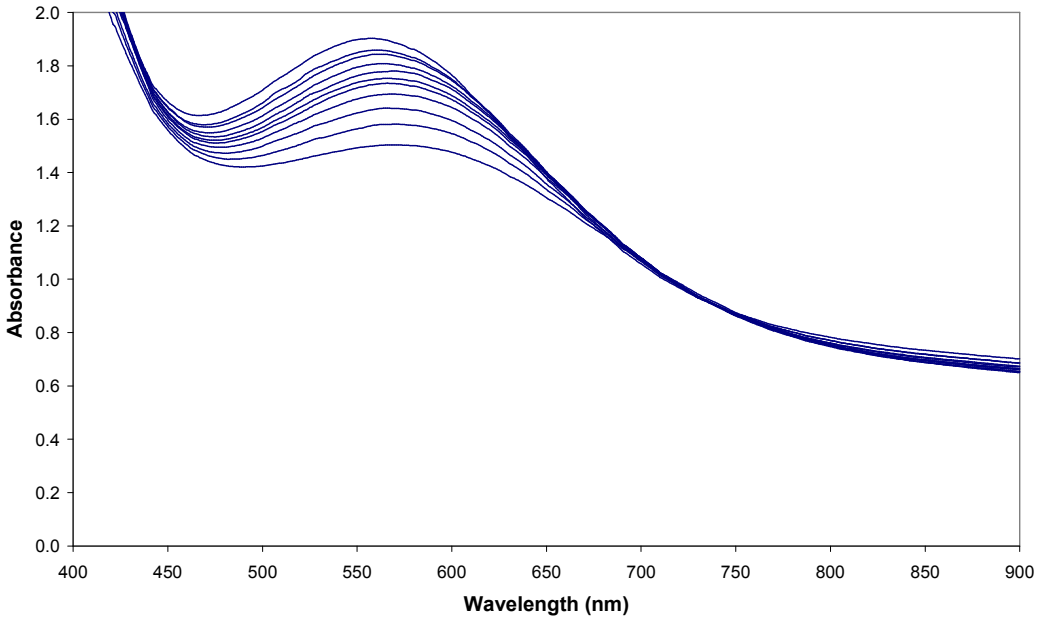

Figure 5-14 – The UV-Vis spectra of a RD/SiO_2 film. The spectra shown were obtained for the following % ethanol levels (from bottom to top): 0, 10, 20, 30, 40, 50, 60, 70, 80, 90 and 100 %.

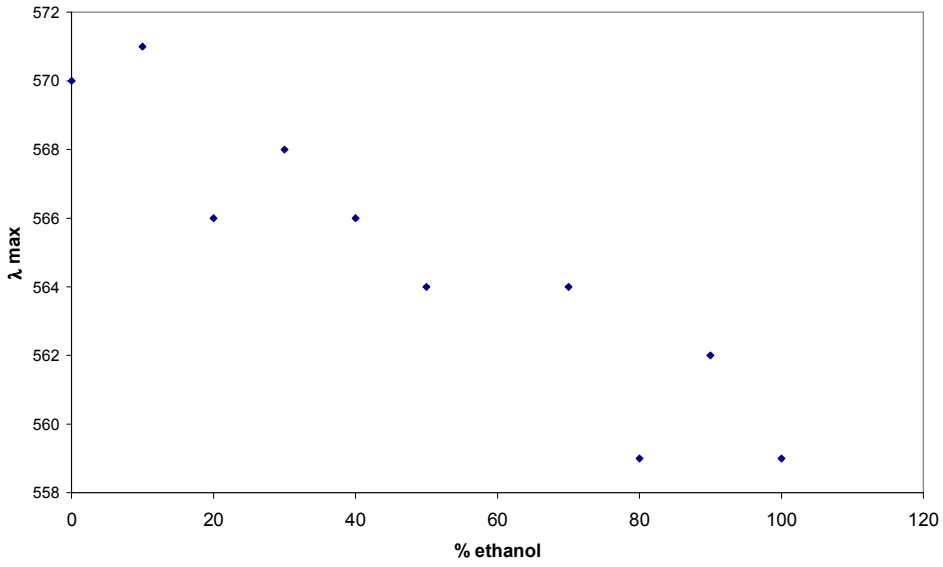

Figure 5-15 – A plot showing the change in λ_{max} with the change in % ethanol. A decrease in λ_{max} signifies an increase in the polarity of the system.

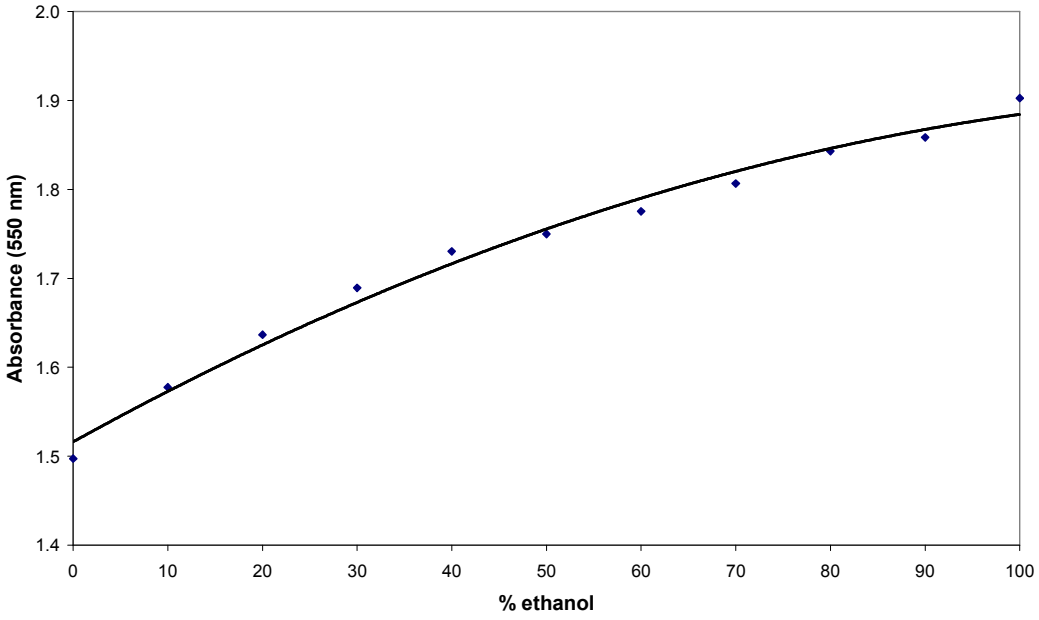

Figure 5-16 – A calibration curve of absorbance versus % ethanol for RD/EC film. The absorbance was measured at 680 nm as this showed a good distinction between each vapour concentration.

5.4.3 Response and recovery characteristics of a RD/SiO_2 film

Given that a major issue with polymer based solvent sensors such as RD/EC films is their significant response and recovery times – see figure 5-12 and table 5-3 – it was necessary to determine these times for the RD/SiO_2 films. As before, ethanol was chosen as the initial test solvent vapour. All the procedures described previously were followed and the following plot was obtained:

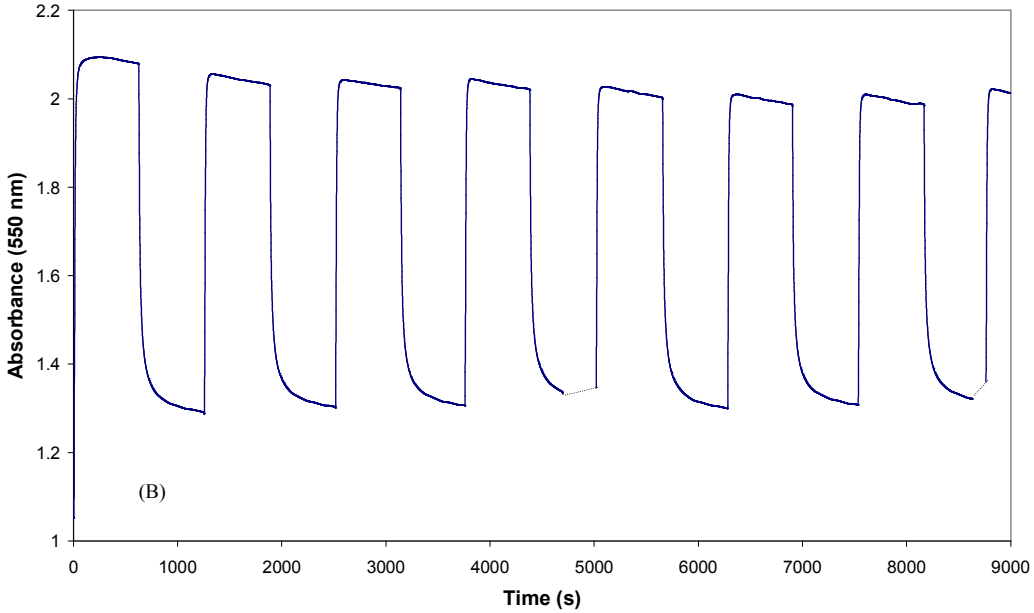

Figure 5-17 – A plot showing the change in absorbance (λ_{max} of ethanol free films) of a silica-Reichardt's disc when exposed repeatedly exposed to ethanol then air. An increase in absorbance indicates exposure to ethanol, while a decrease signifies exposure to air.

The data in Figure 5-17 clearly shows that, like the RD/EC system, the change in absorbance with repeated exposure to air and then ethanol vapour is fairly reversible over an extended period. What is even more interesting is that the change in absorbance seems to occur over a much shorter time period. The t_{50} and t_{90} values calculated from the data in figure 5-17 are shown in table 5-5.

Table 5-5 - t_{50} and t_{90} values for a reichardt's dye containing fumed silica disc, wrt ethanol.

Support	t_{50} Response (s)	t_{50} Recovery (s)	t_{90} Response (s)	t_{90} Recovery (s)
Fumed Silica	10	16	20	106

As can be seen from table 5-5 the RD/SiO_2 films responds to and recover from the presence of solvent vapour much quicker, ca. 3 times as fast, than the RD/EC polymer films. While t_{90} for recovery is approximately 1½ minutes, this is still faster than other reported times for RD-based ethanol sensors and gives promise to the use of the fumed silica system as an optical sensor.

Other alcohols – methanol, propanol, butanol, pentanol, and hexanol – were also studied as part of this work. The response times for the different alcohols are listed in the table below, while the response-recovery profiles for methanol and butanol are shown in figure 5-18 for comparison.

Table 5-6 – the response and recovery times for RD/SiO_2 films exposed to various alcohols

			Response		Recovery	
Vapour (BP°C)	**λ_{max}**	**ΔH_{Vap} (kJ mol^{-1})**	**t_{50}**	**t_{90}**	**t_{50}**	**t_{90}**
Methanol (64.7)	530	37.6	7	17	7.5	21
Ethanol (78.4)	550	40.5	10	20	16	106
Propanol (97.2)	565	43.6	16	49	30	235
Butanol (117.7)	574	45.9	48	226	81	340
Pentanol (138)	579	52.3	93	357	146	434

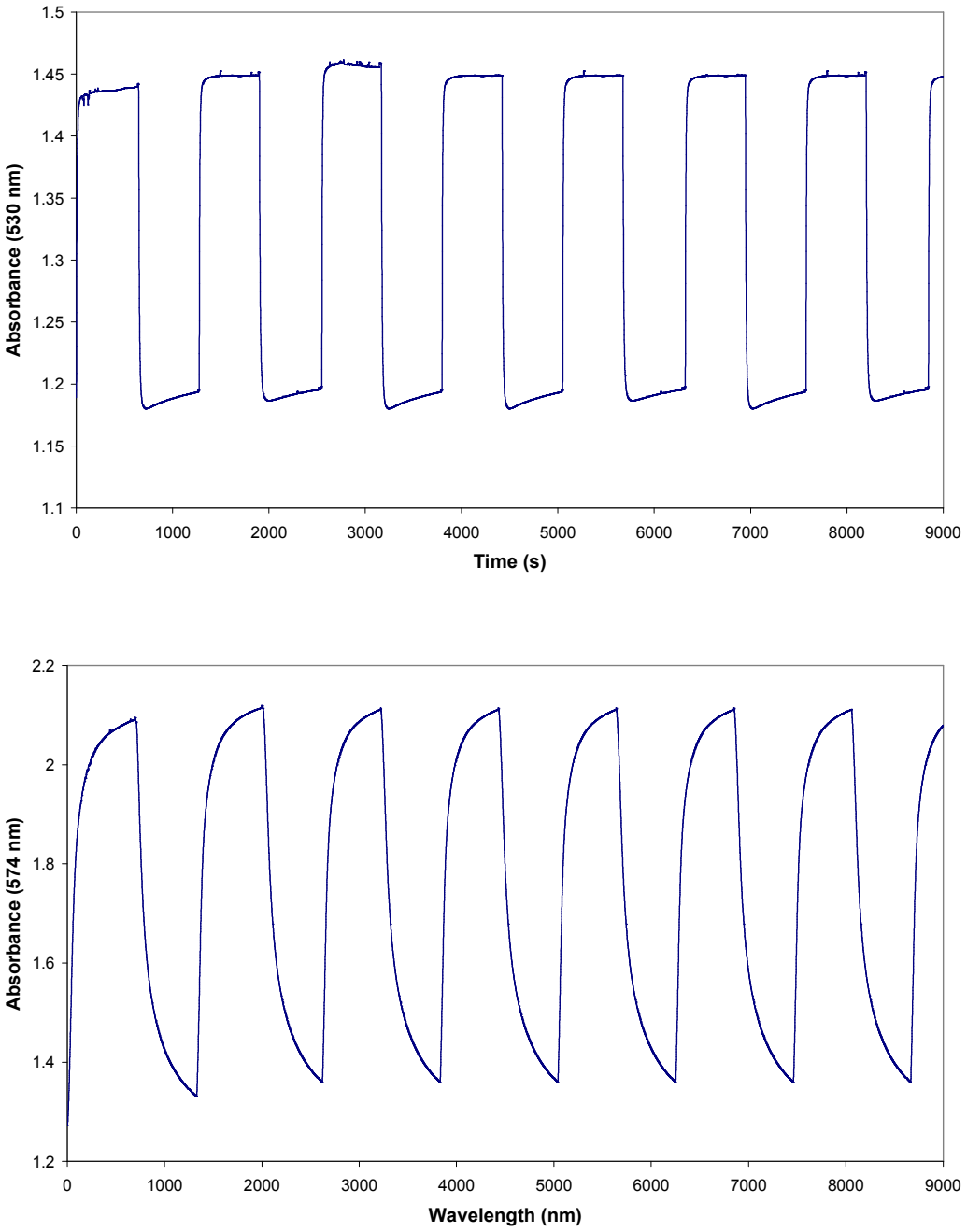

Figure 5-18 – The upper diagram shows the change in absorbance of a RD/SiO_2 film at λ_{max} on exposure to (increase in absorbance) and recovery from methanol (decrease in absorbance). The lower plot shows the change in absorbance of a similar film on exposure to (increase in absorbance) and recovery from butanol (decrease in absorbance).

This response and recovery data correlate well with the variation of the ΔH_{vap} of the alcohols as illustrated in figure 5-19.

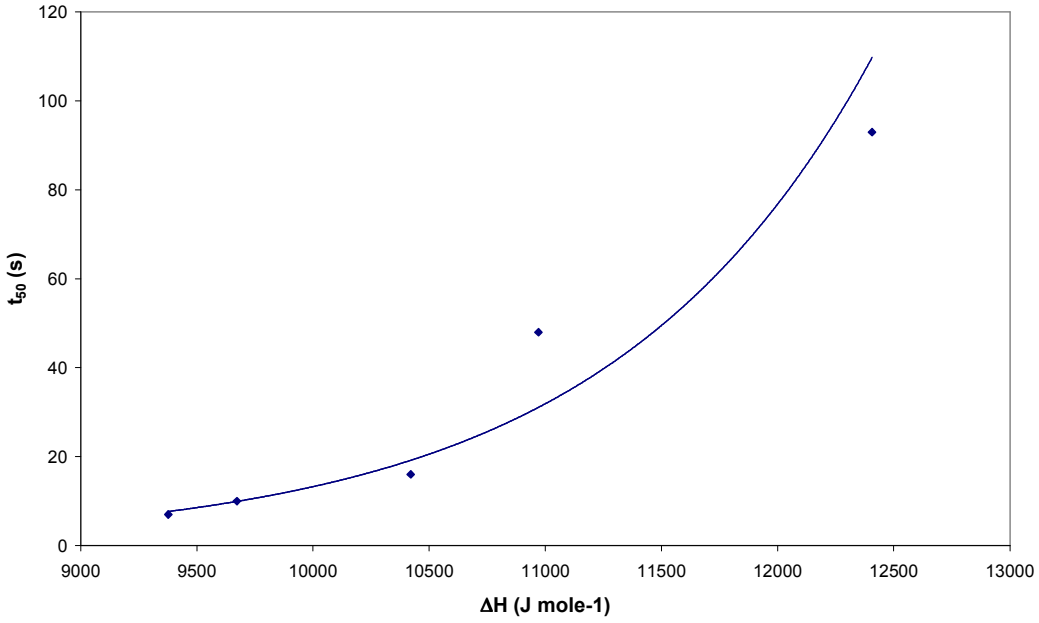

Figure 5-19 – A plot showing how the t_{50} response time of a RD/SiO_2 film increases with increasing ΔH_{vap} of the alcohols from methanol to pentanol.

ΔH_{vap} for any chemical provides a measure of the cohesive forces acting on the pure solvent molecules and therefore the intermolecular forces which, in the case of alcohols, will be dominated by hydrogen bonding. The hydroxylated nature of the fumed silica is likely to favour H-bonding with the alcohol vapours and presumably this is the cause for the correlation between ΔH_{vap} and the response recovery times.

5.4.4 RD/SiO_2 films and $E_T(30)$ values for alcohol vapours

An analysis of the spectral information regarding the absorbance λ_{max} values of the RD/SiO_2 films to different alcohols reveals a surprisingly good correlation between the $E_T(30)$ values recorded for the films and those reported in the literature for RD in the neat solvents, as indicated by the plot in figure 5-20.

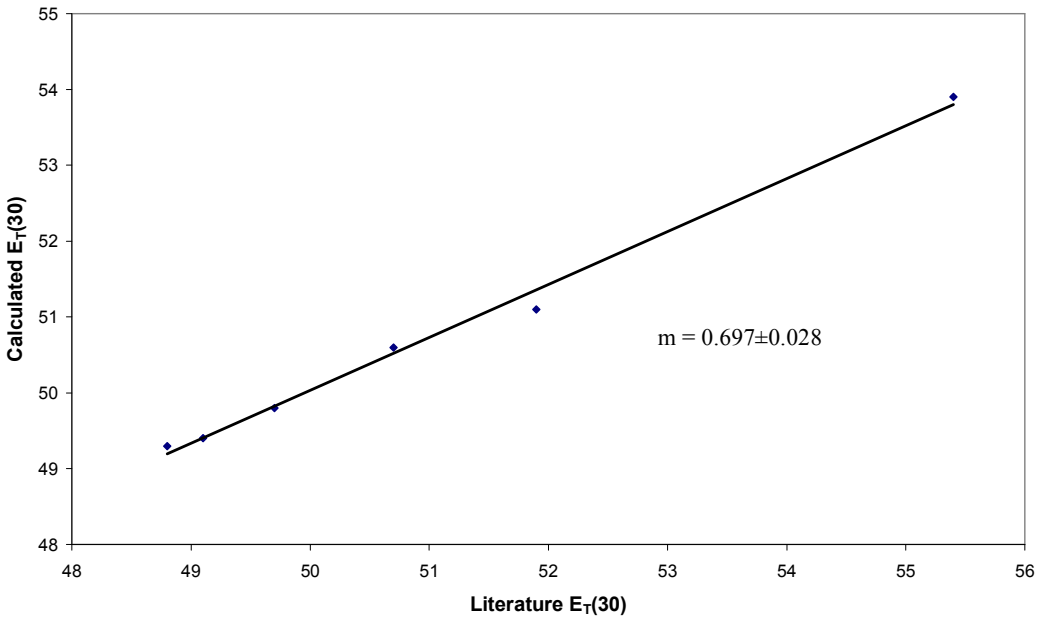

Figure 5-20 – A plot comparing the $E_T(30)$ values of the reichardt's impregnated silica in different alcohol vapours compared to the literature values.

It is not clear why RD/SiO_2 $E_T(30)$ values correlate well with the literature $E_T(30)$ values for the alcohols, but not for other types of molecules (such as ketones and chlorinated solvents). However, it does make this type of indicator useful for quantitative analysis of single alcohols. Thus, it would seem from the results in figure 5-20 that, for the alcohols at least, the fumed silica system may act as a solvent indicator via the λ_{max} or $E_T(30)$ values, where:

$$E_T(30)_{silica} = (0.697 \pm 0.028) \cdot E_T(30) + (15.2 \pm 1.4) \qquad (5.4)$$

5.4.5 RD/SiO_2 films and humidity detection

In a final set of experiments the % relative humidity (at 20^{o}C) in the ambient atmosphere above the RD/SiO_2 film was varied and the spectral response of the film recorded. The results of this work are illustrated in figure 5-21 over the page.

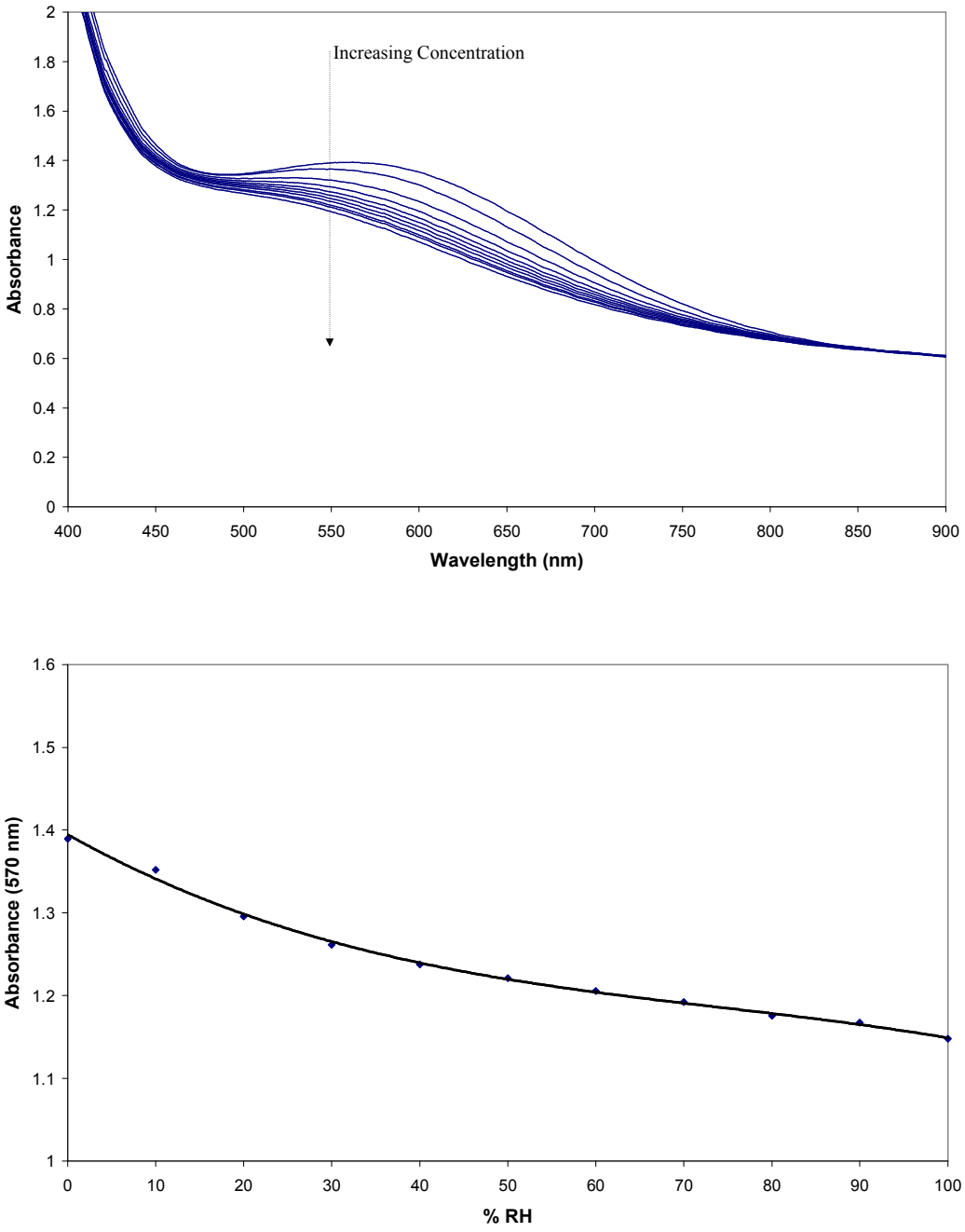

Figure 5-21 – The upper diagram shows the UV/Vis spectra of a Reichardt's dye impregnated silica disc after exposure to various flowrates of water vapour in air. The lower plot is the absorbance vs. flowrate calibration curve for determination of water concentration.

These results show that the RD/SiO_2 films can also be used as an indicator of ambient relative humidity levels.

5.5 Conclusions

Reichardt's Dye has been incorporated into a variety of different polymer films in a bid to create a workable solvatochromic sensor. These polymer sensors show some response to vapours, where complete response is a constant shift in absorbance and λ_{max}, in the order of minutes. This has been demonstrated using ethyl cellulose.

Using a non-reactive inorganic species as support for the solvatochromic dye, such as fumed silica, results in a sensor which responds to the presence of organic vapours in the order of seconds and will do so reproducibly.

As RD displays different colours when dissolved in different solvents so these RD/SiO_2 discs respond differently to different solvent vapours, allowing identification of individual vapours.

The wavelength shifts, and subsequent $E_T(30)$ values, recorded for the RD/SiO_2 do not match those reported for Reichardt's dye in the pure solvent. Thus unknown vapours exposed to the RD/SiO_2 films cannot be identified using the $E_T(30)$ scale.
Further work will be required to make this a qualitative sensor for solvent vapours.

5.6 References

1. Sheppard, S. E., *Reviews of Modern Physics* **1942,** *14*, 303
2. Kosower, E. M., *J. Am. Chem. Soc.* **1958,** *80*, 3253
3. Brooker, L. G. S.; Keyes, G. H.; Heseltine, D. W., *J. Am. Chem. Soc.* **1951,** *73*, 5350.
4. Buncel, E.; Rajagopal, S., *Journal of Organic Chemistry* **1989,** *54*, 798
5. Buncel, E.; Rjagopal, S., *Accounts of Chemical Research* **1990,** *23*, 226
6. Catalan, J.; Lopez, V.; Perez, P.; Martin-Villamil, R.; Rodriguez, J.-G., *Liebigs Annalen Chemie* **1995**, 241
7. Katritzky, A. R.; Fara, D. C.; Yang, H.; Tamm, K., *Chemical Reviews* **2004,** *104*, 175
8. Reichardt, C., *Chemical Reviews* **1994,** *94*, 2319
9. Reichardt, C.; Asharin-Fard, S.; Blum, A.; Eschner, M.; Mehranpour, A.-M.; Milart, P.; Niem, T.; Schafer, G.; Wilk, M., *Pure and Applied Chemistry* **1993,** *65*, 2593
10. Dimroth, K.; Reichardt, C., *Liebigs Annalen Chemie* **1963,** *661*, 1.
11. Blum, P.; Mohr, G. J.; Matern, K.; Reichert, J.; Spichiger-Keller, U. E., *Analytica Chimica Acta* **2001,** *432*, 269.
12. Dickert, F. L.; Geiger, U.; Liberzeit, P.; Reutner, U., *Sensors and Actuators B* **2000,** *70*, 263.
13. Fichou, D.; Hubert, C.; Valat, P.; Garnier, F., *Polymer Communications* **1995,** *36*, 2663.
14. Krech, J. H.; Rose-Pehrsson, S. L., *Analytica Chimica Acta* **1997,** *341*, 53.
15. McGill, R. A.; Paley, M. S.; Harris, J. M., *Macromolecules* **1992,** *25*, 3015
16. Smithrud, D. B.; Diederich, F., *J. Am. Chem. Soc.* **1990,** *112*, 339
17. Ortega, J.; Rafols, C.; Bosch, E.; Roses, M., *Journal of the Chemical Society: Perkin Transactions II* **1996**, 1497
18. Banerjee, D.; Kumar Laha, A.; Bagchi, S., *Journal of the Chemical Society: Farady Transactions I,* **1995,** *91*, 631
19. Acree, W.; Powell, J.; Tucker, S., *Journal of the Chemical Society: Perkin Transactions 2* **1995,** 529

20. Rafols, C.; Roses, M.; Bosch, E., *Journal of the Chemical Society: Perkin Transactions 2*. **1997,** 243.

21. Demas, J. N.; Carraway, E. R.; DeGraff, B. A., *Langmuir* **1991,** *7*, 2991

6 Optical Sensing Systems for Photocatalysis

6.1 Photocatalysis

The basic process that underlies most examples of semiconductor photocatalysis (SPC) can be summarized as follows[1-5].

$$\text{organic pollutant} + O_2 \xrightarrow[\text{Semiconductor}]{h\nu \geq E_{bg}} \text{minerals} \qquad (6.1)$$

where E_{bg} is the bandgap energy of the semiconductor, which is usually anatase titanium dioxide. The latter form of titania is commonly chosen because of its chemical and biological inertness, mechanical toughness, high photocatalytic activity and low cost.

Extensive research into SPC using TiO_2 has shown that it is able to photocatalyse the complete oxidative mineralization of a wide range of organic materials, including many pesticides, surfactants and carcinogens, by oxygen. Not surprisingly, many commercial products have emerged in recent years based on titania photocatalysis, including: water and air purification systems and self-cleaning tiles and glasses[6]. The latter in particular have met with significant commercial success and are now sold world-wide by most of the major glass manufacturers including the following (with the trade name of their commercial product in parentheses): Pilkington Glass (Activ™)[7], St-Gobain (Bioclean™)[8] and PPG (SunClean™)[9].

In the case of the above, the films of anatase titania on glass employed are self-cleaning in that most of the organic pollutants that go to make up the dirt and grime that deposit on window glass are readily mineralized by oxygen via the photocatalytic process (6.1)[10]. These films are also more easily wetted by water, i.e. hydrophilic, after UV irradiation, making it difficult for hydrophobic organic pollutants to adhere to the surface. Although it remains, as yet, unclear how UV-induced, hydrophilicity and SPC

activity are related, it is clear that any titania film which is SPC active also exhibits UV-induced hydrophilicity. It follows that for a fully functioning, self-cleaning glass it is essential that the titania coating exhibits SPC activity.

In order to compare the effectiveness of one self-cleaning glass with that of another, and to be able to effect and demonstrate a commercially acceptable high degree of quality control on any SPC product it is essential to have a set of agreed standard methods of assessment of SPC activity. The creation, validation and promotion of such a set of standard methods is currently in progress by an internationally-recognised body (ISO). Presented here is a comparison of existing methods of SPC analysis with those newly developed in the laboratory.

6.2 Existing Methods of Analysis

6.2.1 The stearic acid (SA) test

The stearic acid (SA) test involves the initial deposition of a thin layer of SA onto a photocatalytic film and then monitoring its destruction as a function of time, from which a rate for the disappearance of SA is usually gleaned and can be compared with values determined for other samples under the same conditions[10-17]. This reaction has gained considerable preference over the years, especially with the self-cleaning glass companies, for a number of reasons; SA provides a reasonable model compound for the solid films that deposit on exterior and interior surfaces, it is very stable under UV illumination in the absence of a photocatalyst film, the films are very easily laid down from a methanol or chloroform solution, the kinetics of removal of SA are usually simple and typically zero-order, and there are many possible ways in which the mineralisation process can be monitored.

The overall reaction can be summarized as follows:

$$CH_3(CH_2)_{16}CO_2H + 26O_2 \xrightarrow[h\upsilon \geq E_{bg}]{TiO_2} 18CO_2 + 18H_2O \qquad (6.2)$$

It is no surprise that this process has been studied a number of different ways including by monitoring the amount of CO_2 generated, using gas chromatography[13], and the change in thickness of the stearic acid film, using ellipsometry[18]. However, the most commonly employed method of studying the reaction is via the disappearance of the SA film using infra-red absorption spectroscopy, since SA absorbs strongly in the region 2700-3000 cm^{-1}, with peaks at 2958 cm^{-1}, 2923 cm^{-1}, and 2853 cm^{-1}, due to asymmetric in-plane C-H stretching in the CH_3 group and asymmetric and symmetric C-H stretching in the CH_2 groups, respectively[15, 16, 19-21]. The integrated area due to these peaks, over the range 2700-3000 cm^{-1}, A_{int}, is proportional to the amount of stearic acid present. Figure 6-1 illustrates the FT-IR absorbance versus wavenumber, σ, spectra, recorded for a sample of Activ^{TM} coated with stearic acid, as a function of irradiation time, where the irradiation source comprised six 8W blacklight bulbs, i.e. 365 ± 20 nm light.

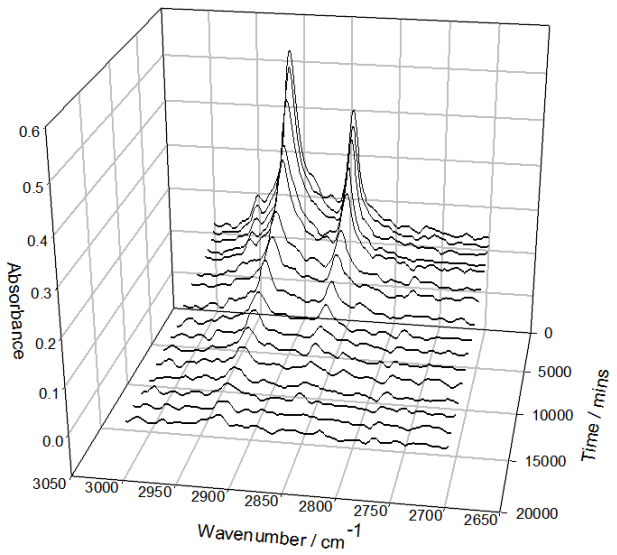

Figure 6-1 – A plot showing the change in the IR spectrum of a stearic acid film with irradiation time. Published with permission of Professor Andrew Mills.

An experiment carried out under the same conditions, but using plain glass instead, i.e. in the absence of a coating of titania, reveals no significant change in the stearic acid IR

absorption spectrum over the irradiation period. Figure 6-2 illustrates plots of A_{int} versus irradiation time profiles for plain glass, Activ™ and a 90 nm thick film of Degussa P25, respectively. The greater activity exhibited by the latter, compared to Activ™ is mainly due to its greater absorbance at 365 nm due to its greater film thickness[20].

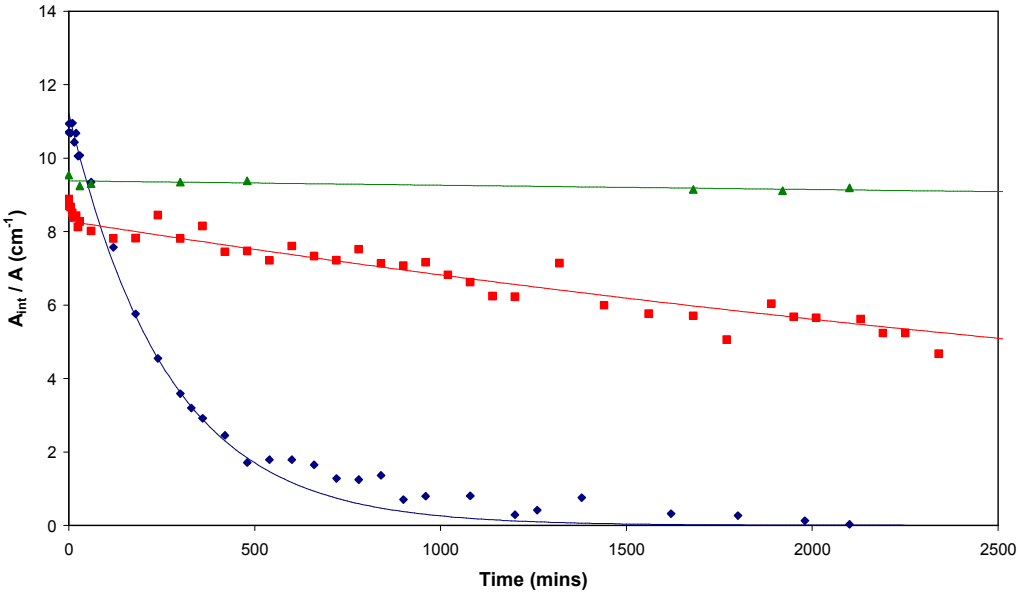

Figure 6-2 – A graph showing the integrated area (A_{int}) from 2700 – 3000 cm^{-1} of a stearic acid film as a function of time. Show are the profiles obtained for stearic acid films coated on plain glass, Activ™ glass and a 90nm thick film of Degussa P25.

A brief inspection of reaction (6.2) reveals that the overall mineralization process involves the transfer of 104 electrons and raises the concern that the observed temporal variation in [SA] upon UV irradiation of a SA layer on a titania film may not follow the stoichiometry indicated by reaction (6.2), due to the formation of recalcitrant or volatile intermediates. Certainly Minabe et. al.[13] have reported that the photocatalytic decomposition of SA sensitized by a TiO_2 sol-gel film does not go to completion, but instead halts after ca. 69% of the compound has been decomposed. This finding implies that long-lived, recalcitrant oxidation intermediate products are formed, preventing the SA:CO_2 stoichiometric ratio achieving the ultimate value of 1:18 as expected from

reaction (6.2). In contrast, and more reassuringly, others, including the Mills group, have reported that sol-gel and CVD produced titania films are able to completely remove a SA covering layer via semiconductor photocatalysis. In addition, very recently, both the destruction of SA and concomitant stoichiometric generation of CO_2 via semiconductor photocatalysis using a 110 nm thick sol gel titania film, were monitored simultaneously using FT-IR spectroscopy[17].

A typical set of IR spectra recorded as part of this work are illustrated in figure 6-3 and show the disappearance of the SA film and simultaneous appearance of the CO_2 as a function of irradiation time[17].

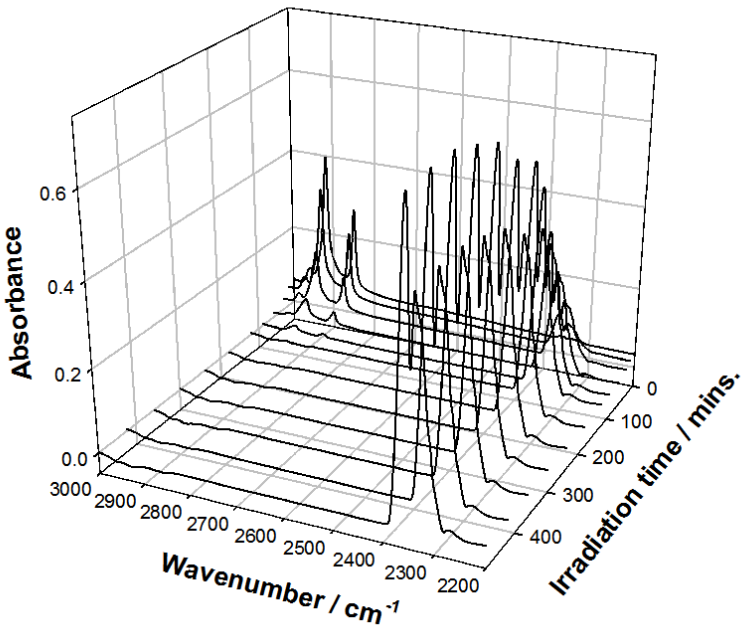

Figure 6-3 – IR spectra, recorded over time, of a stearic acid layer on a thick sol-gel TiO_2 film irradiated with UV light. Published with permission of Professor Andrew Mills[17].

This data, and other work, shows that no major intermediates, volatile or otherwise, are generated via the photocatalytic mineralisation of the SA film, i.e. the only major and readily observable IR active species present during the course of the photomineralisation process are SA and CO_2. The FT-IR data generated in this study

were used to produce the plots illustrated in figure 6-4 of the variation in the number of moles of stearic acid, (1/18) x the number of moles of CO_2 and, the sum of both as a function of irradiation time for the sol-gel TiO_2 film.

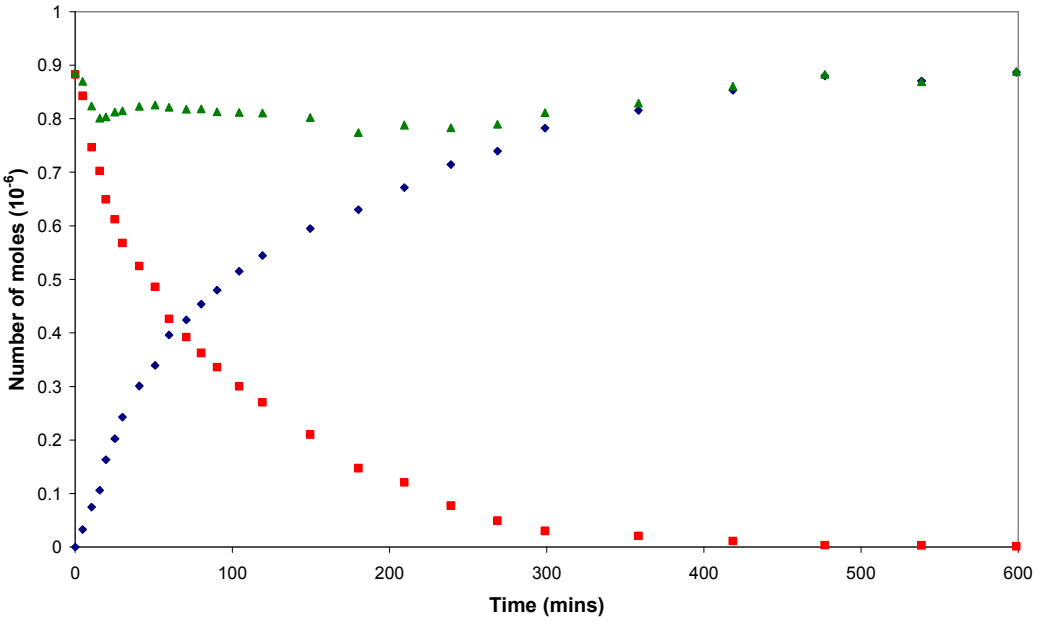

Figure 6-4 – Plots of the variations in: (i) the number of moles of stearic acid, (1/18) time the number of moles of CO_2, and the sum of both as a function of irradiation time for a P25 TiO_2 film. The data for the plots was derived from the integrated areas under the IR peaks, such as shown in 6-3, and appropriate calibration plots.

These plots show that, apart from the initial stages of the photomineralisation process, the degradation of SA and the concomitant generation of CO_2 are described by the reaction stoichiometry of reaction (6.2)[17] .

6.2.2 The methylene blue (MB) test

The methylene blue (MB) test is fast-becoming the most popular method for assessing photocatalytic activity of titania films and powders and is based on the photobleaching of the cationic, thiazine dye, methylene blue, MB[22-33]. The overall mineralization process can be summarized as follows:

$$2C_{16}H_{18}N_3S^+ + 51O_2 \longrightarrow 32CO_2 + 6HNO_3 + 2H_2SO_4 + 2H^+ + 12H_2O \qquad (6.3)$$

The initial step in the mineralization of this dye appears to be the cleavage of the bonds of the R-S^+=R' functional group in MB by a photogenerated $OH^\bullet$ radical, both adsorbed on the surface of the titania photocatalyst, to form the sulfoxide[23], i.e.

$$R\text{-}S^+\text{=}R' + OH^\bullet \longrightarrow R\text{-}S(\text{=}O)\text{-}R' + H^+ \qquad (6.4)$$

A second oxidative attack of the sulfoxide will produce an unstable sulfone, which is thought to dissociate to form the two benzenic rings and lead to a complete loss in colour of the original dye molecule. Herrmann and his co-workers have established that prolonged, titania-based photocatalysis of MB in aqueous solution leads to its complete mineralization as described by the reaction stiochiometry in equation (6.3). In most work where MB is used to assess the photocatalytic activity of a semiconductor, only the bleaching of the dye is monitored via UV/Vis absorption spectroscopy, presumably due to dye oxidation via reaction (6.4)[11, 22-33].

In aqueous solution MB absorbs most strongly at ca. 660 nm and, given its molar absorbtivity is ca. 10^5 dm^3 mol^{-1} cm^{-1} at this wavelength[27], it is easy to translate any absorbance data generated in a study of the photocatalytic destruction of MB into a plot of [MB] vs t, from which either an initial rate or a first order rate constant, k_1, can be obtained. Using this procedure as a guide, a 10^{-5} M, air-saturated, aqueous solution of MB was placed in a 1 cm spectrophotometer cell, 1 face of which was replaced with a piece of glass covered with a 4 micron sol-gel titania film. The spectra of this solution were then recorded as a function of UVA (1 mW cm^{-2}) irradiation time and the results are illustrated in figure 6-5. The insert diagram is a plot of the change in absorbance of the MB solution at 660 nm, ΔAbs, as a function of irradiation time and fits first order kinetics, with $k_1 = 0.0097$ min^{-1}, using data from the main diagram.

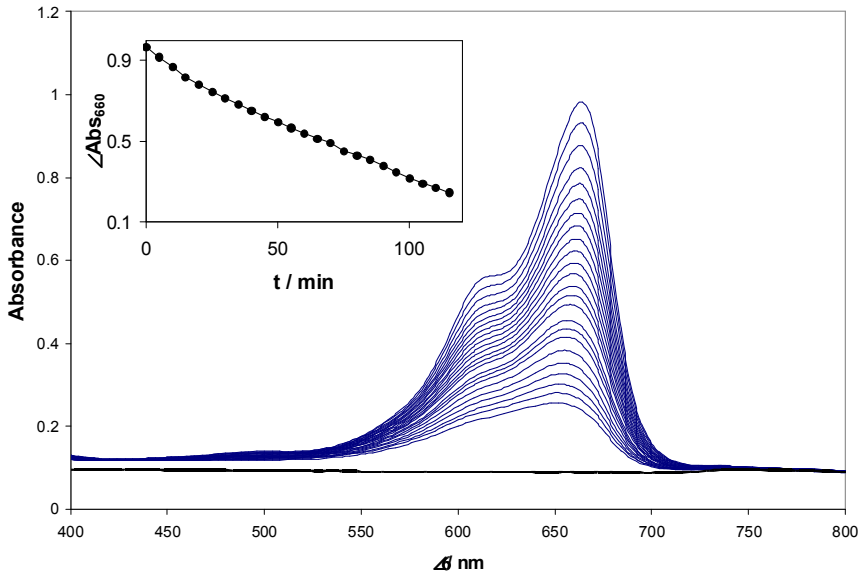

Figure 6-5 – a plot showing the absorbance spectrum, changing with time, of a methylene blue solution in contact with a 4 micron sol-gel titania film irradiated with 1mW cm^{-2} UVA light.

These results show that a thick titania film generated by the sol gel process[19] is effective at bleaching MB under the reaction conditions used, i.e. an initially neutral solution with a UVA intensity = 1 mW cm^{-2}. Note that in the absence of a titania film, over the same irradiation period the [MB] remains largely unchanged. The ease of this method of assessment, and its ability to provide a very visible and dramatic demonstration of the efficacy of semiconductor photocatalysis for water purification, have helped contribute to the ever-increasing popularity of this test method.

It is possible to claim some ambiguity in the interpretation of the MB test method, due to the ease of reduction of MB to its doubly reduced form, *leuco*-methylene blue, LMB, which, like the initially oxidized form of MB, is colourless, i.e.

$$MB + 2e^- + H^+ \longrightarrow LMB \qquad (6.5)$$

This reduction reaction is possible because E^o(MB/LMB) is ca. 0.53 V vs NHE at pH 0, and the reduction potential of the photogenerated electrons on a titania photocatalyst is

-0.32 V vs NHE at pH 0. It is well-known that it is very easy to effect reaction (6.5) with UV light, using a titania photocatalyst and a sacrificial electron donor, SED, provided that oxygen is absent from the reaction solution, e.g. by sparging with nitrogen[27, 34-37].

Although the probability appears low that reaction (6.5) can be effected by a titania photocatalyst, if a SED is not deliberately added to the system, in practice it is very readily effected by UV irradiation of a titania photocatalyst film or powder in contact with just an anaerobic MB solution and no obvious SED present. In this case it appears that MB itself, or other adventitious impurities, are able to act as a SED. That LMB has been generated in such an experiment is easily demonstrated, by exposing the final *anaerobic*, photo-bleached solution to air, which rapidly restores most of the original colour of the reaction solution, via the oxidation of to LMB to MB, i.e.

$$2LMB + O_2 \longrightarrow 2MB + H_2O \qquad (6.6)$$

The above results pose the question: is the photobleaching of MB in *aerobic* solution – i.e. the process that is a fundamental feature of the MB test – due solely to the photo-oxidation of the dye, via reaction (6.4), and not some or all of the photoreduction, of MB, via reaction (6.5)? In neutral or slightly alkaline solution, the kinetics of reaction (6.6) are so facile that any photo-bleaching of MB appears to be due solely to its photo-oxidation, i.e. reaction (6.4), as demonstrated by the results in figure 6-5. These results show that the neutral MB aqueous solution is photo-bleached upon irradiation with UV light. Other work shows that it does not recover its colour even with continued purging with air in the dark, indicating that no LMB has been photo-generated, since under the latter conditions, any LMB present would have been expected to react with the oxygen in the dark and recover some of the original colour of the MB solution.

Interestingly, reaction (6.6) is much slower under acidic conditions and, as a result, the photo-bleaching of MB by titania is more likely to show some evidence of LMB production, via reaction (6.5), as well as photo-oxidation, via reaction (6.4) if carried

out at a low pH. This is nicely demonstrated by performing an experiment in which a 10^{-5} M MB solution containing 0.01 M $HClO_4$ was placed in contact with a film of P25 titania and UV irradiated in an oxygenated solution for 30 min, and then left in the dark for a further 60 min during which the solution was purged with nitrogen (first 30 min) and then oxygen (last 30 min). The results of this work are illustrated in figure 6-6, plotted in the form of the change in absorbance at 660 nm of the MB solution, ΔAbs, as a function of time.

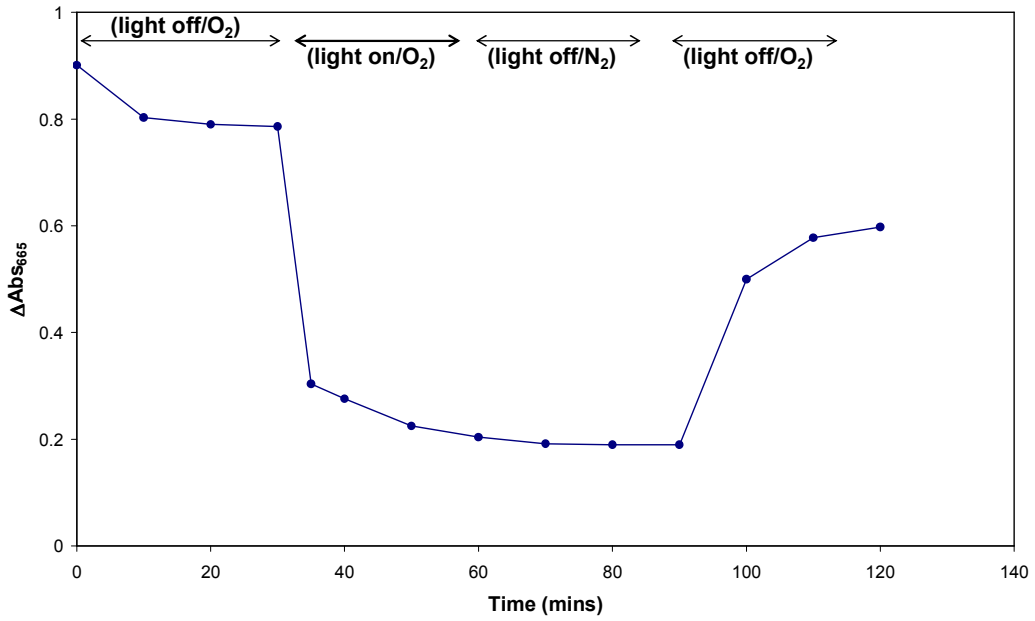

Figure 6-6 – a plot showing the change with time in absorbance at 660nm of a 10^{-5} M MB solution, in contact with a TiO_2 film, in 0.01 M $HClO_4$. During the 'light on' stage the solution was irradiatied with 1 mW cm^{-2} UVA light.

These show that, as with the non-acidic MB solution, the MB is photo-bleached by the titania particles in an oxygen–saturated solution and does not recover any of its colour when the light is switched off and the solution purged with nitrogen for 30 min. However, in marked contrast to the work carried out in neutral solution, under acidic conditions, purging of the photo-bleached reaction solution with oxygen allows the MB solution to regain 2/3's of its original colour, as illustrated by the results in figure 6-6. The most likely explanation for these observations is that in oxygenated solution, MB in aqueous solution is photo-oxidatively and irreversibly bleached under neutral or alkaline conditions, whereas under acidic conditions it is largely photo-reductively and

reversibly bleached to LMB-reduced, which is quite stable even in oxygen-saturated solution, since reaction (6.6) is very slow under acidic conditions. Previous work also established that this latter reaction is favoured in neutral and acidic conditions upon UV irradiation of the MB/TiO_2 under anaerobic conditions.

Any ambiguity in a method of assessment, as exists for the MB test system, is clearly highly undesirable. Although reaction (6.5) is a possible cause for ambiguity in the MB test, it appears to be only a concern when the MB solution is acidic, or not fully saturated with oxygen. However, less than fully air or oxygen saturated conditions may arise not only if the solution is poorly stirred or purged – both of which can be eliminated by good practice - but also if the photo-catalyst under assessment is highly active. A rather nice demonstration of this is illustrated by the ΔAbs vs UV irradiation time profiles in figure 6-7 that were generated using samples of plain glass, Activ™, and a thick sol gel film (4 microns) in contact with an unstirred, and stirred, air-saturated aqueous solution of 10^{-5} M MB.

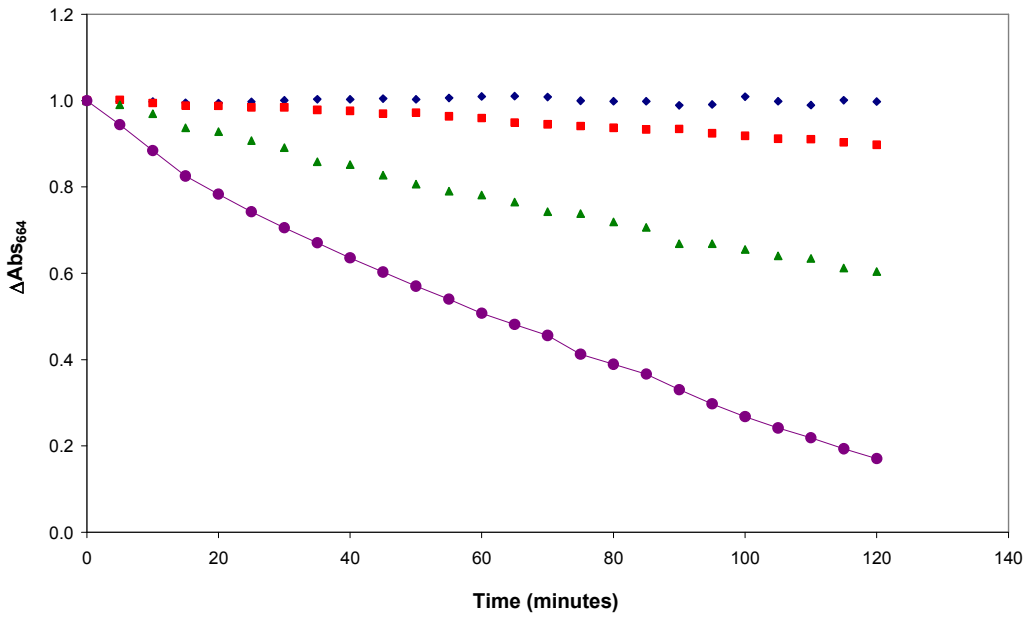

Figure 6-7 – a plot showing the change in absorbance at 665nm of 10^{-5} M MB solutions, irradiated with 1 mW cm^{-2} UVA light in contact with: plain glass, Activ Glass, Sol-Gel TiO_2 (unstirred soln.), and Sol-Gel TiO_2 (stirred soln.). Stirred solutions for the plain glasses showed were no different to the unstirred solutions.

From these plots it is clear that MB in contact with plain glass is not photo-degraded by the UV light to any great extent, with or without stirring, over the timescale of the experiment. In addition, the ΔAbs vs t profile for Activ™, with its very low SPC activity, is largely the same with and without stirring (initial rate (r_i) = ca. $9.0x10^{-4}$ Ab min^{-1}) for Activ™. However, for the much more active, thick sol-gel film, the measured initial rate of MB bleaching is $9.2x10^{-3}$ AbsU min^{-1} when stirred, but ca. 2.7 times less, when left unstirred, presumably due to oxygen depletion and/or LMB production.

The results of the above work show that a set of test conditions in which an air-saturated, neutral, quiescent MB solution is used may be appropriate if a slow-acting photocatalyst film, such as Activ™ is under test, but clearly inappropriate if a more active photocatalyst film is being assessed. Clearly if the MB test does become a standard test procedure, - and there is a strong suggestion that it will - the protocol should be defined as such that the test is able to assess the activities of photocatalyst films with high and low activities.

6.3 Newly Developed Method of Analysis

6.3.1 The resazurin (Rz) ink test

Both the stearic acid and the methylene blue tests do not appear apt for making measurements in the field, since they require at least one piece of sophisticated and expensive electrical analytical equipment and, usually, a trained technician to run and maintain it. In addition, because most commercial self-cleaning glasses utilize only a very thin layer of titania, the kinetics of the photomineralisation of SA or MB are very slow and so it can take hours, if not days, to completely destroy a stearic acid layer or a MB solution under solar UVA conditions (typically ca. 4.5 mW cm^{-2} for a clear, sunny day).

It is apparent that the photocatalytic activity of a semiconductor film would be more easily assessed, and appropriate for use in the field, if the test involved a simple color change, especially if the latter were rapid, i.e. within a few minutes of UV exposure. Researchers have tried staining SPC films and powders directly with dyes[38-40] and, with more success, incorporating a dye in a deposited polymer film layer[41]. However, the major problem with these approaches is that they rely on the colour change being effected by the photo-oxidation of the dye or dye/polymer combination and this is usually a slow process, as evidenced by the SA test. Such a dye or dye/polymer test might be adequate for assessing the SPC activities of very active, usually thick, titania films, where the kinetics of photomineralisation are rapid, but, clearly inappropriate for most commercial, self-cleaning photocatalytic products, including glasses and tiles, that exhibit much slower rates of photocatalysis. Instead, what is required is an indicator ink that can be printed, coated or written onto any SPC film, be it transparent or opaque, and which rapidly, i.e. within a few minutes at most, will change color upon UV irradiation of an underlying thin photocatalyst film.

Such an ink has been reported recently by this group[42] and comprises: 3 g of a 1.5 wt% aqueous solution of hydroxyethyl cellulose (HEC), 0.3 g of glycerol and 4 mg of the redox dye, resazurin, Rz. The film is usually spun-coated onto the substrate under test and dried in an oven at 70^{o}C for 10 min, although drying in air, rather than in an oven, does not alter its performance. A typical dried ink film has a λ_{max} at 610 nm, and is ca. 590 nm thick when coated onto a test substrate, such as plain glass or Activ™. The UV-Vis spectrum of this film, as well as the associated spectra recorded during UVA irradiation, is shown in figure 6-8.

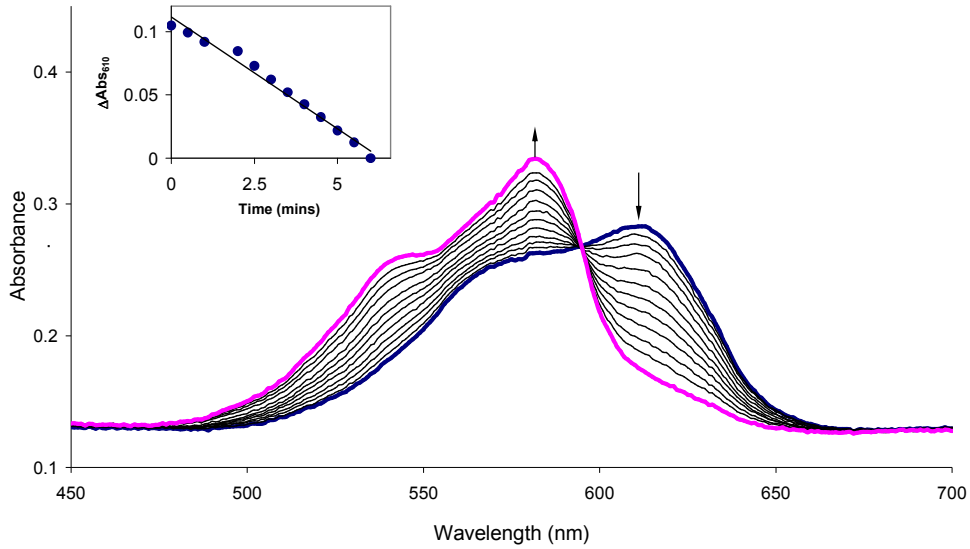

Figure 6-8 – the change in the absorbance spectra of the resazurin ink with time while in contact with a photocatalyst film (Active Glass) and irradiated with UV light.

In contrast, as illustrated by the results in figure 6-8, the ink did change rapidly in color, i.e. within minutes, from blue to pink upon UVA irradiation when deposited on a commercial sample of self-cleaning glass, such as Activ™. Other work shows that this colour change always occurs if a titania photocatalyst is present, regardless of its form (film or powder) or supporting substrate (glass, tile, paper, plastic or metal). Further irradiation (hours) of this system bleaches the ink, although the polymer remains apparently intact. However, the unreacted polymer component of the ink is readily removed with a damp cloth, since the ink is water-soluble, or when subjected to prolonged UV irradiation (days), since this effects its complete mineralization by the underlying photocatalytic film.

In contrast to the stearic acid and methylene blue tests, the Rz photocatalyst indicator ink test described above does not work via a photo-oxidative mechanism, but rather by a novel, photo-reductive mechanism in which the photogenerated holes react irreversibly with the sacrificial electron donor present, glycerol, and the photogenerated electrons (E° (TiO_2 (e^-)) = -0.52 V) reduce the indicator ink dye molecules, Rz, contained therein,

to a differently coloured form, namely, resorufin, Rf. The various steps of the process are summarised in figure 6-9.

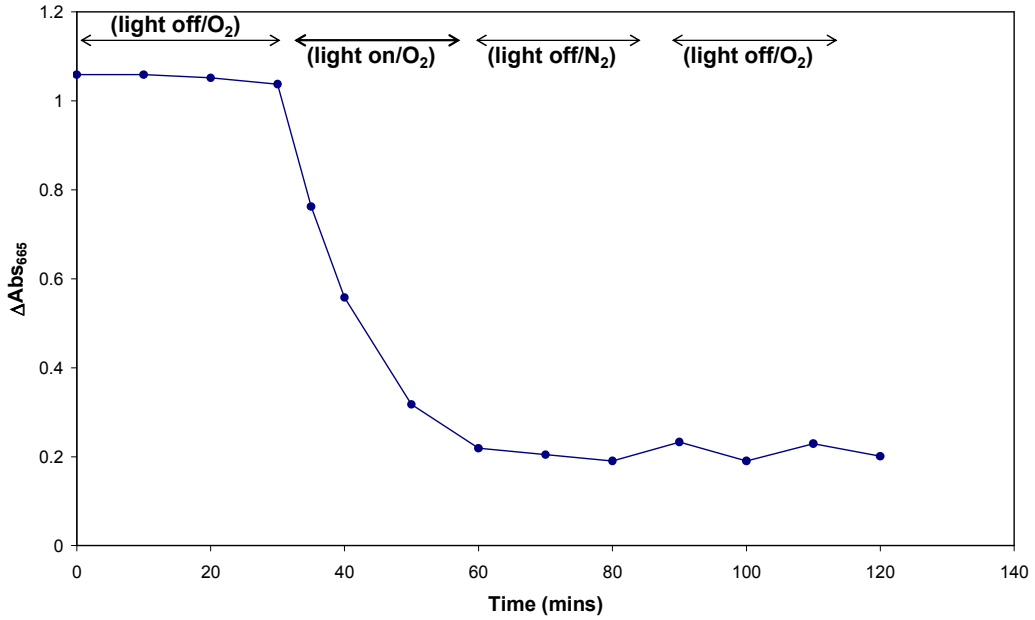

Figure 6-9 – the change in absorbance at l_{max} of a Resazurin film on Activ Glass when irradiated with UV light and then left in the dark.

The Rz/glycerol/HEC photocatalyst indicator ink described above works very rapidly for photocatalyst films with low SPC activities, such as commercial samples of self-cleaning glass, as illustrated by the results in figure 6-8 for Activ™ [43]. However, clearly its value as a photocatalyst indicator would be greatly enhanced if the initial rate of dye bleaching, R_{ink}, correlated with the initial rate of stearic acid removal, R_{SA}, which is so often used to assess the SPC activities of such films. In order to address this issue a series of CVD coated samples of anatase titania on glass with different SPC activities were prepared by varying the deposition conditions. These films, and a commercial sample of self-cleaning glass, Activ^{TM}, were first assessed for SPC activity using the stearic acid test and then cleaned and coated with the photocatalyst ink and assessed for SPC activity via the measured values of R_{ink}. A plot of the rate data arising from this work, i.e. R_{ink}, vs R_{SA} is illustrated in figure 6-10 and reveals a good correlation between the two sets of rate data, the important difference being that for each sample

the R_{ink} data were obtained in a few minutes, whereas the R_{SA} data required hours of illumination.

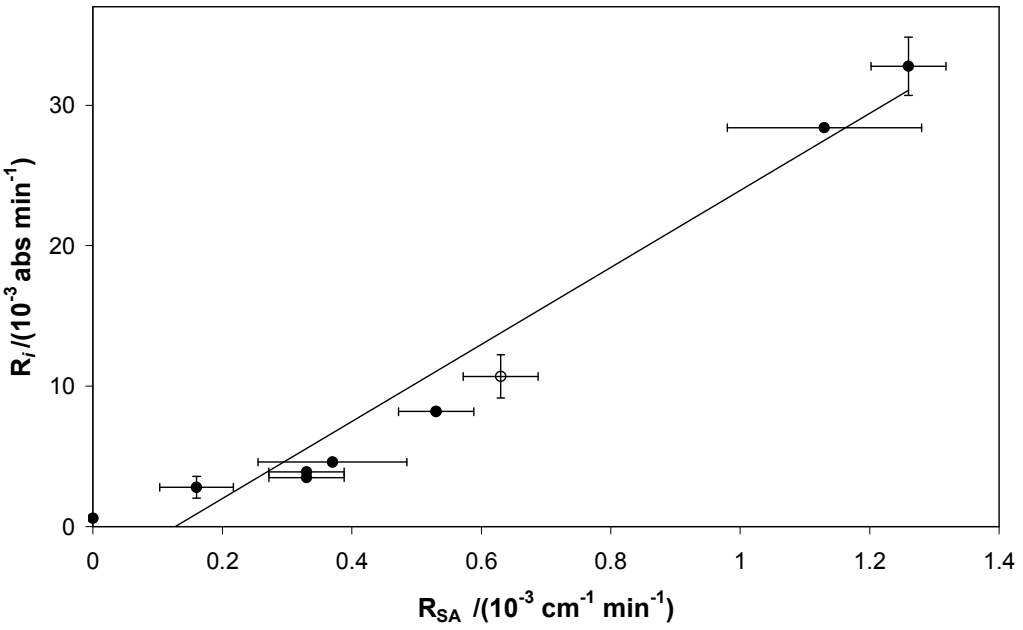

Figure 6-10 – a plot showing a comparison of the rates of reaction of the resazurin test against the same values obtained for the stearic acid test.

Finally, the efficacy of the photocatalyst indicator ink for work in the field was illustrated by placing some of the Rz ink in an empty felt-tipped pen and using it to write on a piece of plain and Activ™ glass. Upon exposure to 3 min of UVA light (7.4 mW cm^2) the writing on the Activ™ coated glass had changed from blue to pink, whereas the writing on the plain glass remained blue even after prolonged (6h) irradiation with the same UV source. Figure 6-11 is a photograph of the pen and the two inscribed pieces of glass after irradiation.

Figure 6-11 – a picture showing the resazuring ink on Activ Glass and plain glass after irradiation with UV light, alongside the pen used to put down the ink.

Given that most methods of assessing photocatalyst activity are slow and require expensive analytical equipment to service them, the Rz photocatalyst indicator ink reported here appears an attractive test for SPC activity, either in the laboratory for quantitative work, or in the field, for a semi-qualitative assessment. It is of particular merit since it can be delivered using a simple felt-tipped pen or rubber stamp and it allows the semi- quantitative assessment of a photocatalytic film to be made in the field, using sunlight as the light source and the human eye as the detector of a colour change.

6.4 Conclusions

Two major established, and one new, methods of assessing the photocatalytic activities of films, such as found on self-cleaning glass, are reviewed. The SA test is currently most popular and very reliable. The MB test has a more checkered history, and there remain some genuine concerns regarding its reliability; despite this it is used increasingly in SPC. The new Rz ink test is much faster than the other tests and easier to use, especially in the field.

6.5 References

1. Fox, M. A.; Dulay, M. T., *Chemistry Reviews* **1993,** *93*, 34.
2. Hoffmann, M. R.; Martine, S. T.; Choi, W.; Bahnemann, D. W., *Chemistry Reviews* **1995,** *95*, 69.
3. Kamat, P. V., *Chemistry Reviews* **1993,** *93*, 267.
4. Mills, A.; LeHunte, J., *Journal of Photochemistry and Photobiology A: Chemistry* **1997,** *108*, 1.
5. Ollis, D. F.; Pelizetti, E.; Serpone, N., In *Photocatalysis: Fundamentals and Applications*, Wiley InterScience: 1989.
6. Mills, A.; Lee, S. K., *Journal of Photochemistry and Photobiology A: Chemistry* **2002,** *152*, 233.
7. http://www.pilkington.com (accessed November 2009 - 2006).
8. http://www.saint-gobain-glass.com/fr/index.asp (accessed January 2011 - 2008).
9. http://www.ppg.com/gls_residential/gls_sunclean/ (accessed January 2011 - 2008).
10. Sanderson, K. D.; Mills, A.; Hurst, A. S.; Lepre, A.; McKittrick, D.; Rimmer, D.; Ye, L. In *SVC*, Annual Technical Confrerence Proceedings, Society of Vacuum Coaters, Albuquerque, USA, Albuquerque, USA, 2003; p 203.
11. Fretwell, R.; Douglas, P., *Journal of Photochemistry and Photobiology A: Chemistry* **2001,** *143*, 229.
12. Manning, T. D.; Parkin, I. P.; Clark, R. J. H.; Sheel, D.; Pemble, M. E.; Vernadoue, D., *Journal of Materials Chemistry* **2002,** *12*, 2936.
13. Minabe, T.; Tryk, D. A.; Sawunyama, P.; Kikuchi, Y.; Hashimoto, K.; Fujishima, A., *Journal of Photochemistry and Photobiology A: Chemistry* **2000,** *137*, 53.
14. Paz, Y.; Heller, A., *Journal of Materials Research* **1997,** *12*, 2759.
15. Paz, Y.; Luo, Z.; Rabenterg, L.; Heller, A., *Journal of Materials Research* **1995,** *10*, 2842.
16. Sawunyama, T.; Jiang, L.; Fujishima, A.; Hashimoto, K., *Journal of Physical Chemistry B* **1997,** *101*, 1100.

17. Mills, A.; Wang, J., *Journal of Photochemistry and Photobiology A: Chemistry* **2006,** *182*, 181.
18. Remillard, J. T.; McBride, J. R.; Nietering, K. E.; Drews, A. R.; Zhang, X., *Journal of Physical Chemistry B* **2000,** *104*, 4440.
19. Mills, A.; Elliot, N.; Hill, G.; Fallis, D.; Durrant, J. R.; Willis, R. L., *Photochemical & Photobiological Sciences* **2003,** *2*, 591.
20. Mills, A.; Hill, G.; Bhopal, S.; Parkin, I. P.; O'Neill, S. A., *Journal of Photochemistry and Photobiology A: Chemistry* **2003,** *160*, 185.
21. Mills, A.; Lee, S. K.; Lepre, A.; Parkin, I. P.; O'Neill, S. A., *Photochemical & Photobiological Sciences* **2002,** *1*, 865.
22. Artem'ev, Y. M.; Artem'eva, M. A.; Vinogradov, M. G.; Ilika, T. I., *Russian Journal of Applied Chemistry* **1994,** *67*, 1354.
23. Houas, A.; Lachleb, H.; Ksibi, M.; Elaloui, E.; Guillard, C.; Hermann, J. M., *Applied Catalysis B: Environmental* **2001,** *31*, 145.
24. Lakshmie, S.; Renganathan, R.; Fuijita, S., *Journal of Photochemistry and Photobiology A: Chemistry* **1995,** *88*, 163.
25. Matthews, R. W., *Journal of the Chemical Society: Farady Transactions I* **1989,** *85*, 1291.
26. Matthews, R. W., *Water Research* **1991,** *25*, 1169.
27. Mills, A.; Wang, J., *Journal of Photochemistry and Photobiology A: Chemistry* **1999,** *127*, 1301.
28. Nogueira, R. F. P.; Jardin, W. F., *Journal of Chemical Education* **1993,** *70*, 861.
29. Reeves, P.; Ohlhausen, R.; Sloan, D.; Pamplin, K.; Scoggins, T.; Clark, C.; Hutchinson, B.; Green, D., *Solar Energy* **1992,** *48*, 413.
30. Serrano, B.; de Lasa, H., *Industrial and Engineerig Chemistry Research* **1997,** *36*, 4705.
31. Valladares, J. E.; Bolton, J. R., *Photocatalytic Purification and Treatment of Water and Air*. Elsevier, New York: 1993.
32. Wark, M.; Tschirch, J.; Bartels, O.; Bahnemann, D. W.; Rathoussky, J., *Microporous and Mesoporous Materials* **2005,** *84*, 247.
33. Zhang, T.; Ovama, T.; Aoshima, A.; Hidaka, H.; Zhao, J.; Serpone, N., *Journal of Photochemistry and Photobiology A: Chemistry* **2001,** *140*, 163.

34. Kamat, P. V., *Journal of the Chemical Society: Farady Transactions I* **1985,** *81*, 509.
35. Naskar, S.; Pilay, S. A.; Chanda, M., *Journal of Photochemistry and Photobiology A: Chemistry* **1998,** *113*, 257.
36. Pamfilov, A. V.; Mazurkevich, Y. S.; Pakhomova, E. P., *Kinetika i Kataliz* **1969,** *10*, 915.
37. Yoneyama, H.; Toyoguchi, Y.; Tamura, H., *Journal of Physical Chemistry* **1972,** *76*, 3460.
38. Julson, A. J.; Ollis, D. F., *Applied Catalysis B: Environmental* **2006,** *65*, 315.
39. Kemmitt, T.; Al-Salim, N. I.; Waterland, M.; Kennedy, V. J.; Markwitz, A., *Current Applied Physics* **2004,** *4*, 189.
40. Tatsuma, T.; Tachibana, S.; Fujishima, A., *Journal of Physical Chemistry B* **2001,** *105*, 6987.
41. Mills, A.; Wang, J.; Lee, S. K.; Simonsen, M., *Chemical Communications* **2005**, 2721.
42. Mills, A.; Wang, J.; McGrady, M., *Journal of Physical Chemistry* **2006,** *110*, 18324.

7 Summary

7.1 Viologen Dosimeter

It was shown that viologens will form coloured species when exposed to all wavelengths of ultraviolet light. The rate of formation of this species follows a near linear correlation with the intensity of irradiating light. These coloured species are stable in an oxygen free environment, such as in the low permeability poly(vinyl alcohol). In the presence of oxygen the viologen radicals are rapidly oxidised to their colourless bipyridinium molecules. The use of benzyl viologen, rather than methyl viologen, is preferably as the benzyl species is less likely to be oxidised (although will still react in an oxygen permeable environment).

The mechanism of the reduction remains unclear. The two proposed mechanisms for the reaction involve the donation of electrons from either the halide associated with the viologen or the solvent environment. Increasing the amount of halide in the system by a factor of 10 led to a very small increase in the rate of reaction. Replacing chloride with the less electronegative iodide decreased, rather than increased, the rate of reaction. This is complicated, as the presence of the iodide clearly affects the electronic structure (and thus absorbance spectrum) of the viologen so the effect of the halide isn't simple. Regardless, substituting the halide proves useful in retarding the rate of reaction. The use of electron donating species appears to have little effect on the rate of the viologen reduction, although the species used must be considered carefully as plasticization of the a polymer film may occur, leading to the problems caused by oxygen outlined above.

A viologen system has been shown to respond to erythemal levels of UV radiation, producing a strong colour change it does so, with an absorbance of 0.8 at 550 nm after reaching the MED for skin type II. This same system has been shown to respond in a similar fashion under varying intensities of both artificial and natural light.

7.2 Tetrazolium Dosimeter

The tetrazolium salts have been shown to respond to ultraviolet light of different wavelengths, much like the viologens, and neotetrazolium chloride has been shown to produce the greatest response in that regard. These extent of colouration can be controlled by dye concentration and film thickness, much like the viologen films. The tetrazolium systems are not sensitive to oxygen so a wider variety of polymer materials may be used as the films for a tetrazolium based dosimeter. A tetrazolium system has been shown to respond to erythemal levels of ultraviolet light, producing a strong colour change after reaching the MED of an a skin type II individual.

7.3 Solvatochromic VOC sensor

Reichardt's dye was embedded within an ethyl cellulose film and the film was shown to change colour depending on the solvent vapour it was exposed to. The colour changes were not equal to, or directly correlated with, those reported for the Reichardt's dye in pure solvent. It was shown using ethanol that, by carefully choosing the analysis parameters, these RD/EC films could be used to quantitatively measure the level of solvent vapour in the environment.

The response and recovery characteristics of the RD/EC films were shown to be similar to other polymer-dye films reported in the literature, with the complete colour change of the film when exposed to (and removed from) the solvent vapour occurring in over 1 minute.

Reichardt's dye was also adsorbed onto a fumed silica support. These RD/SiO_2 films also displayed colour changes when exposed to solvent vapours, although these were markedly different to those displayed in the polymer films. This difference is due to the different polarities of silica and ethyl cellulose.

The RD/SiO_2 films responded much quicker than the polymer films, with colour changes taking <30 seconds to come to completion for ethanol. These films were also capable of quantifying the amount of solvent in the surrounding environment.

Interestingly, the E_T30 values of the RD/SiO_2 films under a series of alcohols showed a linear correlation with the E_T30 values recorded in the pure solvents. If these sensors are not useful for directly identifying individual solvents they can at least be used for identifying specific alcohols.

The RD/SiO_2 films were also shown to be sensitive to water and, while not a VOC, may be useful as humidity indicators.

7.4 Sensor systems for Photocatalysis

Existing and new systems for assessing the activity of photocatalytic films were reviewed. The Stearic acid test was shown to be a reliable and well understood system for monitoring the activity of a photocatalytic material, either by direct monitoring via IR spectroscopy or by monitoring the evolution of CO_2 through the same. The advantage to this system is that it closely mimics the real-world application of many photocatalyst films – the destruction of a thin layer of organics – but this comes at the cost of taking a long time to perform, with times of 1000+ minutes reported for complete testing.

The Methylene Blue test, which looks set to become a new standard method of assessing photocatalytic activity, was shown to be quicker than the stearic acid test (times <120 mins) and can be regarded as easier to monitor; While a spectrometer gives accurate results the experimenter can gauge the extent of reaction by simply watching the colour change.

The review highlighted difficulties with the Methylene Blue test, showing that the precise mechanism of the reaction varies depending on the surrounding conditions such as pH and O_2 concentration. These show that the results obtained from this test will only be reliable if the conditions are understood and good experimental practice is followed to ensure that each film under receives the same test.

The newest test developed by the Mills group, using the reduction of Resazurin as the analysis method, has been shown to be much faster the the two established methods,

with complete reaction occurring in less than 5 minutes. The colour change displayed by this method occurs at levels of UVA associated with natural sunlight and so can be used to give semi-qualitative analysis in the field without the need for specialist equipment, especially if delivered by the proposed method of a felt-tip pen or rubber stamp

7.5 Further Work

- It is suggested that more work needs to be done to fully understand the mechanism of the viologen system. The author is inclined to believe that the mechanism is based on the donation of electrons from the solvent environment, rather than donation from the halide, but this has not been proved conclusively. Kamogawa even argues that changing the solvent simply changes the mobility of the viologen cation and halide anion, so any change in reactivity is simply a matter of solubility rather than the solvent directly causing the reaction.

- The author tried to completely replace the halide with another type of anion – dodecylsulfide – and saw no colour change (results not reported). However this species was dissolved in a non-aqueous polymer and so it is impossible to say either way what caused the loss of reactivity. If the halide were to be replaced by another anion that allowed dissolution in the same polymer mixture then it may be possible to say whether the halides are contributing to the reaction. By understanding what causes the reaction it will be easier to identify ways of altering and controlling the rate of reaction.

- The work performed by this author shed little light on the tetrazolium system other than it was a UV dosimeter system unaffected by the presence of oxygen. It was suggested that work similar to that with the viologens and using electron donors, and perhaps even reaction blocking species, be carried out to demonstrate that the rate of the tetrazolium reaction can be controlled and made

applicable to all skin types. (This work was carried on by Mrs Pauline Grosshans – see appendix).

- The solvatochromic system was shown to give a quantitative response to different levels of solvent vapour but the qualitative response was shown to be non-simple when compared with the pure solvent. One direction to take this would be to build up a library of E_T30 values for the RD/SiO_2 films exposed to different solvent vapours. This would remove the difficulty of direct comparison with the values recorded for Reichardt's dye in pure solvent.

- A project which could come out of the work would be the development of an optical nose system using this dye. The broad spectral peaks obtained from these films make it difficult to correctly identify a maximum wavelength and this may result in solvents of similar polarity being confused. If an array were built with RD dissolved in a variety of different solid supports, each recording a different E_T30 value for a given solvent, then it may be possible to develop unique spectral pictures for any given solvent. This would allow the development of a more 'complete' library than the one suggested above.

- Now that the solvatochromic system has been shown to work, it is suggested that work is carried out to determine whether it can detect levels of solvent in the ppm/b range more commonly associated with VOCs in real world situations.

APPENDIX

Anal Bioanal Chem (2006) 386: 299–305
DOI 10.1007/s00216-006-0605-0

ORIGINAL PAPER

Andrew Mills · Michael McFarlane · Stefan Schneider

A viologen-based UV indicator and dosimeter

Received: 7 April 2006 / Revised: 16 May 2006 / Accepted: 8 June 2006 / Published online: 22 July 2006

Abstract A UV indicator/dosimeter based on benzyl viologen (BV^{2+}) encapsulated in polyvinyl alcohol (PVA) is described. Upon exposure to UV light, the BV^{2+}/PVA film turns a striking purple colour due to the formation of the cation radical, $BV^{\bullet+}$. The usual oxygen sensitivity of $BV^{\bullet+}$ is significantly reduced due to the very low oxygen permeability of the encapsulating polymer, PVA. Exposure of a typical BV^{2+}/PVA film, for a set amount of time, to UVB light with different UV indices produces different levels of $BV^{\bullet+}$, as measured by the absorbance of the film at 550 nm. A plot of the change in absorbance at this wavelength, ΔAbs(550), as a function of UV index, UVI, produces a linear calibration curve which allows the film to be used as a UVB indicator, and a similar procedure could be employed to allow it to be used as a solar UVI indicator. A typical BV^{2+}/PVA film generates a significant, semi-permanent (stable for >24 h) saturated purple colour (absorbance ~0.8–0.9) upon exposure to sunlight equivalent to a minimal erythemal dose associated with Caucasian skin, i.e. skin type II. The current drawbacks of the film and the possible future use of the BV^{2+}/PVA film as a personal solar UV dosimeter for all skin types are briefly discussed.

Keywords UV dosimeter · UV indicator · Methyl viologen · Photoreduction

Introduction

The major source of UV radiation is the sun, although other sources include fluorescent lamps, welding arcs, plasma torches and some lasers. On the surface of the Earth, the wavelengths of solar UV lie in the UVB and UVA waveband regions, i.e. 290–320 nm and 320–400 nm [1], typically 0.16 and 4.49 mW cm^{-2}, respectively, on a sunny day (UVI=3.7); terrestrial levels of solar UVC (200–290 nm) are negligible. Most fluorescent white light sources emit small amounts of UVA (≤4.8 μW cm^{-2}) and UVB (≤9.3 nW cm^{-2}), both of which are well below (typically <14% of) current recommended UV exposure limits [2]. Black–light blue (BLB) lamps (λ_{max} (emission)=355 nm; half-peak bandwidth=34 nm) are UVA fluorescent lamps; they are commonly used in stores to check for fluorescent markings on banknotes and to set UV-sensitive glues or paints. UVC (i.e. germicidal, fluorescent tubes, λ_{max} (emission)=254 nm) are most commonly used by the water industry as a means of disinfection; they are also used to disinfect the air in air-conditioning units, especially in hospitals [3]. UVA and UVB fluorescent tubes are often used in the sun-tanning industry [4].

UV is a well-recognised potential health hazard [5–8]. The damage it can cause depends upon many factors, including the biological material concerned (usually skin or eyes), the type of UV, its intensity, the length of exposure and the sensitivity of the individual. For example, short-term exposure of the skin to UV can cause damage ranging from erythema, i.e. skin reddening or sunburn, to blistering that is similar to that associated with second-degree thermal burns. Prolonged exposure can lead to premature skin ageing and skin cancer. Exposure of the eyes and eyelids to UV can cause keratoconjunctivitis, i.e. welder's flash or snow blindness [6–8]. Prolonged exposure of the eyes can cause cataracts and/or clouding of the lens of the eye. Finally, there is increasing evidence that the human immune system is suppressed upon acute and low-dose UV exposure, and this effect is independent of skin type sensitivity [9].

Each year, about 133,000 new cases of malignant melanomas and approximately three million nonmelanoma skin cancers are diagnosed, most of which are directly attributable to UV damage [10]. It is no surprise therefore there is growing public recognition that we all should make an effort to reduce the harmful effects of UV when out in the sun. The latter is particularly important where

A. Mills (✉) · M. McFarlane · S. Schneider
Department of Pure and Applied Chemistry,
University of Strathclyde,
Glasgow G1 1XL, UK
e-mail: a.mills@strath.ac.uk
Tel.: +44-141-5482458
Fax: +44-141-5484822

Journal of Photochemistry and Photobiology A: Chemistry 201 (2009) 136–141

Contents lists available at ScienceDirect

Journal of Photochemistry and Photobiology A: Chemistry

journal homepage: www.elsevier.com/locate/jphotochem

UV dosimeters based on neotetrazolium chloride

Andrew Mills*, Pauline Grosshans, Michael McFarlane

WestCHEM, University of Strathclyde, Department of Pure and Applied Chemistry, Thomas Graham Building, 295 Cathedral Street, Glasgow G1 1XL, UK

ARTICLE INFO

Article history:
Received 4 July 2008
Received in revised form 6 October 2008
Accepted 10 October 2008
Available online 21 October 2008

Keywords:
UV dosimeter
Tetrazolium
UV index
MED

ABSTRACT

A novel UV dosimeter is described comprising a tetrazolium dye, neotetrazolium chloride (NTC), dissolved in a film of polymer, polyvinyl alcohol (PVA). The dosimeter is pale yellow/colourless in the absence of UV light, and turns red upon exposure to UV light. The spectral characteristics of a typical UV dosimeter film and the mechanism through which the colour change occurs are detailed. The NTC UV dosimeter films exhibit a response to UV light that is related to the intensity and duration of UV exposure, the level of dye present in the films and the thickness of the films themselves. The response of the dosimeter is temperature independent over the range 20–40 °C and, like most UV dosimeters, exhibits a cosine-like response dependence upon irradiance angle. The introduction of a layer of a UV-screening compound which slows the rate at which the dosimeter responds to UVR enables the dosimeter response to be tailored to different UV doses. The possible use of these novel dosimeters to measure solar UV exposure dose is discussed.

1. Introduction

Tetrazolium salts are water soluble organic heterocycles that can be readily reduced to form partially soluble and insoluble formazans. Tetrazoliums are generally colourless or pale yellow in solution while formazans are highly coloured species typically red, blue and purple. A general tetrazolium reduction reaction is as follows:

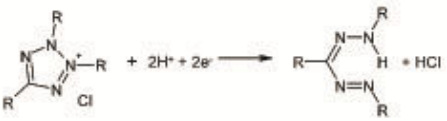

colourless coloured (1)

This colour changing reaction has made tetrazolium salts a popular choice of indicator for the evaluation of bacterial metabolic activity [1] as well as the detection of diseases such as tuberculosis [2]. The literature has numerous references to the "Tetrazolium Test" or the "Nitro Blue Test" [3–7] in which the tetrazolium dyes provide a quick visual indication of cell activity *via* its addition to a cell culture.

As well as occurring *via* electron transfer in biological environments, the reduction of tetrazoliums can also be induced by γ-radiation, which enables tetrazoliums to be used as dosimeters for measuring absorbed dose of γ-rays. Much work in this area has been carried out using triphenyl tetrazolium chloride (TTC) [8–11] the structure of which is illustrated in Fig. 1, along with some other cited compounds.

TTC based dosimeters for γ-radiation monitoring have been proposed in the form of aqueous [8,9] and alcoholic [10] solutions but also as agar gels [8]. Less well studied has been the use of tetrazolium dyes in films for UV dosimetry.

Ultraviolet radiation (UVR) plays an important role in maintaining the human body. The main benefit of UVR is generally ascribed to its role in the synthesis of vitamin D3 [12], which is required in many important functions within the human body, such as aiding the absorption of dietary calcium in the gut required to sustain healthy bones [12,13]. Individuals suffering from skin conditions such as psoriasis can also benefit from UV phototherapy [14]. Overexposure to UVR can, however, be hazardous to human health [15] with the severity of the damage caused depending on the type of UV, the intensity and length of the exposure and the sensitivity of the individual. Acute effects arising from short-term exposure to the skin and eyes include erythema i.e. the reddening of the skin more commonly known as sunburn, photokeratitis and photoconjunctivitus, the reversible sunburn of the cornea and conjunctiva, respectively [15,16]. Long-term exposure can lead to chronic conditions such as photoaging [12,17] and skin cancer [12–21] and cause clouding of the lens of the eye, i.e. cataracts [22]. There is also evidence that the human immune system is suppressed due to

* Corresponding author. Tel.: +44 141 548 2458; fax: +44 141 548 4822.
E-mail address: a.mills@strath.ac.uk (A. Mills).

1010-6030/$ – see front matter © 2008 Elsevier B.V. All rights reserved.
doi:10.1016/j.jphotochem.2008.10.010

Available online at www.sciencedirect.com
ScienceDirect
Catalysis Today 129 (2007) 22–28
CATALYSIS TODAY
www.elsevier.com/locate/cattod

Current and possible future methods of assessing the activities of photocatalyst films

Andrew Mills *, Michael McFarlane

Department of Pure & Applied Chemistry, University of Strathclyde, Glasgow, G1 1XL, UK

Available online 20 August 2007

Abstract

The continuing interest in semiconductor photochemistry, SPC, and the emergence of commercial products that utilise films of photocatalyst materials, has created an urgent need to agree a set of methods for assessing photocatalytic activity and international committees are now meeting to address this issue. This article provides a brief overview of two of the most popular current methods employed by researchers for assessing SPC activity, and one which has been published just recently and might gain popularity in the future, given its ease of use. These tests are: the stearic acid (SA) test, the methylene blue (MB) test and the resazurin (Rz) ink test, respectively. The basic photochemical and chemical processes that underpin each of these tests are described, along with typical results for laboratory made sol–gel titania films and a commercial form of self-cleaning glass, Activ™. The pros and cons of their future use as possible standard assessment techniques are considered.

Keywords: Stearic acid; Methylene blue; Photocatalysis; Titania; Resazurin; Ink

1. Introduction

The basic process that underlies most examples of semiconductor photocatalysis, SPC, can be summarized as follows [1–5].

$$\text{Organic pollutant} + O_2 \xrightarrow[\text{Semiconductor}]{h\nu \geq E_{bg}} \text{minerals} \quad (1)$$

where E_{bg} is the bandgap energy of the semiconductor and, usually, the semiconductor is anatase titanium dioxide. The latter form of titania is commonly chosen because of its chemical and biological inertness, mechanical toughness, high photocatalytic activity and low cost [1–5].

Extensive research into SPC using TiO_2 has shown that it is able to photocatalyse the complete oxidative mineralization of a wide range of organic materials, including many pesticides, surfactants and carcinogens, by oxygen [1–5]. Not surprisingly, many commercial products have emerged in recent years based on titania photocatalysis, including: water and air purification systems and self-cleaning tiles and glasses [6]. The latter in particular have met with significant commercial success and are now sold world-wide by most of the major glass manufacturers including the following (with the trade name of their commercial product in parentheses): Pilkington Glass (Activ™) [7], St-Gobain (Bioclean™) [8] and PPG (Sun-Clean™) [9].

In the case of the above, the thin, typically 15 nm, films of anatase titania on glass employed are self-cleaning in that most of the organic pollutants that go to make up the dirt and grime that deposit on window glass are readily mineralized by oxygen via the photocatalytic process (1) [10]. These films are also more easily wetted by water, i.e. hydrophilic, after UV irradiation, making it difficult for hydrophobic organic pollutants to adhere to the surface. Although it remains, as yet, unclear how UV-induced, hydrophilicity and SPC activity are related, it is clear that any titania film which is SPC active also exhibits UV-induced hydrophilicity. It follows that for a fully functioning, self-cleaning glass it is essential that the titania coating exhibits SPC activity.

In order to compare the effectiveness of one self-cleaning glass with that of another, and to be able to effect and demonstrate a commercially acceptable high degree of quality control on any SPC product, such as self-cleaning glass, it is essential to have a set of agreed standard methods of assessing SPC activity. The creation, validation and promotion of such a set of standard methods is currently in progress by an

* Corresponding author. Tel.: +44 141 548 2458; fax: +44 141 548 4822.
E-mail address: a.mills@strath.ac.uk (A. Mills).

0920-5861/$ – see front matter © 2007 Elsevier B.V. All rights reserved.
doi:10.1016/j.cattod.2007.06.046